12-2016

Laser-processed parchment paper for fabrication of chronic wound dressings with selective oxygenation

Manuel Ochoa
Purdue University

Graduate School Form
30 Updated 12/26/2015

PURDUE UNIVERSITY
GRADUATE SCHOOL
Thesis/Dissertation Acceptance

This is to certify that the thesis/dissertation prepared

By Manuel Ochoa

Entitled

LASER-PROCESSED PARCHMENT PAPER FOR FABRICATION OF CHRONIC WOUND DRESSINGS WITH SELECTIVE OXYGENATION

For the degree of Doctor of Philosophy

Is approved by the final examining committee:

Babak Ziaie
Chair

Zhihong Chen

Saeed Mohammadi

Çağri Savran

To the best of my knowledge and as understood by the student in the Thesis/Dissertation Agreement, Publication Delay, and Certification Disclaimer (Graduate School Form 32), this thesis/dissertation adheres to the provisions of Purdue University's "Policy of Integrity in Research" and the use of copyright material.

Approved by Major Professor(s): Babak Ziaie

Approved by: Venkataramanan (Ragu) Balakrishnan 10/12/2016

Head of the Departmental Graduate Program Date

LASER-PROCESSED PARCHMENT PAPER FOR FABRICATION OF CHRONIC WOUND DRESSINGS WITH SELECTIVE OXYGENATION

A Dissertation

Submitted to the Faculty

of

Purdue University

by

Manuel Ochoa

In Partial Fulfillment of the

Requirements for the Degree

of

Doctor of Philosophy

December 2016

Purdue University

West Lafayette, Indiana

This dissertation is dedicated to my parents, Manuel and Gloria, and to my sister, Alejandra, with my endless gratitude for their unwavering support, love, and encouragement.

ACKNOWLEDGMENTS

The work in this dissertation could not have been completed without the help from many people; I am grateful to everybody who supported me along the way. I cannot mention everyone here, as I would surely run out of paper, but I would like to especially thank here those who were most influential in the completion of this work.

My endless gratitude goes to my parents, Mr. Manuel Ochoa and Mrs. Gloria Ochoa, and my sister, Ms. Alejandra Ochoa. I thank them for their patience, encouragement, and support as I pursued this academic endeavor. I could not have accomplished this without their love and care.

I especially wish thank my academic advisor and mentor, Professor Babak Ziaie, for all of his valuable guidance, support, and inspiration during my time as a graduate student. His enthusiasm and scientific intuition inspires everyone in his lab to develop creative out-of-the-box solutions that target real-world challenges. I appreciate his leadership and patience, his understanding of students as real people with diverse lives outside of research, and his motivation through brainstorming sessions, group dinners, and exciting conference travel, all of which create an exceptional atmosphere for conducting doctoral research.

I would also like to thank all the wonderful people I met during my time at Purdue who have been very influential and supportive, many with whom I had the pleasure of collaborating on research. Firstly, I thank all the members of my committee, Professor Zhihong Chen, Professor Saeed Mohammadi, and Professor Çağri Savran, for their support and feedback during my graduate studies. I am also especially grateful to Mr. Rahim Rahimi, Mr. Chang K. Yoon, Mr. Hongjie Jiang, Ms. Tiffany L. Huang, Mr. Pablo Jiménez-Corredor, Dr. Neslihan Alemdar, and Dr. Michael Zieger, as the work in this dissertation is a direct product of our working together and it would not have been possible without them. A very special thanks goes to all my senior colleagues and friends who have always

been very supportive and who showed me the light towards graduation, including Dr. Seung Huyn Song, Dr. Jun Hyeong Park, Dr. Albert Kim, Dr. Girish Chitnis, Dr. Charilaos Mousoulis, Dr. Teimour Maleki, Dr. Xuemei Chen, Dr. Nithin Raghunathan, Dr. Kul Inn, Dr. Sultan Helmi, Dr. Hossein Pajouhi, and Dr. Pankaj Jha.

A very dear thanks goes to all my friends that have helped to keep me motivated throughout this endeavor. These include my close friends from my hometown, including Mr. Jason Salamat, Mr. Horacio Ochoa, Mr. Steven Moya, and Dr. Mario Roa; my wonderful officemates from BRK 1238 who livened up the office with our fun conversations; my friends and colleagues from the Nanotechnology Student Advisory Council; the helpful staff at the Birck Nanotechnology Center; and of course all my colleagues from from the Ziaie Biomedical Microdevices Laboratory (ZBML). ZBML is more than just a group of coworkers; we are friends who work together, laugh together, travel together, and together create an energizing atmosphere in the lab. I thank (in addition to those mentioned above) Ms. Farah Alimagham, Mr. Marcus Brown, Ms. Swetha Chandrasekar, Mr. Zachariah Hughes, Mr. Vaibhav Jain, Mr. Sam Kenknight, Mr. Junyoung Kim, Mr. Seung Seob Lee, Mr. Rodolfo Leiva, Ms. Rebeca Hannah Olivera, Mr. Mark Oscai, Mr. Tejasvi Parupudi, Mr. Tianlin Tan, Mr. Lior Ben Yehoshua, Mr. Wuyang Yu, Mr. Jiawei Zhou, and all my other lab colleagues.

I am also grateful for the many exciting collaborations with wonderful colleagues who provided me with help and guidance and who contributed to the rich interdisciplinary nature of my graduate studies. In particular, a big thank you goes to my collaborators from Harvard Medical School and Tufts University on the NSF EFRI team, including Professor Sameer Sonkusale, Professor Ali Khademhosseini, Dr. Mehmet R. Dokmeci, Dr. Ali Tamayol, and Dr. Pooria Mostafalu. I am also grateful to Professor Sophie Lelièvre, Professor Rodolfo Pinal, Dr. Andrew Otte, Dr. Rajiv Sood, and Mr. Joonhyeong Park for their continued support throughout various other projects in my graduate career.

Finally, I would like to take this opportunity to thank those who provided me with professional development and financial support. Firstly, I would like to thank the Purdue Department of Mathematics, in particular my supervisors Dr. Dominic Naughton Dr. Rita

Saerens, for the many teaching opportunities and financial support throughout my graduate career. I am also grateful to the Andrew W. Mellon Foundation, in particular the Melon-Mays Undergraduate Fellowship (MMUF), for providing a fellow network, as well as professional development and financial support during my undergraduate and graduate studies. Finally, I also thank the National Science Foundation; funding for this work was provided in part by NSF grant EFRI-BioFlex #1240443.

TABLE OF CONTENTS

Page

Page

LIST OF TABLES

LIST OF FIGURES

ABSTRACT

Ochoa, M. Ph.D., Purdue University, December 2016. Laser-Processed Parchment Paper for Fabrication of Chronic Wound Dressings with Selective Oxygenation. Major Professor: Babak Ziaie.

Chronic non-healing wounds (e.g., diabetic foot ulcers and bed sores) impact over 6.5 million Americans per year, costs in excess of $25 billion to treat on an annual basis, and are on the rise due to increasing levels of obesity and diabetes compounded by an aging population. A major inhibitor of healing is suboptimal oxygenation of the wound bed. Unlike acute injuries that receive sufficient oxygen via a functional blood vessel network, chronic wounds often suffer from the lack of a proper vascular network; thus being incapable of providing sufficient oxygen for tissue growth. Typical medical treatment of hypoxic chronic wounds typically employs hyperbaric oxygen therapy, which requires bulky equipment and often exposes large areas of the body to unnecessarily elevated oxygen concentrations that can damage healthy tissue. A more recent and convenient approach is topical oxygen therapy (TOT), in which the dressing itself can generate and deliver the required oxygen; various such systems exist commercially, but they are not economical, they do not provide selective delivery to only hypoxic regions, and their design does not permit further expansion for other wound-healing therapies on the same platform. A more practical implementation of such dressings would comprise an inexpensive dressing platform for adaptive oxygen therapy which is capable of delivering appropriate oxygen gas where and when it is needed. This work presents a low-cost alternative for continuous oxygen delivery comprising of an inexpensive, paper-based, biocompatible, flexible platform for locally generating and delivering oxygen to selected hypoxic regions. The platform takes advantage of recent developments in the fabrication of flexible microsystems including the incorporation of paper as a substrate and the use

of inexpensive laser machining. The use of paper simultaneously provides structural strength and flexibility as well as selective filtering functionality, i.e., it allows for oxygen to pass through while preventing aqueous solutions to reach the tissue. The laser machining enables the precise definition of oxygen generating regions that match the hypoxic wound profile. Together these two technologies enable the development of a low-cost patch/wound-dressing with customized, wound-specific oxygen generating regions.

1. INTRODUCTION

1.1 Problem definition

Cutaneous wounds pose major health and financial burdens for millions of people throughout the world. In the US alone, chronic non-healing wounds, in particular, (e.g., diabetic foot and bed sores) impact over 6.5 million Americans per year, costs in excess of $25 billion to treat on an annual basis, and are on the rise due to increasing levels of obesity and diabetes compounded by an aging population [1, 2]. Chronic wounds are those which do not follow the standard cascade of biological processes (i.e., inflammation, proliferation, and maturation) by which common acute wounds heal [3]. Instead, their healing is impaired by conditions such as local hypoxia, irregular vascular structure, external mechanical pressure, and bacterial infections [3–9]. Current treatments are expensive and labor-intensive, relying on regular cleaning, debridement, oxygen therapy, surgery, and topical or systemic administration of antibiotics [10–12]. Commercially-available dressings (e.g., alginate, hydrogels, hydro-colloids, foams, etc.) have not proven to be significantly effective in reducing the burden. An ideal dressing integrates sensors (pH, oxygen, and inflammatory mediators), drug/cell delivery (antibiotics, growth factors, stem cells, and oxygen), and electronic intelligence to drastically improve wound care by measuring individual responses and enabling appropriate adjustments to therapy (i.e., precision/personalized wound care) [13, 14]. In order to do so, it is important to address one component at a time.

Among the many issues hampering chronic wound healing, suboptimal oxygenation of the wound bed is one of the most critical and treatable. Unlike acute injuries that receive sufficient oxygen via a functional blood vessel network, chronic wounds often suffer from the lack of a proper vascular network, thus, being incapable of providing sufficient oxygen for tissue growth [7, 8, 15]. While the lack of oxygen may trigger vascular

regeneration, the severity and depth of wounds can prevent adequate regeneration, causing wound ischemia. Modern medical treatment of hypoxic chronic wounds typically employs hyperbaric oxygen therapy, which requires bulky equipment and often exposes large areas of the body to unnecessarily elevated oxygen concentrations that can damage healthy tissue [16–18]. A more practical approach is topical oxygen therapy (TOT) in which the dressing itself can generate and deliver the required oxygen. Moreover, an ideal strategy would be to develop a dressing for adaptive oxygen therapy capable of delivering appropriate O_2 where and when it is needed. Various commercial systems exist which provide or generate oxygen to be delivered topically; however, they suffer from one or more of the following shortcomings: high cost ($2000 per two weeks), inability to selectively deliver oxygen to specific wound regions, and a lack of modularity for incorporation with other wound sensing components.

1.2 A low-cost solution

As a first step towards the development of a multi-functional smart wound healing bandage, this dissertation presents a low-cost alternative for continuous O_2 delivery comprising of an inexpensive, paper-based, biocompatible, flexible platform for locally generating and delivering oxygen to selected hypoxic regions. The platform takes advantage of recent developments in the fabrication of flexible microsystems including the incorporation of paper as a substrate [19–22] and the use of inexpensive laser machining [23–25]. The use of paper simultaneously provides structural flexibility as well as selective filtering functionality, i.e., it allows for oxygen to pass through while preventing aqueous solutions to reach the tissue. The laser machining enables the precise definition of oxygen generating regions that match the hypoxic wound profile.The silicone-based composition of the paper 's binder enables seamless integration with other flexible (e.g., PDMS) microfluidic and therapeutic components. Together these two technologies enable the development of a low-cost patch/wound-dressing with customized, wound-specific oxygen generating regions.

1.3 Organization of this dissertation

This dissertation is organized as follows. Chapter 2 presents a brief overview of cutaneous wounds, an overview of modern treatment practices for chronic wounds, a case for the need for advanced wound dressings, and a description of modern rapid prototyping technology that is ideal for the development of such new dressings. Chapter 3 introduces parchment paper as an ideal substrate for wound dressing applications, specifically laser-treated parchment paper as an oxygen generation platform; it discusses the various merits of such paper in light of the requirements for a wound dressing. Chapter 4 presents a practical catalysis-based approach to generating oxygen on the wound dressing. Chapter 5 demonstrates an oxygen generation platform for wound dressings, including various practical embodiments of the platform. Chapter 6 summarizes the work and remarks on the contributions of this research to the existing technologies. Finally, Chapter 7 discusses the remaining challenges for manufacturing integrated, smart dressings for the treatment of chronic wounds.

2. CHRONIC WOUNDS AND APPROPRIATE THERAPIES

2.1 Chronic dermal wounds

This chapter provides background about chronic wounds and their treatment approaches. Portions of this text are taken from publications by the author [14, 26].

2.1.1 Dermal composition and wound classification

Skin is composed of various layers of cells which can be classified as two distinct tissue layers, the epidermis (outer) and the dermis (inner), Figure 2.1. The epidermis (about 40–400 µm thick, depending on the body location) [27] serves as a protective barrier which shields the underlying tissue from external threats such as bacteria in the environment. It consists primarily of keratinocytes (95 %) but also contains some melanocytes, Langerhans cells, and Merkel cells.

Beneath the epidermis lies the dermis, a layer containing connective tissue composed of protein fibers, primarily collagen (and to a lesser extent elastin), as well as various types of cells, including fibroblasts, mast cells and histiocytes [28]. This layer also contains a network of capillaries (5–10 µm diameter) with a cross-sectional density in the range of 36–81 capillaries per mm^2 [29]; they are the primary source of nutrition/oxygen for dermal tissue.

When the epidermis or dermis are damaged (e.g., by scraping the epidermis or by a burn incident), the surrounding tissue responds immediately by releasing enzymes which trigger inflammation as well as signal proteins such as vascular endothelial growth factor (VEGF). In acute wounds, wounded tissue typically remains properly interspersed with (capillary) oxygen/nutrient sources such that the entire wound bed receives sufficient oxygen and nutrients (as is the case with un-injured tissue). Thus, as long a the

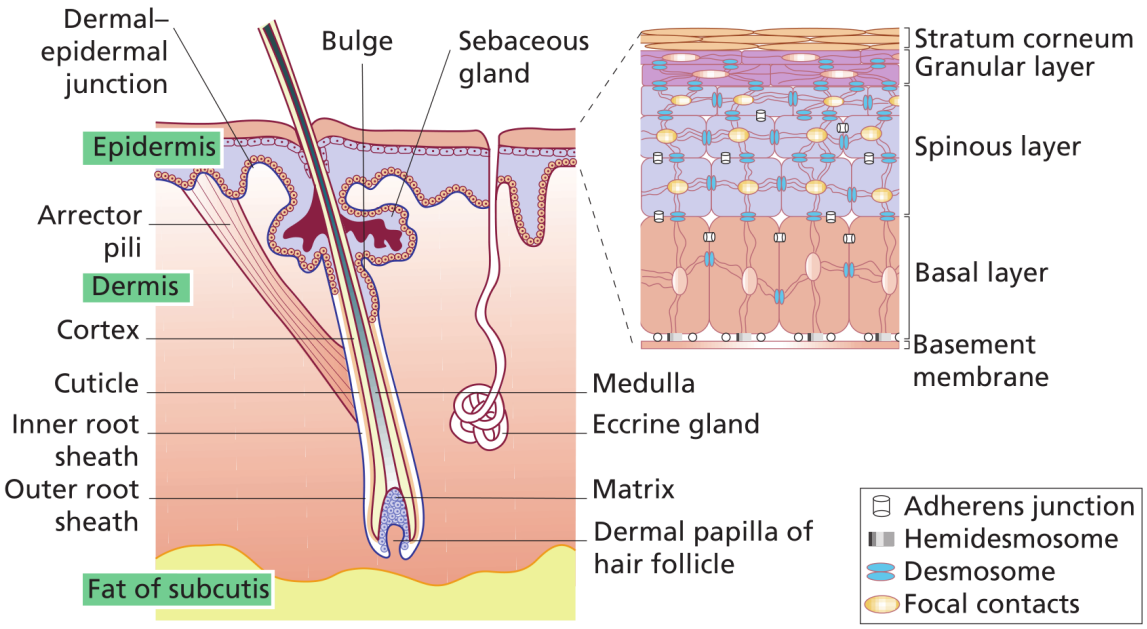

Figure 2.1. A cross-section of the skin, showing the two primary layers, the epidermis and the dermis. Reproduced from Ref. [28] with permission from John Wiley and Sons.

wound is maintained moist (e.g., with a traditional bandage), wound healing progresses through distinct inflammatory, proliferative, and maturation phases in an orderly fashion, Figure 2.2. The surrounding tissue provides adequate signal proteins to the wounded region to regenerate the tissue and recreate vascular structure to adequately nurture the new skin. In such acute wounds, the entire healing process lasts no more than about three months.

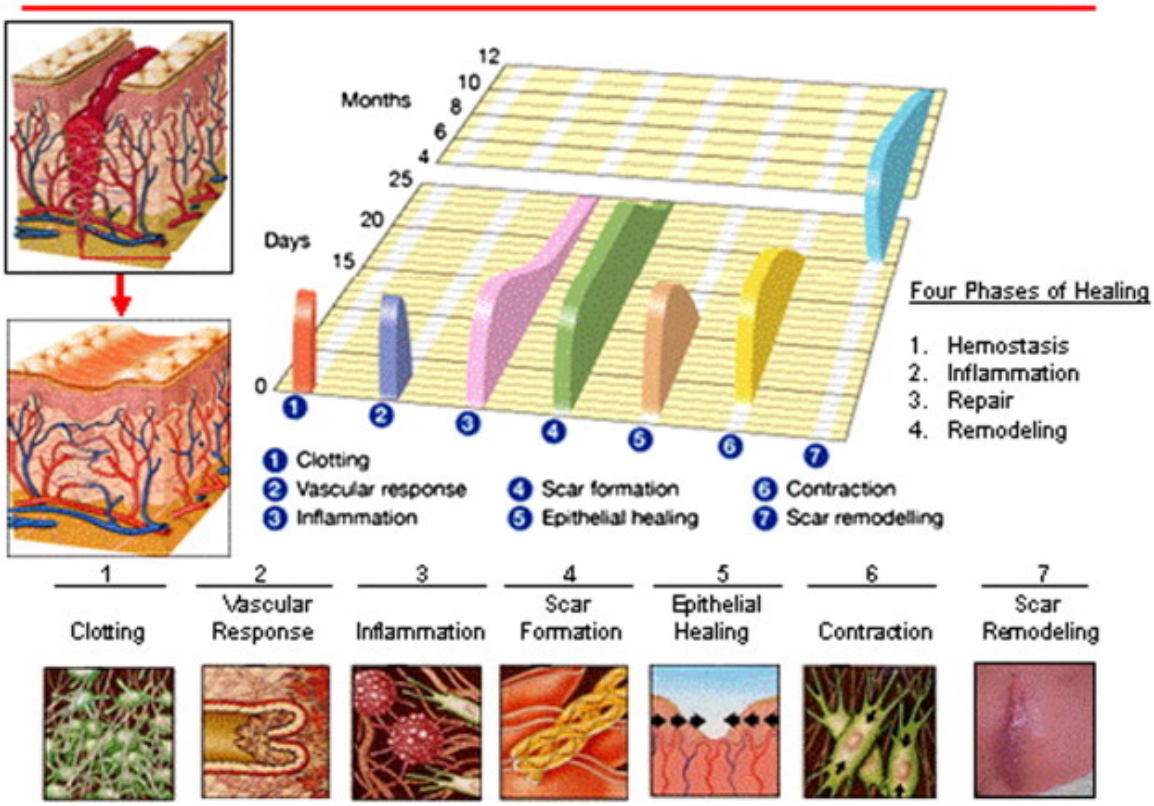

Figure 2.2. Sequence of molecular and cellular events in skin wound healing. Reproduced from Ref. [3] with permission from Elsevier.

If, however, a wound is incapable of receiving proper nutrition (e.g., oxygen) from the surrounding tissue, it may become chronic. A chronic wound is a type of wound that does not heal in an orderly or timely (i.e., within three months) manner. These wounds, unlike (healing) acute wounds, either remain in an non-healing state or worsen rather than improving. One major reason is inadequate oxygenation. Such wounds often occur

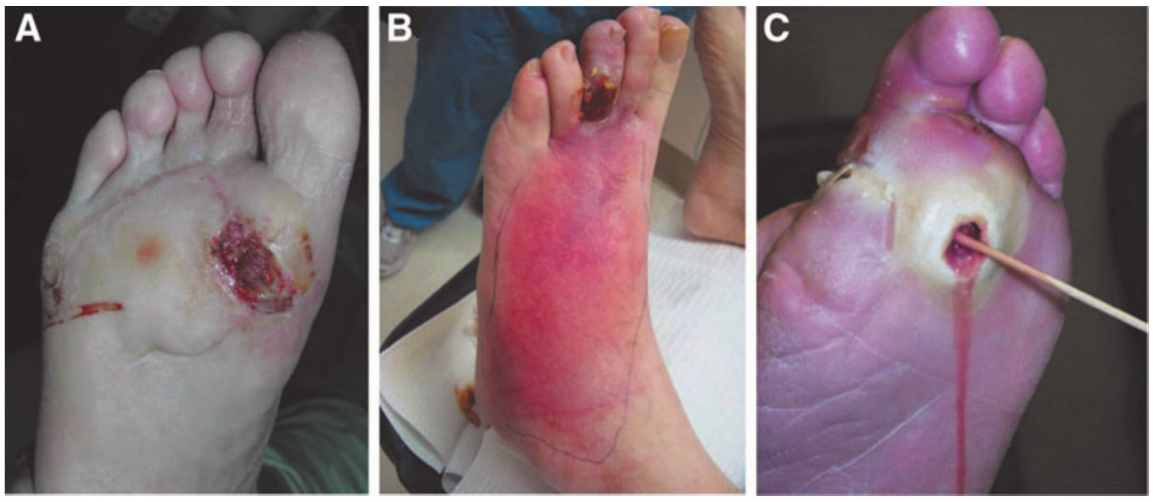

Figure 2.3. Example of chronic wounds (pressure ulcers) on the foot. (a) Recurring foot ulcer; (b) cellulitis from ischemia; (c) probe-to-bone test to check for osteomyelitis. Reproduced from Ref. [31], used under CC BY-NC 4.0.

in patients that are bedridden due to other unrelated health problems. Their inactivity causes prolonged constant pressure on specific areas of the body, resulting in pressure ulcers with a disturbed vascular structure and an ideal ground for bacterial infection growth [15, 30]. A graphic example of a (chronic) foot ulcer is shown in Figure 2.3. In order for this wound to heal, the dermal tissue must be regenerated. To ameliorate this situation, it is possible to supplement the hypoxic regions of the wound bed with oxygen from an external source.

2.1.2 Standard treatment protocols for chronic wounds

Modern protocols for the treatment of chronic wounds call for attentive care and regular application and replacement of wound dressings. Their primary purpose is to physically protect the wound and maintain adequate moisture levels while allowing air exchange [3, 10, 11, 32]. Since the exact optimal healing environment for a particular wound varies depending on its severity and healing state, various types of dressings are

available for treating a wide range of wounds, Figure 2.4 [3, 12, 33, 34]. Each of these addresses a unique condition in the wound and each follows a different replacement schedule (from twice per day to twice per week). The most common and least expensive is the standard gauze, Figure 2.4(a), which is indicated for shallow wounds or as a base component in multi-layer dressings. For increased moisture retention, a porous transparent film dressing, Figure 2.4(b), may be used instead or in addition to the gauze. Such dressings permit gas exchange but prevent wound-bed dry-out. If, on the other hand, the wound-bed is excessively wet, one may opt for a more absorbent dressing such as a gel or a hydrocolloid, Figure 2.4(c). These materials absorb excess exudate but maintain the wound sufficiently moist to promote tissue regeneration. In more extreme cases of deeper or more exudate-prone wounds, a sponge-based dressing is the preferred alternative, Figure 2.4(d); such dressings can more effectively fill a deep wound and absorb significant exudate. In addition to moisture management, many chronic wounds also require infection control. These cases would benefit from the application of antiseptic-loaded carriers such as silver-ion alginate dressings, Figure 2.4(e) [35]. This broad variety of modern dressings may seem sufficient for targeting many wound conditions; however, the high complexity of chronic wounds often results in the simultaneous expression of multiple symptoms that can be more efficiently addressed with improved wound monitoring systems.

To specifically address hypoxia, treatment of hypoxic chronic wounds typically employs hyperbaric oxygen therapy [17, 36–39], which requires bulky equipment and often exposes large areas of the body to unnecessarily elevated oxygen concentrations that can damage healthy tissue. For example, hyperbaric oxygen therapies (e.g., Figure 2.5) for foot ulcers are expensive, cumbersome, can result in systemic toxicity, and have shown marginal benefits. Hence, such methods require very careful and periodic oxygen administration to avoid hyper-oxygenation of tissue surrounding the wound. In a more practical approach, recent research has endorsed transdermal oxygen therapy (TOT) as a viable and effective method for oxygenating a hypoxic wound [8, 18, 40–42]. A variety of wound dressings can be used to create an enclosure around a wound which can entrap

Figure 2.4. Various types of commercially available wound dressings. (a) Common gauze pads/rolls, (b) transparent film, (c) hydrocolloid dressing, (d) foam dressing, (e) silver-loaded alginate dressing, and (f) soft silicone-coated dressing. Reproduced from Ref. [14] with permission from IEEE © 2014.

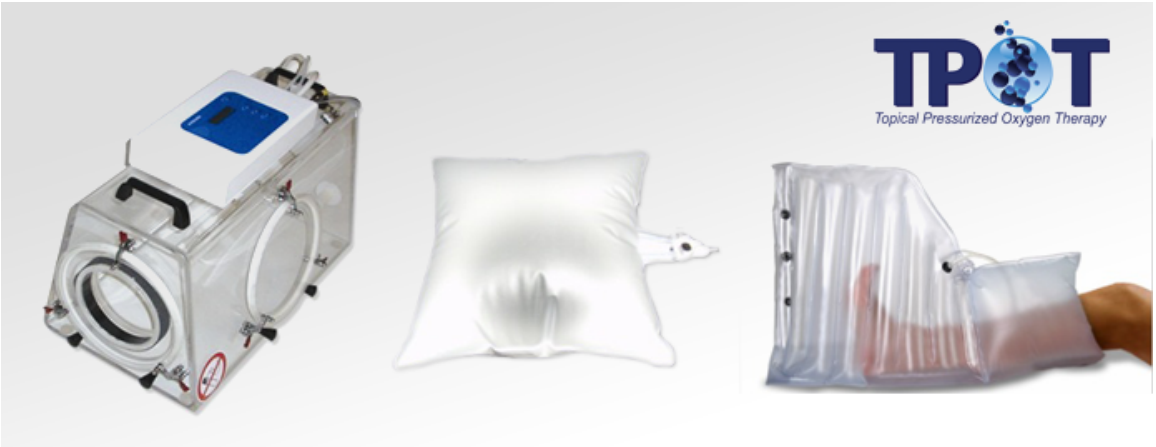

Figure 2.5. Example of a typical hyperbaric foot therapy system for extremities by Therapeutic Surface Solutions Inc. [43]. Figure taken from www.tsswoundcare.com. © Therapeutic Surface Solutions Inc.

oxygen generated from an external source (e.g., oxygen tank), restricting oxygen exposure only to the wound region while reducing the amount of healthy tissue that is exposed to hyper-oxygenation.

Commercial TOT systems

One of the commercial TOT technologies is a hand-held system (EPIFLO, Ogenix, Ft. Lauderdale, FL, Figure 2.6(a)) that concentrates oxygen from the environment and pumps it through a piece of tubing that it feeds into the wound dressing [44, 45], shown in Figure 2.6(a). The system is capable of producing oxygen continuously at a rate of 3 mL/h for up to 15 days, which has been shown to be sufficient for an expedited healing process. Average cots per day for a patient is approximately $ 47. This product is definitely an improvement over previous systems, as it allows for patient mobility and limits oxygen exposure to the wound bed. However, the system is still bulky, expensive, and does not provide a means to selectively deliver oxygen to the hypoxic regions within the wound.

A similar device is the Natrox (Inotec AMD) system (Figure 2.6(b)), consisting of a portable oxygen generator which generates oxygen via electrolysis and directs it through

flexible tubing into an oxygen delivery wound dressing. The generator module runs on a battery which is replaced daily. The dressing is replaced every 2–3 days. The average cost for a 7-day therapy is about $ 750. Like the EPIFLO systems, this is a two-part system.

Another example is the OXYGENESYS O2 patch (Halyard Health, Inc., formerly Kimberly-Clark Health Care), Figure 2.6(c). This devices contains embedded oxygen created during the fabrication process via a chemical reaction. Oxygen is not limited to only certain areas of the patch; instead, it is available everywhere, allowing the patch to be cut to the desired size. Once cut, the patch is applied to the wound, where, upon contact with moisture, it begins to release oxygen into the wound bed. The dissolved oxygen in the patch travels into the wound at a rate which is controlled by the dissolved oxygen gradient in the wound bed. For a 10 cm × 10 cm patch, this corresponds to 221–369 mL/h. Each patch costs approximately $ 93.

The OxyBand (OxyBand Technologies, Figure 2.6(d)) Wound Dressing is another TOT dressing which is pre-filled with oxygen. It consists of an oxygen reservoir capped on one end (non-wound end) by a gas-impermeable cover, and on the wound side by a gas-permeable membrane. When placed on the wound, it exposes the wound bed to pure oxygen for continuous diffusion for the duration of the therapy. The patch can operate continuously for up to 5 days and has a cost of $ 55 per patch.

These four commercial systems represent the current state of the art in the generation and delivery of oxygen to dermal wounds. Their key parameters are summarized in Table 2.1; here, cost comparison is based on a typical 7 day therapy to allow comparisons among single-unit and multi-unit systems (e.g., those where only one unit is replaced). None of these offer selective oxygenation within a wound (e.g., to prevent oxygenation of normoxic cells), nor do they permit integration with flexible medical sensors in a seamless fabrication technique. The treatment of such wounds would greatly benefit from the use of a localized method for oxygen delivery with improved spatial and temporal precision.

(a) Ogenix EPIFLO™ O_2 pump [45]. Photograph taken from www.ogenix.com. Ogenix and EPIFLO are registered trademarks of Neogenix, LLC dba Ogenix.

(b) NATROX™ oxygenation system [46]. NATROX is a trademark of Inotec AMD Limited.

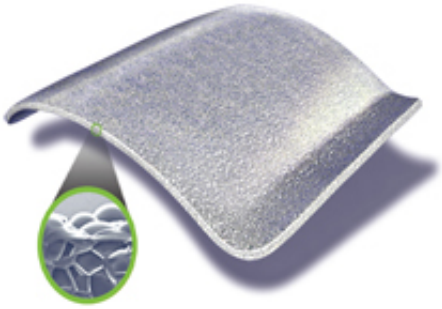

(c) OXYGENESYS™ O_2 patch [47]. OXYGENESYS is a registered trademark or trademark of Halyard Health, Inc.

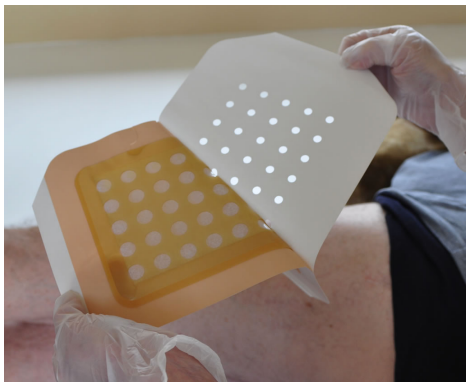

(d) OxyBand™ wound dressing [48]. © OxyBand Technologies.

Figure 2.6. Commercially available systems for topical O_2 delivery; all supply O_2 to the entire wound, without allowing selectivity towards hypoxic regions.

Manufacturer	Product	O2 generation rate	Continuous operation time	Selective delivery	Integratable with flexible sensor farbication	Refillable/ rechargeable	Cost ($USD) of 7 days of therapy	Notes
Ogenix	*EPIFLO*	3 mL/h	15 days	No	No	No	329	Device, separate from dressing
Inotec AMD	*Natrox*	13 mL/h	24 hours (then replace battery; use for 2-3 days)	No	No	Yes (battery)	750	Device + dressing
OxyBand	*OxyBand*	pre-filled	5 days	No	No	No	165*	Size: 7in x 9in (17.78cm x 22.86cm)
Halyard (Kimberly-Clark)	*OXYGENESYS*	221-369 mL/h	N/A	Yes (can be cut)	No	No	280*	Size: 10cm x 10cm

Table 2.1.

Comparison of state-of-the-art, commercial oxygen-generating systems. *For the shorter-term-use patches, the cost of 7 days of therapy is computed assuming 3 patches are used (changed every 2–3 days, as is standard for wound dressings).

2.2 Smart wound dressings

To place the need and viability of advanced precision wound oxygenation dressings in proper context, it is important to first review the advantages of smart wound dressings, their material requirements, and current and emerging technologies for their development. These concepts are covered in this section.

2.2.1 Rationale for developing more complex dressings

The future of wound dressings lies in 'smart' dressings, comprised of arrays of sensors and drug/oxygen delivery modules (e.g., TOT modules) that can address the therapeutic requirements of the wound in a localized, responsive manner. This can be accomplished by the incorporation of bio/chemical sensors (e.g., pH, oxygen, inflammatory signals) and drug delivery capabilities (e.g. via nanomedicine [49] or microfluidics [50]) into the dressings [51, 52] by either (i) developing new wound dressing platforms or (ii) embedding flexible sensors into existing commercial ones. These smart systems can help optimize the healing process, decrease the healing time, and prevent infections. They can evaluate the local wound environment, release wound healing agents as needed, detect the optimal replacement time, and alert the patient/caregiver of any unusual phenomena (preferably through a wireless link). The fabrication of such systems requires a deviation from traditional MEMS and transducer fabrication methods in order to create devices with mechanical and electrical properties which are optimized for the unique environment of wounds (i.e., soft, deformable, wet, and warm). Although the unit cost of such systems may surpass that of current dressings, their ultimate efficacy can result in an overall reduced expenditure. As reported by Kerstein et al., while a pressure ulcer that is properly treated shows satisfactory healing progress with either inexpensive gauze dressings or more expensive hydrocolloid ones, the total cost of the treatment is lower for the latter due to their less frequent replacement schedule and a reduced need for professional medical attention [53]. Additionally, the techniques should be economical, adaptable for moderate-volume production, and preferably customizable

(i.e., for a precision medicine approach). As a result, researchers have embraced the use of commercially-available materials and rapid prototyping equipment for the development of low-cost, conformable, disposable devices for wound healing and other wearable applications. Processes such as inkjet printing, screen printing, micro-gravure coating, and laser machining are particularly suited for these applications due to their scalability and ease of implementation [54, 55].

2.2.2 Material requirements for wound dressings

Cutaneous wounds present a unique environment in which dermal monitoring devices must operate, Figure 2.7. They consist of an exposed subcutaneous tissue (dermis; and in deep wounds hypodermis, fat tissue, and possibly muscle) that is wet/moist, warm, and loaded with cellular and bio/chemical components (red and white blood cells, plasma, bacteria in case of infection, and inflammatory/regenerative biomolecules) [3,32]. Furthermore, the wound bed contains delicate regenerating tissue which may be sensitive to chemical, thermal, or mechanical stimuli. As a result, any device designed for such cutaneous interfaces must conform to a set of requirements, mimicking the properties of typical wound dressings. Despite the large variation in structural and physical properties, current wound dressings have certain core requirements for their functional efficacy. First is flexibility, i.e., such dressings must be sufficiently flexible to conform to the wound and not limit the patient's mobility [56]. Second is gas permeability, which is essential for maintaining an adequate oxygen supply; alternatively, some dressings may supply oxygen at required levels [57]. Third is moisture control [58]; the dressing should keep the wound bed moist but absorb excess exudate. Finally, the material in contact with the wound bed should be sufficiently soft to avoid causing mechanical insults and interfering with the epithelization process (a minimal adhesion is often preferred to reduce the mechanical load).

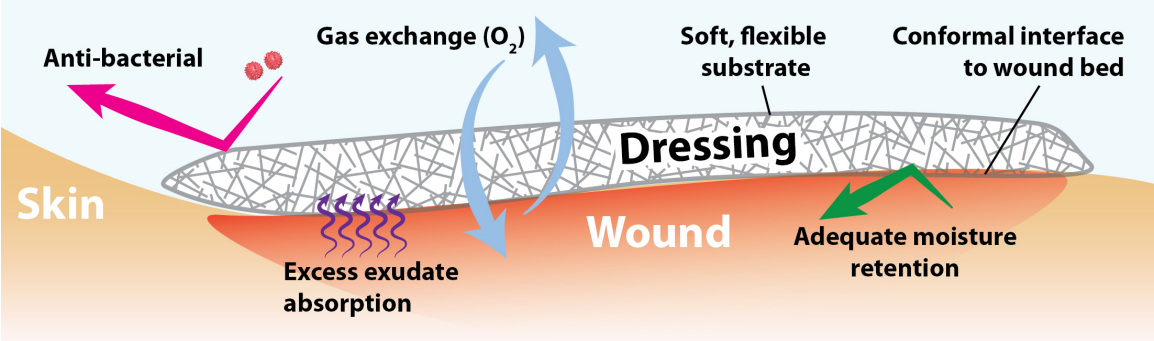

Figure 2.7. Wound dressing requirements for proper healing. The dressing should conform to the wound bed, prevent bacterial infections, retain adequate moisture, remove excess exudate, and promote oxygenation. Reproduced from Ref. [26] with permission from Springer.

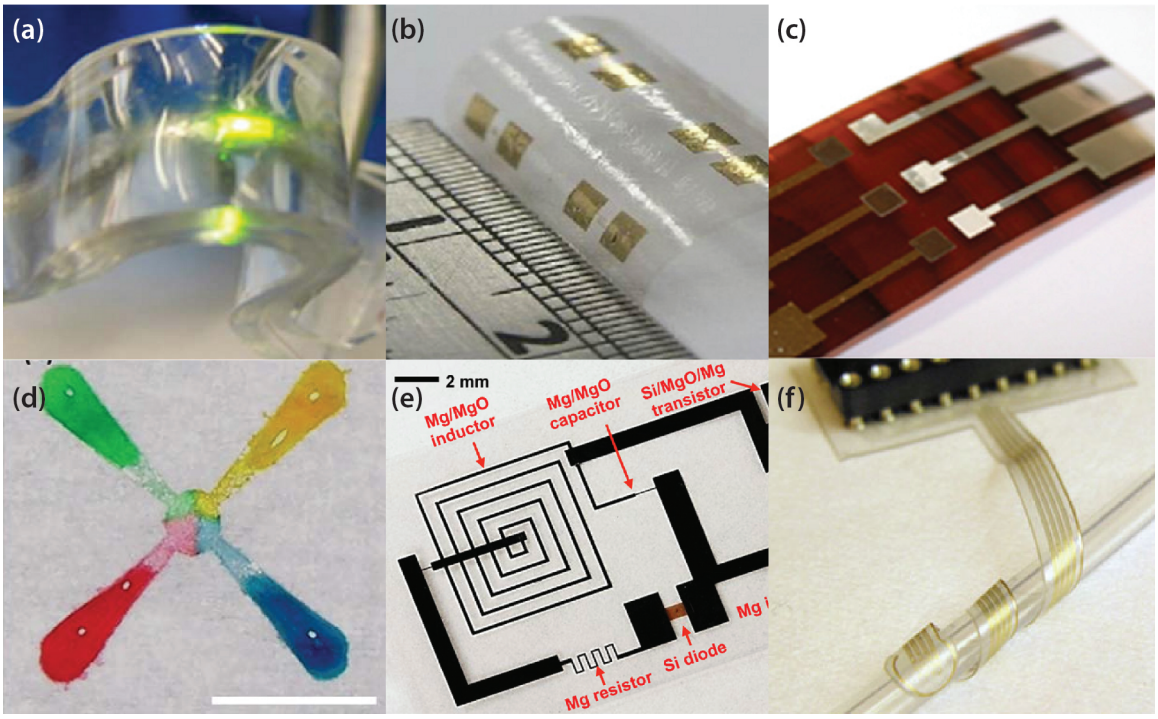

Figure 2.8. Flexible devices for medical applications. These include (a) PDMS, (b) Parylene-C, (c) polyimide, (d) paper, (e) silk, and (f) Parylene-C/PDMS bilayer. Reproduced from Ref. [14] with permission from IEEE © 2014.

2.2.3 Materials and processes for smart wound dressings

Flexible substrates and materials are particularly attractive for wound applications since they can conformally cover the wound and do not apply excessive force/stress to the healing area (most commercially available wound dressing are flexible and conformal). Recent efforts in this area have leveraged large scale integration of ultra-thin inorganic semiconductors with flexible and biodegradable substrates to fabricate several multi-functional systems for biological applications [59, 60], e.g., Figure 2.8. Other materials which have been used for fabrication of such medical devices are summarized in Table 2.2.

Material	Young's Modulus (MPa)	Bio-compatible	Spin-coatable	Stretchable	Flexible	Hydrophilic	Glass transition temperature (°C)	WVP×10^{10} *	References
PDMS	0.360–1.24	Yes	Yes	Yes	Yes	Yes	−125	72000	[61,62]
Poly(vinyl alcohol) (PVA)	49.5±3.2	Yes	Yes	No	Yes	No	85	9.03–4190	[63,64]
Whatman filter paper	460–1700	Yes	No	No	Yes	Yes	–	989–8140	[65–67]
PTFE	500	Yes	Yes	No	Yes	Yes	130	8.45	[62]
polylactide (PLA)	1030–4000	Yes	Yes	No	Yes	No	55–60	200**	[68–70]
PET	2500	Yes	No	No	Yes	Yes	85	151	[71]
Polyimide	3200	Yes	Yes	No	Yes	Yes	>400	417–5040	[62,72]
Parylene	4000	Yes	No	No	Yes	Yes	80–100	9.25**	[73–75]

* Water Vapor Permeability multiplied by 10^{10}: $(cm^3 \cdot cm)/(cm^2 \cdot s \cdot cmHg)$

** Water Vapor Trasfer Rate: $(g)/(cm^2 \cdot s)$

Table 2.2.
Flexible materials which have been used as substrates for fabricating medical devices, such as wound dressings. Reproduced from Ref. [14] with permission from IEEE © 2014.

2.2.4 Laser machining as a viable tool for wound dressing fabrication

Processing such unique materials for wound dressing manufacturing requires the use of emerging rapid prototyping technologies. Among these, laser-machining offers a unique set of capabilities directly beneficial for the development of flexible/stretchable low-cost systems for cutaneous wound interfaces. They consist of a laser module connected to a machining enclosure that contains a working stage and a software-controlled lens. The substrate is placed on the stage and the lens module guides the laser beam on the surface of the substrate to cut or ablate regions as defined in a CAD drawing. Most commercial systems use either a 10.6 μm CO_2 laser (typical powers of up to 150 W) suitable for cutting polymers and wood or a 1.06 μm fiber laser (typical powers of up to 40 W) that can mark metals and cut thin foils [76–78]. These systems have a linear scanning speed of a few meters per second and the output power and laser spot size/focus can be adjusted by software.

Laser machining provides the ability to cut materials, etch (ablate) them, alter their surface morphology, and induce surface chemical changes, all of which increase the functionality of the material. For example, laser can be used to tune the hydrophilicity of materials such as paper, or (using different parameters) it can be used to pyrolize polymers to create active carbon materials. Furthermore, the availability of commercial, reliable, and precise laser systems allows them to become part of large-scale (e.g., roll-to-roll) production lines. Such systems are particularly useful for processing various types of paper, such as parchment paper, as is discussed in the following chapter.

3. LASER PROCESSED PAPER AS A SUBSTRATE FOR WOUND DRESSINGS

3.1 Paper for wound healing

3.1.1 Merit of paper for medical devices and wound dressings

Among the many materials available as substrates for future wound dressings, paper stands out as a competent and appropriate solution due to its low cost, adaptability to mass production, and mechanical flexibility (for conforming to wounds). Paper is a classic material whose invention dates back to ancient China. Aside from its traditional application as a writing medium, paper can be repurposed using modern technologies to create novel devices with complex functionality for use as flexible sensors for wound monitoring. Paper offers many unique properties including biocompatibility, low cost, and ubiquity [79]. Moreover, its cellulose mesh composition invites customization of many physical parameters, including thickness, fiber size, porosity, and hydrophilicity. Cellulose is a natural, hydrophilic fiber with strong hydrogen bonding between polymer chains which render it insoluble in water and most organic solvents. These properties have enabled the manufacturing of many different types of commercial paper, including filter paper [21], wax paper [80], and parchment paper [81], among others. These three, in particular have found niche applications in the field of disposable sensor development due to their favorable, tunable physical properties. The first of these is known to have excellent wicking properties. The latter two are naturally hydrophobic, but their surface properties can be altered by plasma treatment or by laser ablation [25]. Parchment consists of a compressed cellulose fiber sheet encapsulated in a thin coating of silicone to achieve a hydrophobic, heat-resistant surface. Wax and palette paper use wax and plastic, respectively, as the coating material. Many researchers have used these properties for

the fabrication of paper-based systems for various biomedical applications, including controlled drug delivery, tissue engineering, sutures, biodegradable vascular grafts [82,83], low-cost microfluidics [84], and various flexible sensors [19, 21, 85–89].

Of all papers types available commercially, parchment paper offers unique advantages of mechanical strength when dry and wet, selective gas permeability over aqueous solutions at low pressures, laser-patterning ability, compatibility with multiple bio-medical device materials, and bio-compatibility. This chapter describes these key features to demonstrate the suitability of parchment paper for wound dressing applications. Portions of this chapter were adapted from [90, 91].

3.1.2 Mechanical flexibility and strength of parchment paper

Mechanical flexibility and strength are two essential parameters of wound dressing substrates. The substrate must be sufficiently flexible to conform to the human body, specifically to wounds (and in some cases to the wound bed itself). For this reason, most commercial bandages or dressings are composed of stretchable fabric, non-woven fabrics, polymeric sponges, or thin polymer-backed hydrocolloids; similarly, medical adhesive tapes are flexible and are composed of either polymers, fabrics, or paper. At the same time, wound dressings require mechanical robustness to prevent them from tearing under the strain from regular wear and to keep them from disintegrating in the presence of (often heavy) moisture (e.g., sweat, wound exudate, applied therapeutics in the wound bed). This subsection compares the mechanical properties of various types of paper in dry and wet conditions, and places them in context of typical values for wound applications.

The mechanical properties of the paper were investigated using a standard tensile stress-strain test. Paper samples (parchment, wax, filter, and a paper-PDMS composite) were laser-cut into strips (5 mm × 20 mm) and separated into two groups. One group was maintained at room temperature while the other were submerged in buffer saline solution (PBS) for several durations (0-7 days). Subsequently, and the ultimate tensile

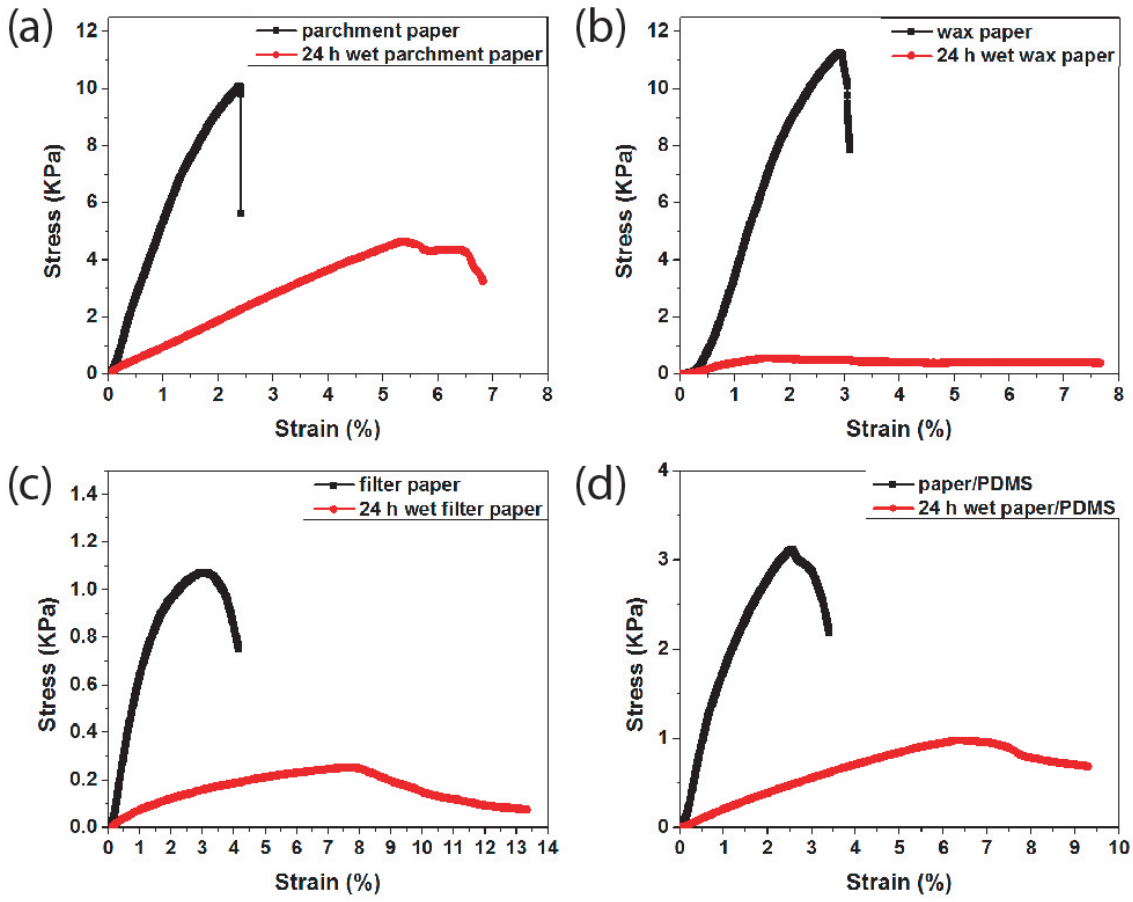

Figure 3.1. Stress-strain curves various types of dry and wet paper: (a) parchment paper, (b) wax paper, (c) filter paper, and (d) paper/PDMS composite. Reproduced from Ref. [90] with permission from The Royal Society of Chemistry.

strength (UTS) and Young's modulus of all samples in both groups were subsequently measured using a universal testing machine (Admet, model eXpert 1000). The tensile strength measurements were performed by fixing the two ends of the film and stretching from 0 % to 12 % strain at a constant extension velocity of 10 mm/min.

Figure 3.1 shows the stress-strain curves of the various papers when dry and after 24 hours in PBS solution. The dry samples exhibit a linear stress-strain profile with limited (2.5 %) elongation before rupture. The sharp drop in the stress indicates the

strain at which the paper tears. The Young's modulus of the various papers is extracted from the stress-strain curves and is graphed in Figure 3.2. The data reveal an high elastic modulus (> 100 kPa) for all dry samples, except for filter paper. Once wet, however, the elastic modulus of each sample drops below 50 kPa. In particular, the elastic modulus of parchment paper changes from over 300 kPa to about 45 kPa, whereas the others drop to significantly lower levels. These values for parchment paper make parchment paper sufficiently rigid for handling (e.g., when using it as a substrate for fabrication) but becomes sufficiently soft for skin application when wet (e.g., in the wound environment). Skin is known to have an elastic modulus of 24.910–101.180 kPa, depending on the skin location [92]. Thus, wet parchment paper matches the elastic properties of skin. As such, it can be compared to other commercial products, such as a commercial wound regeneration matrix (e.g., Integra Dermal Regeneration Matrix, Integra Life Sciences) which is used routinely in burn-related surgeries; this product has a Young's modulus of 25–45 kPa, in the lower range of that for parchmet paper.

Despite being very flexible, parchment paper also exhibits significant strength. Figure 3.3 shows the change in the ultimate tensile strength for the papers/films before and after submersion in phosphate buffered saline (PBS). Figure 3.3 shows the change in UTS for filter paper and various hydrophobic papers before and after various durations of submerging in PBS. All the dry samples exhibit a linear stress-strain profile with a small strain (2.5 %) before rupture. The commercial parchment paper and wax paper have the highest mechanical properties in dry state with the UTS of 69.4 MPa and 73 MPa. Filter paper impregnated with PDMS has a dry UTS of 21.4 MPa, which is three time higher than the pristine filter paper (7.6 MPa). This increase in mechanical strength is explained by the presence of the PDMS filler in the network fiber of the paper forming a stronger composite film. Wet tensile strength results, for all the specimens, show an increase in elasticity but decrease in mechanical strength.

Unlike the dry state, the wet papers show an average 6 % strain followed by necking before rupture. This is understood to be due to the diffusion and plasticizing effect of water molecules in the paper film. The results show that the hydrophobic papers retain

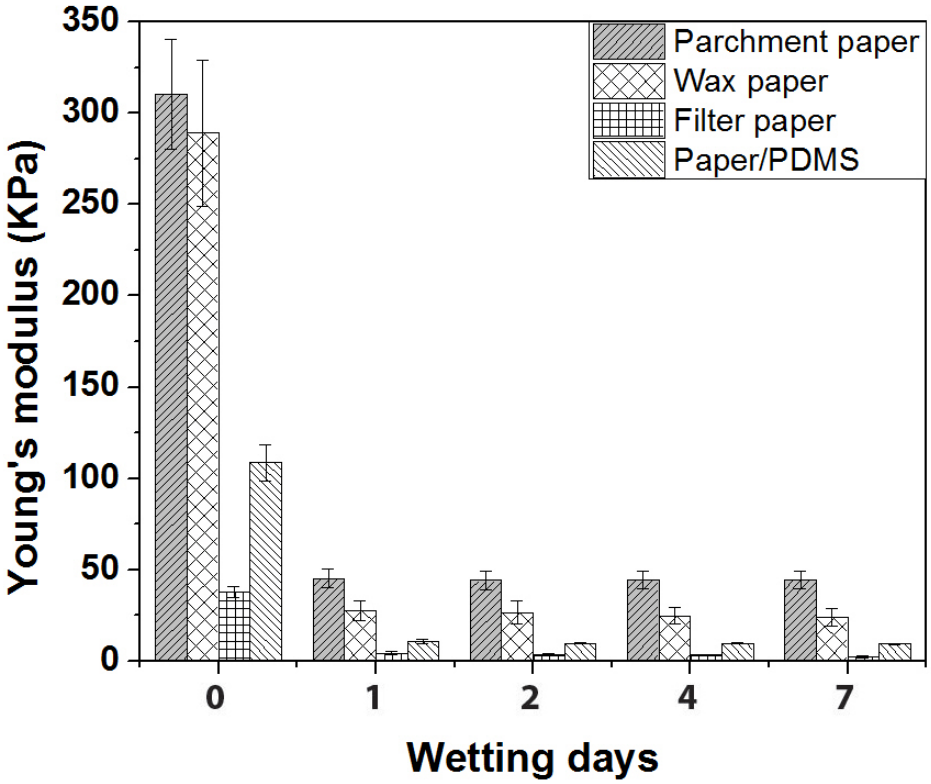

Figure 3.2. Young's modulus of various papers in dry and wet condition. Reproduced from Ref. [90] with permission from The Royal Society of Chemistry.

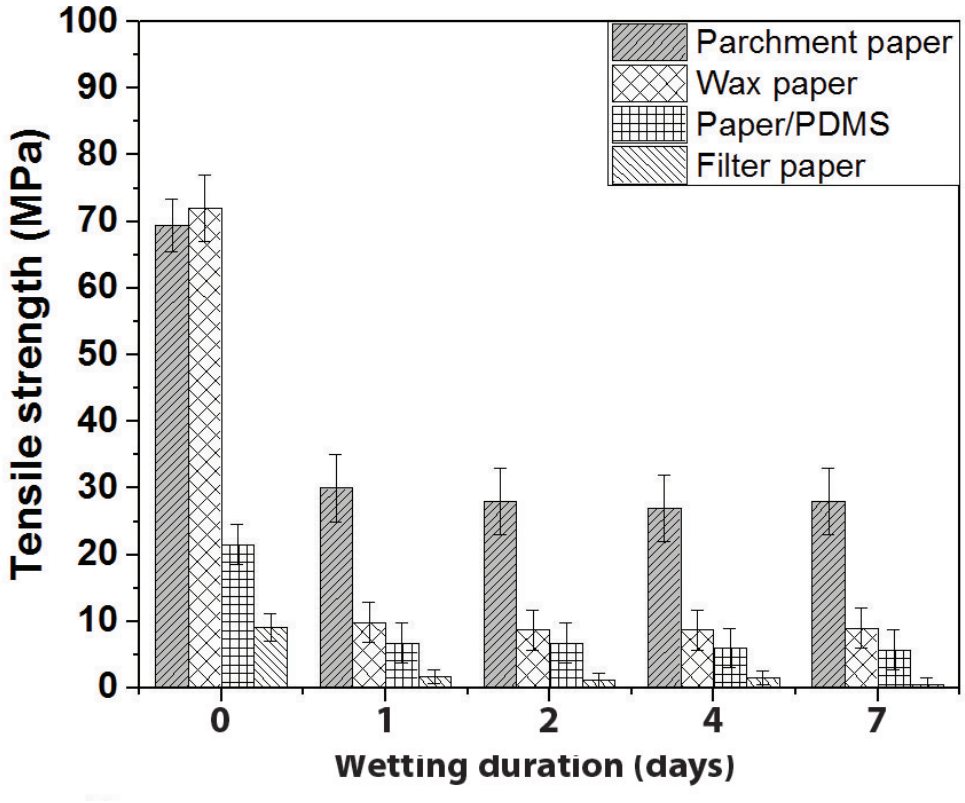

Figure 3.3. Ultimate tensile strength for different papers as a function of wetting duration. Reproduced from Ref. [90] with permission from The Royal Society of Chemistry.

some of their mechanical strength after 24 h submerging in PBS, whereas the filter paper wet UTS drastically decreases to 1.1 MPa and starts to disintegrate in the solution. Among the investigated hydrophobic papers, parchment paper retains more than 40 % of its original dry UTS strength followed by PDMS/paper and wax paper with retentions of 31 % and 14 %, respectively. The parchment paper and wax paper show a stable retention of mechanical strength (UTS) of 29 MPa and 8.9 MPa for 7 days. However, for filter paper and PDMS/paper, a longer wetting duration reduces the mechanical strength (UTS) down to 0.4 MPa and 5.4 MPa, respectively.

3.1.3 Compatibility with other BioMEMS materials/processes

A key requirement for compatibility of parchment paper with other medical devices is the ability to bond securely between common materials. One of the most common materials for medical device prototyping is polydimethylsiloxane (PDMS); this material can be used for microfluidics as is discussed in Chapter 5. Given the superiority of parchment paper with respect to strength, flexibility, and diffusion of oxygen the following tests focused only on parchment paper itself.

To test the bond strength between parchment paper and PDMS, we used a paper-capped PDMS chamber as the test structure. The structure consisted of a 14 mm × 14 mm × 4 mm piece of PDMS with a circular chamber of 8 mm diameter and 2 mm height. The surfaces were treated with air plasma (75 W, 1 min), then brought into contact, and finally allowed to completely cure on a hotplate at 65 °C. For the bond strength tests, the PDMS chamber was bonded to a piece of parchment paper either (1) directly, (2) with a binding layer of partially cured PDMS, or (3) with a binding layer of uncured PDMS. In all cases, both surfaces were treated with air plasma (75 W, 1 min), then brought into contact, and finally allowed to completely cure on a hotplate at 65 °C. The best bonding technique (using partially cured PDMS) was then used to fabricate a test device with the same design for characterizing the gas permeability of the parchment paper (described in the subsection below).

The bond strength of the PDMS-paper interface was measured using the modified test devices, Figure 3.4(a). A stainless steel needle was used for the fluid connection and its perimeter was sealed with silicone adhesive. A syringe pump was used to pump water into the device at a rate of 250 µL/h while the pressure was measured using a digital pressure gauge (DPG4000, OMEGA Engineering Inc.). The pressure immediately before device failure was recorded. A similar setup was used to assess the permeability of parchment paper to air. A syringe pump was used to pump air into a test PDMS-parchment paper device bonded using partially cured PDMS and plasma. The pressure in the chamber

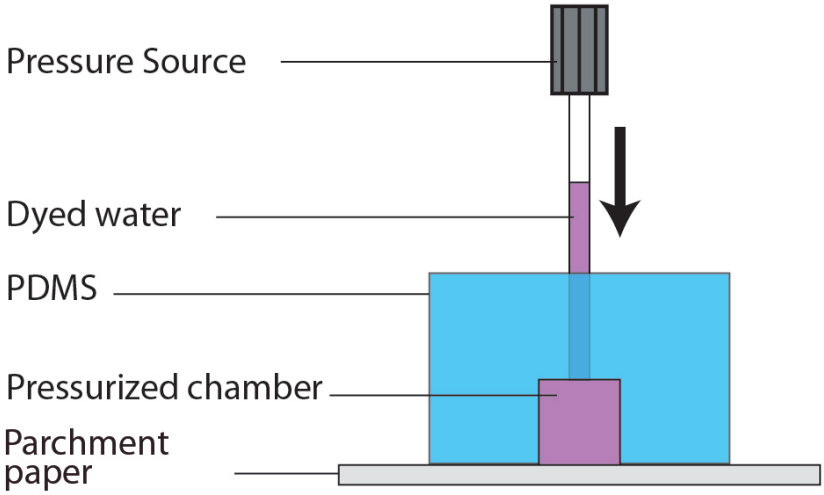

(a) Experimental setup

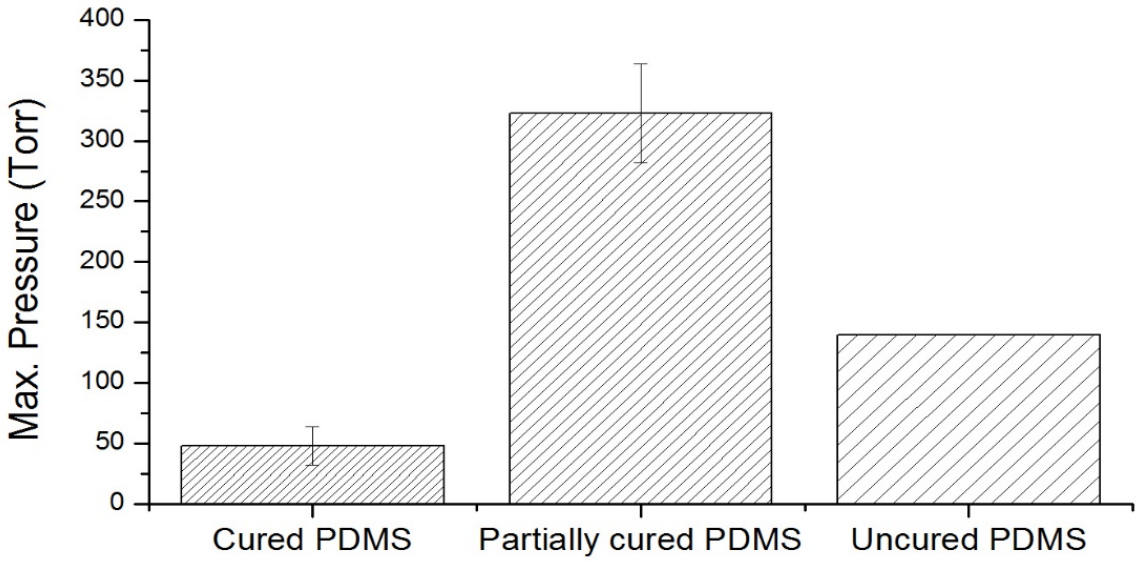

(b) Measured bond strength

Figure 3.4. Strength of bond between parchment paper and PDMS. Reproduced from Ref. [91] with permission from Elsevier.

was measured at various gas flow rates and was used to calculate the permeability of the paper.

The characterization data for the PDMS-parchment paper bond strength is shown in Figure 3.4(b). This test compared the bond strength of parchment paper bonded to PDMS as described in the fabrication section using (1) fully cured PDMS, (2) partially cured PDMS, and (3) uncured PDMS. The results show that a maximum pressure was achieved when bonding the two materials using partially cured PDMS. This method created a bond capable of withstanding up to 323 Torr. During these tests, the parchment paper was also observed to be impermeable to aqueous solutions for pressures below 110 Torr. Hence, the flow of H_2O_2 in the channels was not expected to affect cell cultures on the opposite side of the parchment paper as long as the liquid pressure remained below this level.

3.1.4 Selective permeability of parchment paper to gases over water

In addition to strength, flexibility, and material inter-compatibility, wound dressings should also be permeable to air, in particular oxygen, to allow proper oxygenation of the wound bed during healing. One way to assess the oxygen transport across the paper is to investigate the diffusion of oxygen from the air, into a chamber of water capped with paper. For this, we designed a custom setup to compare the various papers. The setup consists of a cylindrical chamber filled with 20 mL of deoxygenated deionized water and covered by 20 mm-diameter circular sample of the paper. For all tests, the dissolved oxygen is first removed by purging the water for 8 h with nitrogen gas. The oxygen permeability is evaluated with real-time measurements of the dissolved oxygen using an optical oxygen sensor (NeoFox, OceanOptics, Dunedin, FL) positioned in the DI water chamber. All measurements are performed at room temperature and atmospheric pressure. We evaluated the oxygen permeability of different membranes via the rate of dissolved oxygen increase in the water.

Figure 3.5 shows the permeability of dissolved oxygen in a wet environment (setup shown in inset). For all measurements the initial dissolved oxygen of the DI water was close to zero (0.5 ppm) and increased with time up to the oxygen saturation level in the water (8 ppm). The increase was due to the diffusion of the oxygen gas in ambient condi-

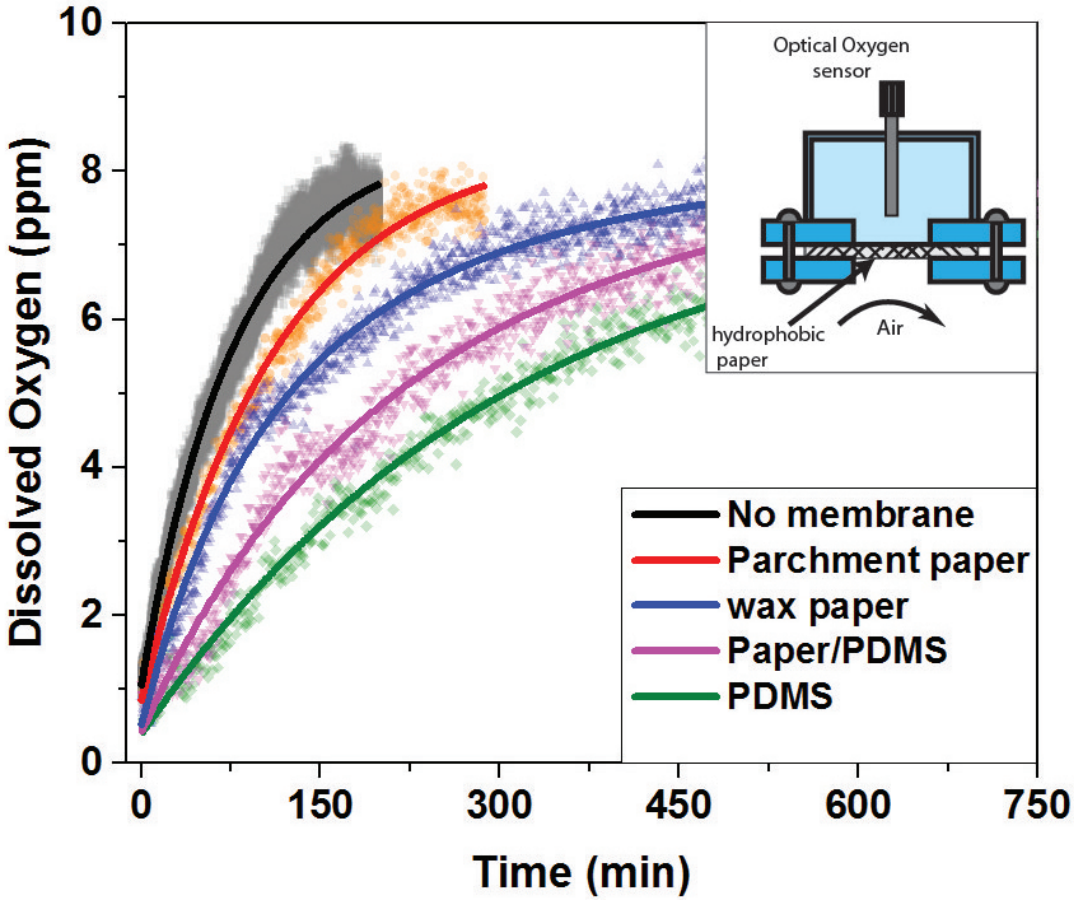

Figure 3.5. Oxygen diffusion of different hydrophobic papers. Reproduced from Ref. [90] with permission from The Royal Society of Chemistry.

tion through the membrane and its dissolution in the water. Without any membrane, the water equilibrates to its steady-state saturation level of about 8 ppm in less than 140 min. However, when the chamber was covered, the time required for oxygen saturation increases. The results showed the longest oxygen equilibration time occurred for a pristine 100 µm membrane of PDMS (720 min). Parchment paper had a larger oxygen permeability (time to saturation of 210 min, with an average rate of 2.4 ppm/h). No signs of water leakage were observed with the hydrophobic films during any of the measurements. The mechanical strength and gas permeability results showed the superior performance of the parchment paper.

The paper was also tested for oxygen generation and permeation. Given the superiority of parchment paper with respect to strength, flexibility, and diffusion of oxygen this test focused only on parchment paper itself. The test structure used for the bonding tests (described above) was used for these experiments. Here, air was pumped into the chamber at various flowrates while the pressure was monitored. Figure 3.6 shows the gas permeability data for parchment paper measured using the test device. The pressure (P) versus gas flow rate (Q) data reveals a slope of 0.014 Torr/μL/min. Since the test devices have a parchment paper area (A) of 50.24 mm^2, the gas permeability (κ) of the paper can be computed to be

$$\kappa = \frac{\Delta Q}{\Delta P} \cdot \frac{1}{A} \approx 1.42\,\mu L/(\text{Torr} \cdot mm^2 \cdot \text{min}) \tag{3.1}$$

For a maximum pressure of 110 Torr (after which aqueous solutions may permeate through the paper), the paper is suitable for oxygen generation rates of up to 3 mL/h with only eleven 200 μm-diameter oxygenation regions. Such regions will be described in the subsequent two chapters and will be used as oxygen generation regions. The results here show that oxygen can penetrate the paper at rates that compare to the oxygen transfer rate of commercial oxygenation (TOT) systems.

3.2 Laser-patterned parchment paper as a dressing substrate

3.2.1 Paper patterning for hydrophilicity or hydrophobicity

Patterning paper to create hydrophilic-hydrophobic structures for microfluidic platforms used in medical diagnostic tests was first demonstrated by Müller and Clegg in 1949 [93]. They created a narrow channel in paper using paraffin which led to faster diffusion with smaller amount of samples. This device consisted of a single channel patterned on filter paper using hot-stamping of paraffin. In 2007, the Whitesides group reinvented the idea of using hydrophobic barriers to create a network of microchannels in paper. In their original work [21], they used SU8-soaked chromatography paper which was subsequently patterned by lithography to create microfluidic channels. Since then,

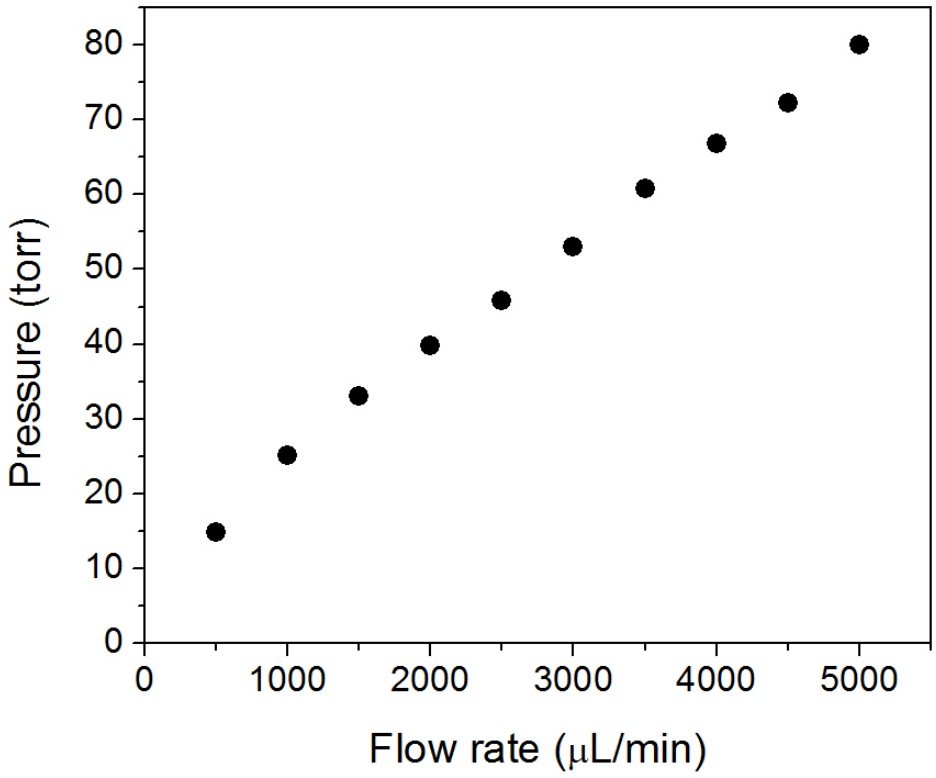

Figure 3.6. The gas permeability of parchment paper was determined from the pressure vs. air flow rate profile. Parchment paper dimensions: A =50.24 mm^2, t =30 μm. Reproduced from Ref. [91] with permission from Elsevier.

many researchers have used SU-8 based lithography, wax-printing, screen-printing, ink-jet printing of chemical, and xerography for paper surface patterning. However, these methods suffer from one or more of the following shortcomings: 1) limited resolution (millimeter scale in wax printing), 2) multi-step processing sequence (wax re-melting is done after printing in order to ensure its complete penetration across the paper thickness), and 3) low mechanical strength of the substrate when submerged in aqueous media for long periods of time. An alternative technique, developed by our group, is laser surface-treatment of commercially available hydrophobic papers (e.g., parchment paper, wax paper, and palette paper) [81]. In contrast with the methods described by the Whitesides group which start with a hydrophilic plain paper and are predominantly additive, our approach is subtractive and can selectively convert hydrophobic areas to hydrophilic ones in a single step process. Since the hydrophobic agent is already present throughout the thickness of the paper, our method does not require heat treatment after patterning to create islands of hydrophilic patterns, as is the case in the wax printing technique. This approach brings several major improvements and allows for the fabrication of more complicated platforms not feasible with other methods. These include: 1) higher resolution, 2) single-step patterning, 3) simultaneous surface processing and micromachining, and 4) greater robustness.

3.2.2 Laser processing of parchment paper

Patterning of paper can be achieved via commercial laser engravers; these systems can rapidly process a broad variety of paper substrates, including parchment paper (Reynolds Parchment Paper, 50 μm thick), wax paper (Reynolds Cut-Rite Wax Paper, 30 μm thick), and palette paper (Canson Palette Paper, 70 μm thick). Among these, parchment paper is particularly well-suited for creating biomedical microdevices due to its robustness and its silicone coating which allows seamless integration with other silicone (e.g., PDMS) devices. To pattern hydrophilic designs onto parchment paper, the paper is placed flat on the cutting surface of a laser engraver while a computer is used to control the laser

parameters to transfer the pattern from a CAD design. The two primary parameters are laser power and beam scanning speed. Increasing the power or lowering the speed imparts higher energy onto the material, resulting in deeper ablation (useful for creating though-paper defects). To avoid completely cutting through the paper (instead of selective surface modification), the laser power and scanning speed must be carefully selected. Commercial laser engraving systems offer satisfactory resolution, control, and processing speed. For the parchment paper selected in our experiments (50 µm-thick silicone coated), the laser source was controlled at 10 % of its maximum power and was operated at a a scanning speed of 35 mm/s. Even for other types of paper, namely wax and palette paper, successful surface treatment is achieved with these parameters.

When parchment paper is laser-machined, its morphology changes, as can be seen in Figure 3.7. This SEM images shows the top view of the paper before and after laser treatment. The image show a clear change in morphology with exposed micro/nano fibers on the surface of the paper after laser treatment. To more clearly observe the morphological changes, one can look at the cross-section of the parchment paper, Figure 3.8. As evident in these images, the thickness of the paper changes as a result of laser treatment. While the initial thickness of the paper is 60 µm, the laser-ablated region was protruded out of the plane by 15 µm over the original surface. This can be attributed to the decomposition/re-deposition of the silicone coating in the paper upon laser exposure, leading to the generation of higher-volume porous micro/nano roughness. Together, the roughness and increased volume of the laser-machined parchment paper produce a sponge-like material into which microparticles can be loaded; this is useful for loading oxygen-generation catalysts, as is described in the following two chapters.

In addition to added roughness, laser treatment of parchment paper also results in increased water contact angle. The surface wettability of parchment paper and other paper types was evaluated by measuring the static contact angle of a 10 µL droplet of DI water before and after laser treatment using an optical contact angle measuring device (Rame-Hart goniometer, model 590). All experiments were conducted five times and the mean contact angle was calculated. Figure 3.9 shows that the contact angle of parchment

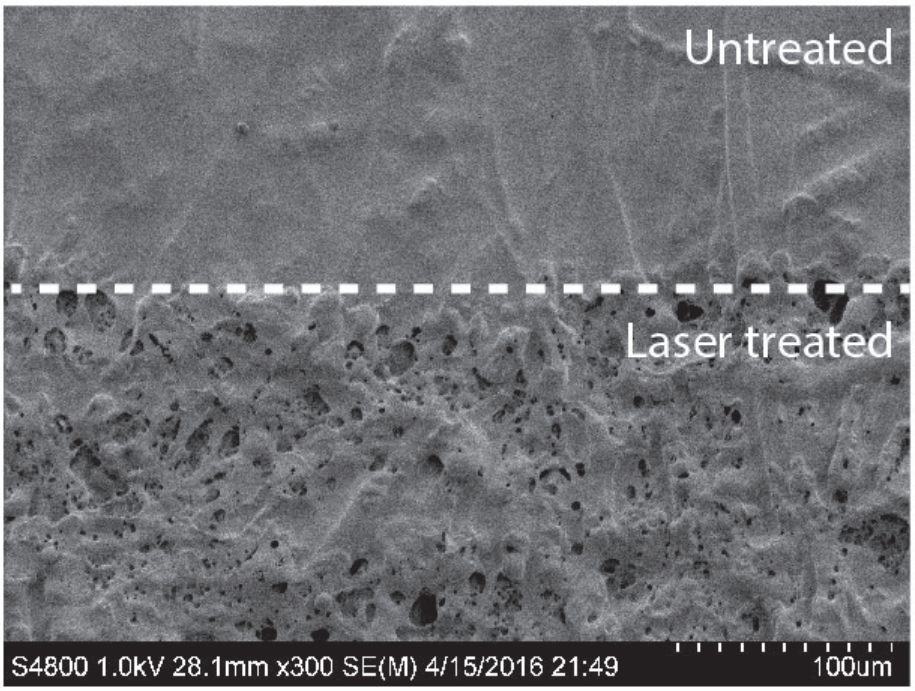

Figure 3.7. Top view of parchment paper before and after laser treatment. Reproduced from Ref. [90] with permission from The Royal Society of Chemistry.

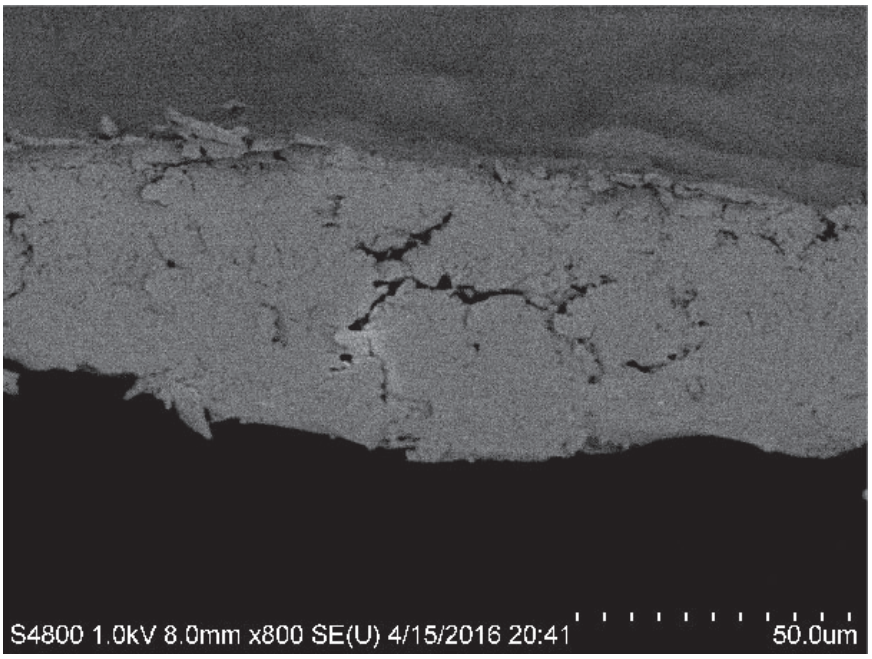

(a) Pristine parchment paper

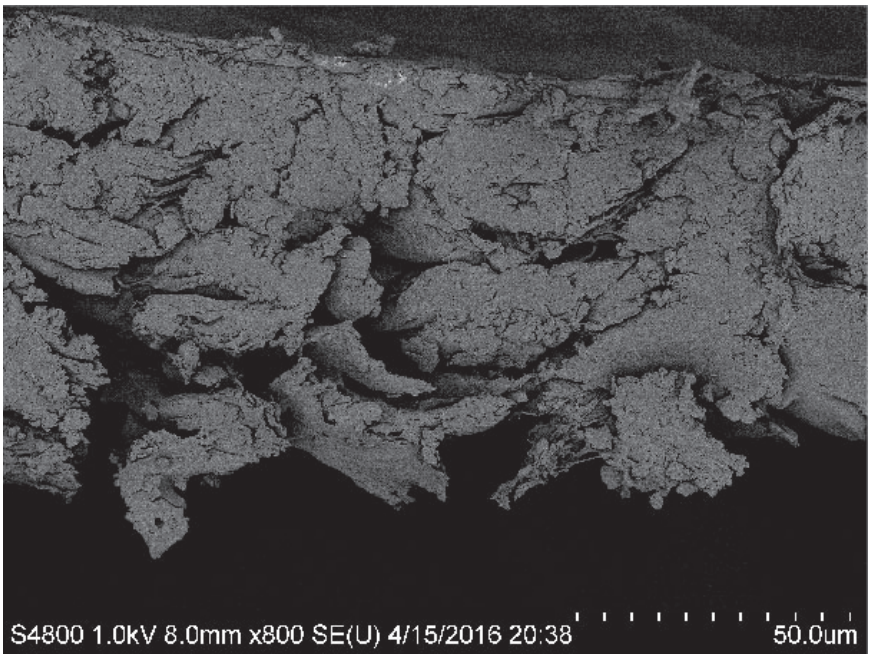

(b) Laser-machined parchment paper

Figure 3.8. Cross-section of parchment paper before and after laser treatment. Reproduced from Ref. [90] with permission from The Royal Society of Chemistry.

paper changes from 121° to 21° as a result of laser treatment. This increase in surface wettability is due to the creation of exposed micro/nano cellulose fibers and addition of hydrophilic −OH, =O groups on the laser-ablated areas. The figure also shows other paper types for comparison. As evident in the figure, parchment paper exhibits the largest change in contact angle, allowing for more clear patterning of the paper.

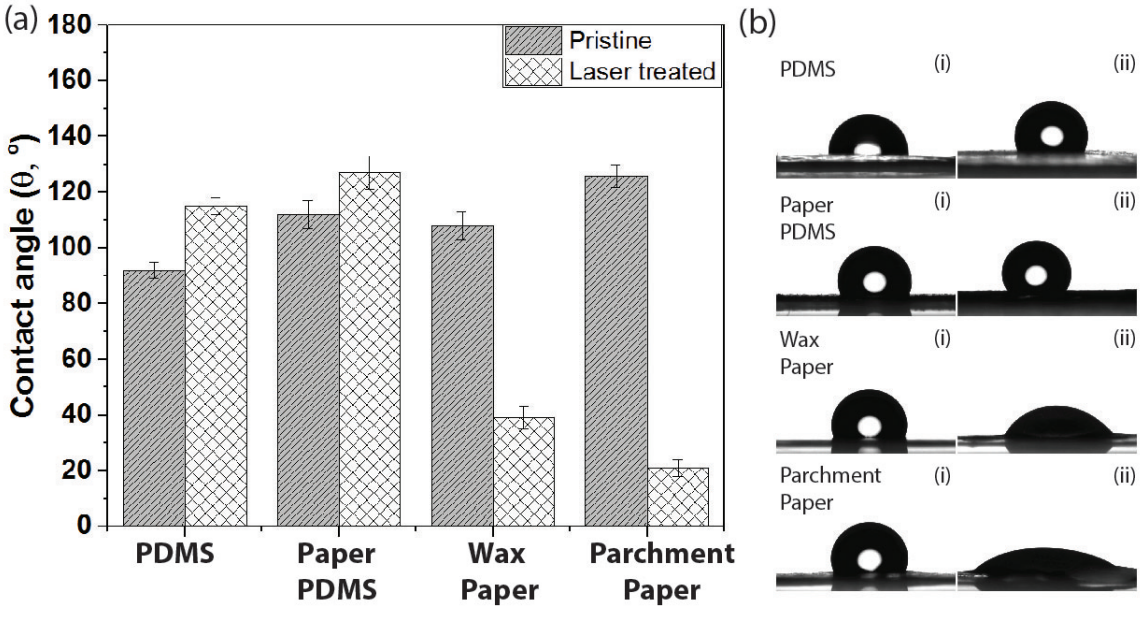

Figure 3.9. Laser treatment of parchment paper results in a decreased water contact angle, from 121° to 21°. The effect of laser on the contact angle of other papers is shown for comparison. Reproduced from Ref. [90] with permission from The Royal Society of Chemistry.

3.2.3 Laser patterning for loading with microparticles

For wound dressing applications, patterning parchment paper allows the rapid creation of hydrophilic traces or regions onto which other materials can be deposited or which can be used for microfluidics. In particular, parchment paper can be loaded with microparticles (e.g., chemical catalysts) for generating oxygen, as is described in the subsequent section. The paper is patterned as described above, and microparticles are

subsequently deposited (e.g., via precipitation) on the hydrophilic regions. Figure 3.10 displays the pattern definition capabilities of the process; the laser-ablated spots are clearly defined and their hydrophilicity allows for precise patterning of the catalyst. The spots have a diameter of 800 µm, but smaller (or larger) custom sizes are possible up to the resolution limit of the laser system (125 µm in our case).

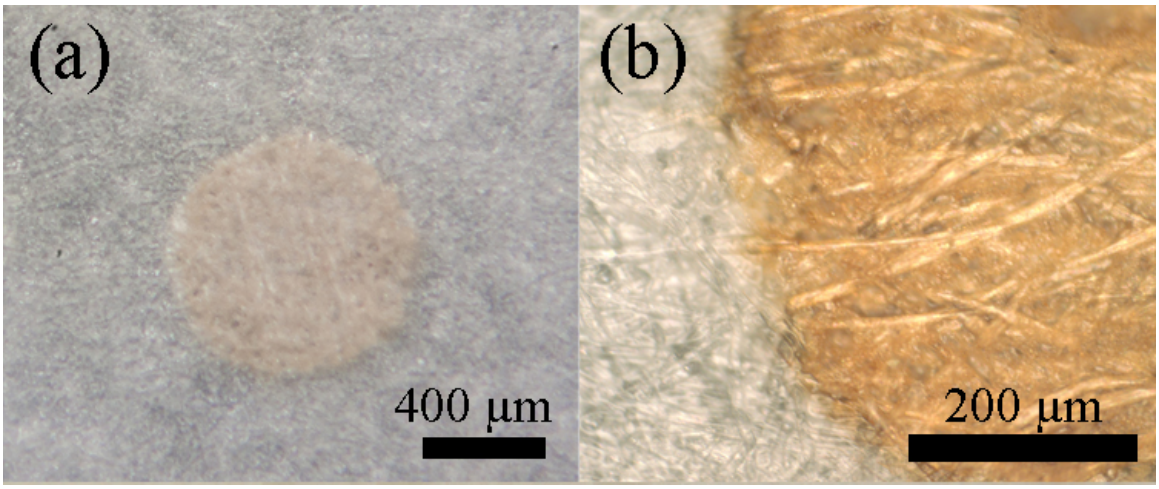

Figure 3.10. Photographs of (a) a catalyst-loaded, laser-patterned disk on parchment paper, and (b) a magnified view of the disk. Reproduced from Ref. [91] with permission from Elsevier.

Magnified views of the catalyst is shown in the SEM images of Figure 3.11. In Figure 3.11a, an aqueous solution of powder MnO_2 was cast on the spot whereas in Figure 3.11b, the same catalyst material was deposited via a chemical reaction of two aqueous reactants (KI, $KMnO_4$). The images show the increased uniformity and smaller particle size achievable with the reaction-deposition approach as opposed to the powder casting method. With the reaction approach, the wicking action of the paper in the catalyst spots absorbs each of the reactants, allowing the catalyst precipitate to be generated within the paper mesh for improved particle entrapment and reduced catalyst washout rate during operation. These images are representative examples of laser-machined parchment paper samples; future work will characterize the repeatability and uniformity of such materials to enable repeatable, reliable production of paper-based wound dressings.

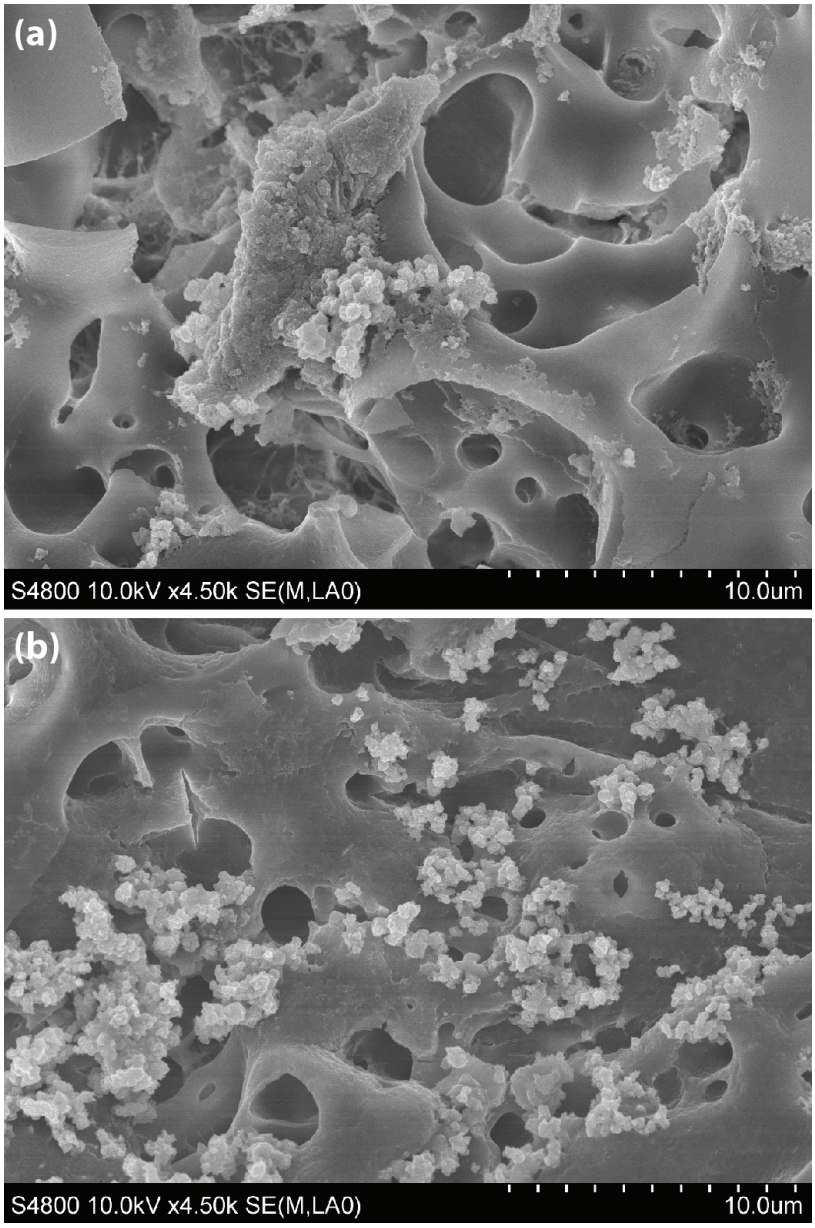

Figure 3.11. SEM images of MnO_2 particles in a laser-ablated spot on parchment paper. (a) Catalyst deposited as an aqueous suspension of MnO_2 particles result in large material clumps on the paper surface. (b) Catalyst deposited by on-spot precipitation via the chemical reaction of two aqueous solutions of KI and $KMnO_4$ results in smaller, more uniformly distributed and entrapped particles. Reproduced from Ref. [91] with permission from Elsevier.

3.2.4 Compatibility with cells

Previous studies have shown that the change in surface wettability with plasma and laser treatment often affects cell growth on different substrates. This method has been widely studied with different cells on various materials such as silk and polymers [94–96]. Here, we investigate the effect on parchment paper since, effective compatibility between parchment paper and mammalian cells is needed if paper is to be used as a medical wound dressing substrate.

For these tests, a pattern of hydrophilic spots was created on parchment paper by laser machining as described above. The laser-treated paper (1.5-cm diameter discs) was placed in 24-well plates and sterilized overnight by exposure to a UV-C lamp. Sterile Teflon rubber rings (od=1.5cm; id=1.2cm) were used to anchor the paper to the well bottom. Adipose stem cells (ASCs) in tissue culture were trypsinized, resuspended and counted with trypan blue. Cells were seeded on each disc at a concentration of 1×10^5 cells/mL and cultured in EGM-2MV for up to 14 days. The medium was replaced every 24 h and the discs were collected over time and stained with eosin phloxine for histological assessment. On day 14, some samples were assessed for the cells differentiation potential. The medium was changed to adipogenic or osteogenic induction medium and after additional culture time discs were processed using Oil Red O or von Kossa stain, respectively.

The results are shown in Figure 3.12. Cells attached preferentially to hydrophilic regions and proliferated over time. The cells remained viable and were induced to differentiate into adipocytes or osteocytes. Thus, laser-treated parchment paper is a suitable matrix for the attachment of ASCs and therefore is suitable for use as a substrate for wound dressings.

3.3 Summary of parchment paper merits

The investigations with parchment paper presented in this chapter reveal that laser-treated parchment paper is ideal as a substrate for advanced wound dressings. In particular, the paper possesses high mechanical strength (> 70 MPa) to withstand human

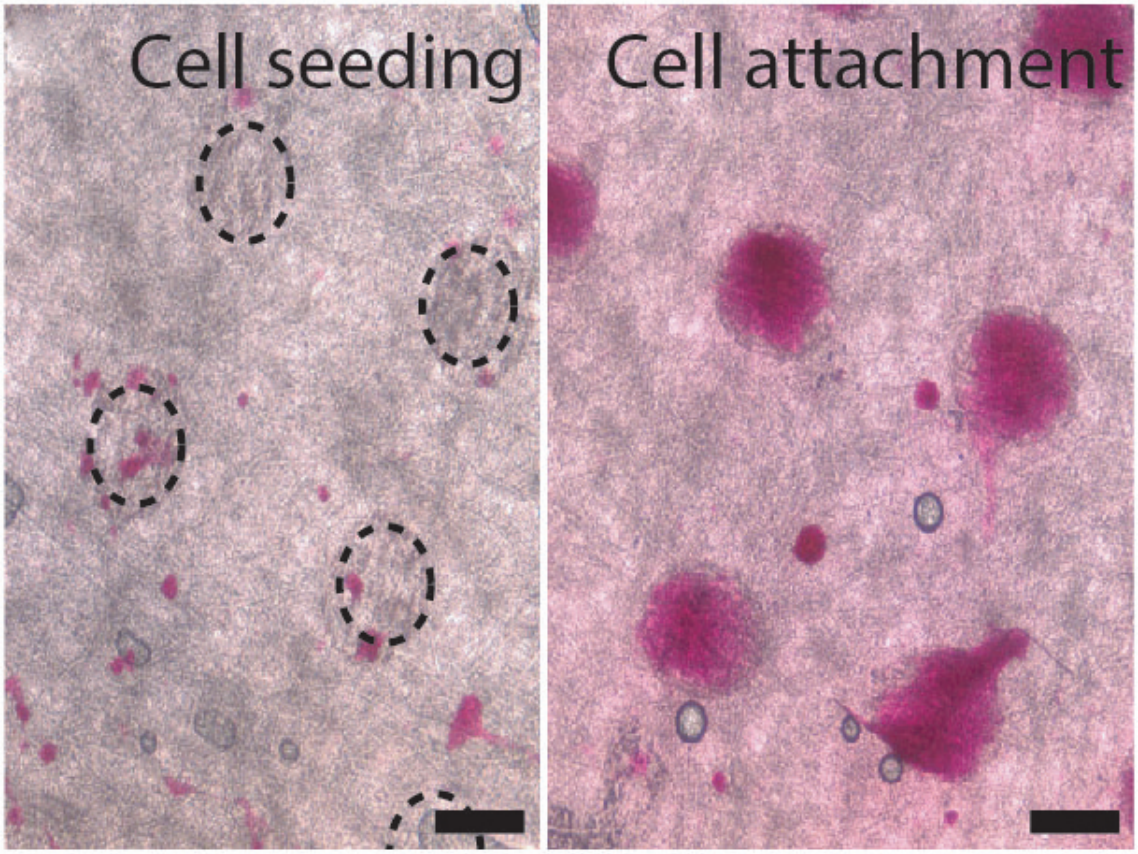

Figure 3.12. Laser-treated parchment paper is shown to be compatible with adipose stem cells. Left: Pristine parchment paper leads to minimal cell adhesion. Left: Laser-rastered parchment paper creates hydrophilic spots onto which cells can attach, allowing patterning of paper with cells. Scale bar: 2 mm. Reproduced from Ref. [90] with permission from The Royal Society of Chemistry.

motion, high elastic modulus when dry (> 300 kPa) for easy handling during fabrication, low elastic modulus (< 50 kPa) when wet for interfacing with similarly soft tissue, permeability to gas and not water at low pressures, and permeable to oxygen diffusion. When laser-rastered, it offers the additional advantages of a roughened surface for deposition of particles (e.g., catalyst for oxygen generation) and a low contact angle (21°) for adsorbing aqueous solutions as well as for promoting attachment of mammalian cells. The laser machining capabilities allow the creation of hydrophilic patterns which can be used as micro oxygen generators for localized oxygenation in wounds, as is described in the following two chapters. It is important to note that laser rastering may change the mechanical properties of the paper (i.e., compared to those shown in Figure 3.3 and Figure 3.2; these variations will be investigated in future work, as described in Chapter 7.

4. PEROXIDE DECOMPOSITION FOR PORTABLE OXYGEN GENERATION

A convenient way to oxygenate wounds is to generate oxygen within the wound dressing. Unlike systems which require a separate (bulky) tank of compressed oxygen gas, on-demand generation allows for smaller, more portable supply of oxygen. Furthermore, generating the oxygen within the wound dressings is particularly attractive, as it eliminates the need for multi-unit wound dressing systems, simplifying the use of the dressings. Using laser-patterned parchment paper as a substrate (as described Chapter 3), appropriate oxygen-producing chemicals can be deposited on the paper selectively to generate oxygen in specific regions of the wound. This chapter presents a practical technique for depositing such chemicals, and discusses the merits of a particular combination for wound healing applications.

4.1 Materials for oxygen generation

Oxygen generation can be achieved by various methods, including via electrolysis and by a a myriad of chemical reactions. Electrolysis is advantageous in settings where electronics and abundant electrical power are readily available; such is the case in many large-scale applications, but for (non-electronic) wound dressings, an alternative method is more favorable. As a result, chemical reactions are a more practical approach when generating oxygen in a wound dressing. These reactions rely on the catalytic decomposition of an oxygen-containing substance. The advantage of such catalytic reactions is that they allow extended operation with only a small amount of the catalyst loaded onto it (as long as the consumable material is abundant or replaced).

Catalytic reactions for oxygen production typically involve the decomposition of peroxides or superoxides, whose general chemical formulas can be expressed as M_2O_2 and

MO_2, respectively (M is a variable representing a metal). An economical and broadly available option is the use of hydrogen peroxide, since it is readily available in the medical environment at safe-to-use concentrations (3 %; 1 mL of this produces 11.4 mL of O_2 at 37 °C). Hydrogen peroxide is a commonly used consumable due to its clean decomposition into oxygen and water by well-known materials. This feature allows it to be safely injected into aqueous systems without risk of producing unwanted contaminants. Hydrogen peroxide can be catalyzed by many transition metals and their compounds to produce oxygen via the following below.

$$2H_2O_2 \rightarrow 2H_2O + O_2 \tag{4.1}$$

Of the various catalyst materials available, manganese dioxide stands out as a convenient option. Manganese dioxide micro-particles are biocompatible and catalyzes hydrogen peroxide cleanly while possessing the additional advantages of being economical, simple to synthesize, and commercially available. Additionally, the catalyst can be synthesized via a precipitation reaction ($KI + KMnO_4$ reacted as aqueous solutions) without requiring complex fabrication techniques. This process also allows facile deposition of the catalyst on various substrates via standard commercial manufacturing techniques (e.g., gravure, printing, inkjet printing, dip coating) by processing each of the two reactants sequentially. In the context of wound dressings, the ability to precipitate the catalyst in place allows for deposition of the catalyst within the fibers of the wound dressing; in particular, the catalyst can be easily printed on laser-machined parchment paper, (as is described in Chapter 5) to create paper-based oxygenation wound dressings. Furthermore, it is possible to pre-treat the catalyst particles to achieve nano-scale surface features for enhanced catalytic activity while retaining its overall micro-scale (i.e., safe) size. The following experiments examine the production of oxygen by hydrogen peroxide decomposition using two sizes of particles which can be used for oxygenation wound dressing applications.

4.2 Characterization of manganese dioxide and hydrogen peroxide for cutaneous oxygenation

4.2.1 Experimental approach

MnO_2 microparticles (150 µm diameter) were obtained from Sigma-Aldrich and used as received. Smaller MnO_2 particles (20 µm diameter) were synthesized by reacting 5 mL 0.1 N $KMnO_4$ with 5 mL of 0.1 N KI. Precipitates were collected by centrifugation and rinsed with deionized (DI) water three times to remove impurities. The particles were then dried in a nitrogen gas environment and maintained in an inert environment until just prior to usage.

The catalytic activity of the catalyst particles was investigated in bulk. For this, 20 mg of the large-size catalyst powder was mixed in a flask with 10 mL of 30 % H_2O_2 and immediately connected to a standard trough setup for collection of generated gas. The volume of generated gas was measured over time by time-lapse photography; the generation rate of oxygen generation was subsequently calculated from the photographs. This experiment was repeated for the small-size particles (same mass of catalyst and peroxide concentration). The particle morphology of the catalyst was also investigated by imaging via scanning electron microscopy (SEM) before and after the catalytic activity experiments. The particle size of both catalyst samples was also analyzed from the SEM images using optical granulometry software (ImageJ plugin).

4.2.2 Results and discussion

The electron microscopy investigations on particle size are presented in Figure 4.1, with the large particles shown in Figure 4.1(a) and the smaller ones in Figure 4.1(b). The particle size distribution (Figure 4.1(c-d)) reveal a median diameter of 158 µm for the larger particles and 19 µm for the smaller ones. Both types of particles are well in the micrometer regime and should not pose any nano-scale-related threats to biocompatibility. A close-up inspection (insets) reveals more details about the surface morphology

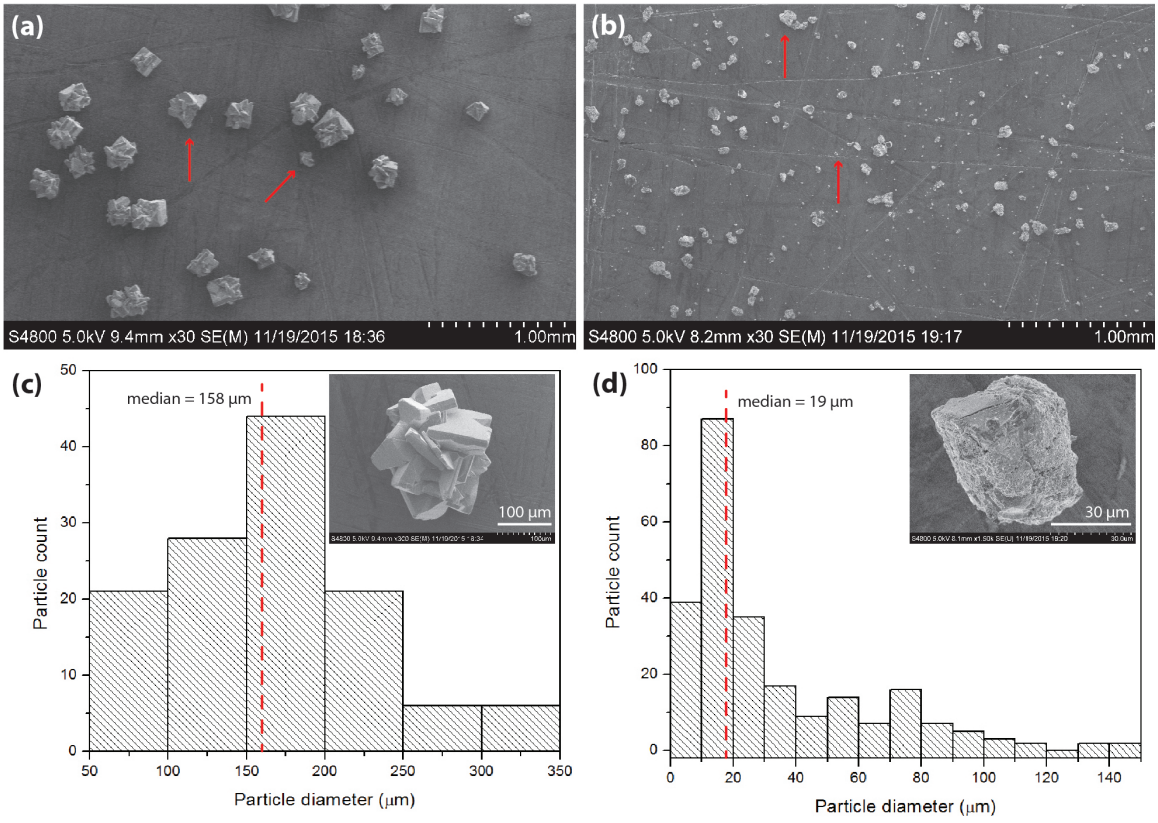

Figure 4.1. SEM of (a) large and (b) small micro-particles of MnO2. Particle size distribution for (c) large and (d) small particles.

of each group; in particular, the larger particles comprise smooth plates, whereas the smaller ones exhibit fewer macro-structures but increase surface roughness. The higher roughness in the smaller ones can be expected to contribute significantly to the catalytic activity.

The characterization experiments for the catalyst reveal a drastic change in catalytic activity between the two particle sizes. The catalytic activity can be interpreted as the rate of oxygen generation in a given solution of H_2O_2. Figure 4.2a shows the normalized gas generation (µL O_2 per minute per µg of MnO_2) for both particles during 20 minutes of immersion in the 30 % H_2O_2 solution. The data show up to an eight-fold increase in rate for the smaller ones, compared to the larger ones. Such large difference for the same

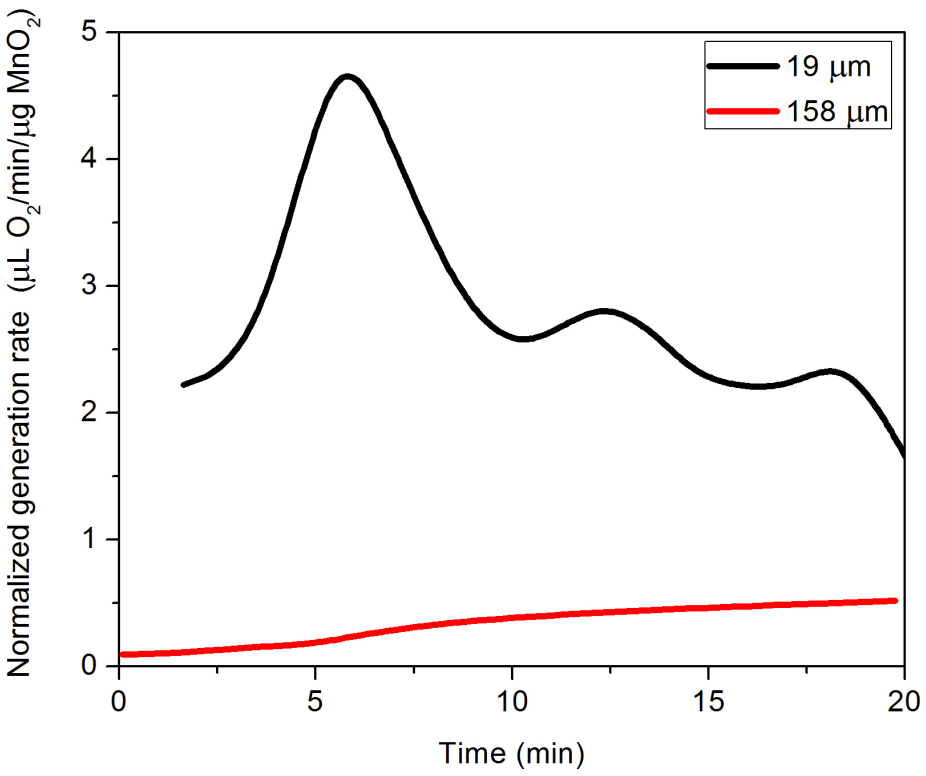

Figure 4.2. Oxygen generation rate increases over time when immersed in H_2O_2. The rate is up to 8 times higher for the smaller particles compared to the larger ones.

mass is expected, since the smaller particles have a much higher surface area available for catalyzing the H_2O_2. Additionally, by the 6 minutes mark, the rate of oxygen generation for the small particles reaches at peak value which is 2.3 times its initial rate, whereas the rate of large particles continues to increase monotonically, reaching nearly 6 times its original rate by the 20 minute mark, Figure 4.3. Thus, in this sense, the smaller particles offer a more stable rate of generation of oxygen, compared to the larger ones.

It is interesting to note that the larger particles experience a larger net percent change in rate than the smaller one. These two effects (the absolute increase in rate for both and the difference in change for each) can be understood by examining the particles

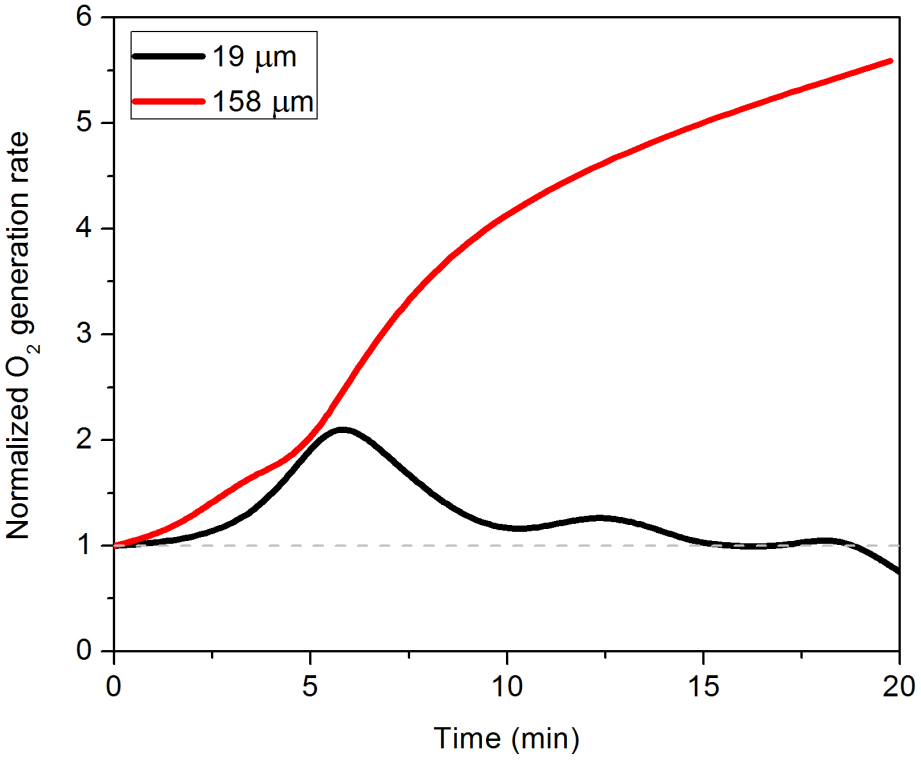

Figure 4.3. Normalized oxygen generation rate of the two particle sizes with respect to the initial rate of each. The smaller particles show less fluctuation in rate (i.e., more stable oxygen generation).

by scanning electron microscopy (SEM). Figure 4.4(a-b) are SEM images of the larger particles (a) before and (b) after exposure to H_2O_2 for 20 minutes. Figure 4.4(c-d) are SEM images of the smaller particles (c) before and (d) after the same exposure. In both cases, the particles achieve a remarkably rough surface (i.e., higher overall surface area) as a result of H_2O_2 exposure. This increase in surface area explains the higher catalytic activity for both [97]. The images also show that the final degree of roughness in both of the exposed particles is approximately equal; as a result, the change in surface is much more drastic for the large particles (which were originally smoother) than for the smaller ones (which started off with a large surface area), leading to a larger change in catalytic activity for the large ones, compared to the small ones. These effects and catalytic rates provide a means for tuning the oxygenation activity during the design phase of wound dressings.

4.3 Summary of wound oxygenation via catalysis of hydrogen peroxide

From the point of view of oxygenation in wound dressings, the use of manganese dioxide and hydrogen peroxide provides a low-cost catalyst-peroxide combination with fast, tunable oxygenation rate. For the 19 µm particles of manganese dioxide investigated here, the maximum generation rate can be converted to 0.27 mL/h/µg MnO_2, assuming 30 % H_2O_2, or 0.027 mL/h/µg MnO_2, assuming 3 % H_2O_2. This generation rate is relevant to wound healing when compared to the oxygen rate which has been shown to improve healing in a rabbit ear wound (0.3 µL O_2/min/mm^2, or equivalently 3 mL O_2/min for a 10 cm × 10 cm area) and to the similar oxygen generation rate of a commercial product (EPIFLO, 3 mL O_2/min, Chapter 2). Based on the results from this chapter, such oxygen generation rates are possible by using no more than 111 µg of the catalyst on a 10 cm × 10 cm area. The rate, of course, can be increased with higher amount of catalyst and can be tuned by the concentration of the hydrogen peroxide. Nevertheless, the rate characteristics measured here identify MnO_2 as a suitable catalyst from the point of view of deposition (via diluted solutions of the reactants) and wound healing requirements.

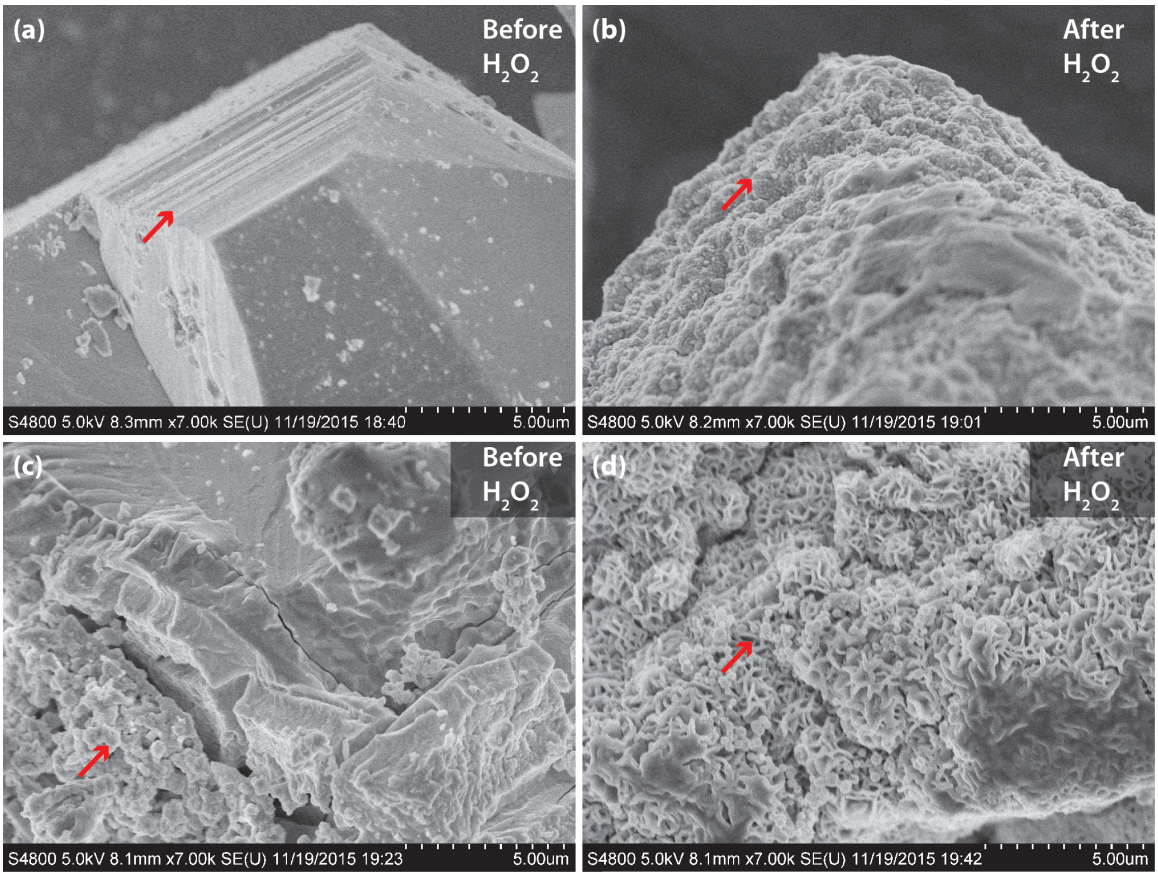

Figure 4.4. Large micro-particles (158 µm) of MnO_2 (a) before and (b) after exposure to H_2O_2. Small micro-particles (19 µm) of MnO_2 (c) before and (d) after exposure to H_2O_2. Both cases reveal increased surface roughness.

5. A PAPER PLATFORM FOR WOUND DRESSINGS WITH SELECTIVE OXYGENATION

This chapter combines the parchment paper from Chapter 3 and the oxygenation reaction from Chapter 4 into a low-cost wound dressing platform for continuous O_2 delivery. Portions of this chapter are taken from [91].

The paper-based oxygenation platform consists of an inexpensive, paper-based, biocompatible, flexible platform for locally generating and delivering oxygen to selected hypoxic regions. It takes advantage of recent developments in the fabrication of flexible microsystems including the incorporation of paper as a substrate [19–22] and the use of inexpensive laser machining [23–25]. As described in Chapter 3, the use of parchment paper simultaneously provides structural flexibility as well as selective filtering functionality, i.e., it allows for oxygen to pass through while preventing aqueous solutions to reach the tissue. The laser machining enables the precise definition of oxygen generating regions that match the hypoxic wound profile. Together these two technologies enable the development of a low-cost patch/wound-dressing with customized, wound-specific oxygen generating regions, ideal for the treatment of chronic wounds with heterogeneous oxygenation.

5.1 Platform design

The platform consists of a flexible microfluidic network bonded to a parchment paper substrate, as illustrated in Figure 5.1. A key feature is the use of laser-patterned parchment paper as the primary structural/functional material. Parchment paper is a hydrophobic material by design; however, it can be ablated using a CO_2 laser to create hydrophilic regions [81]. This technique is applied to define an array of hydrophilic spots. The natural mesh structure of paper allows the spots to be embedded with chemicals suspended in

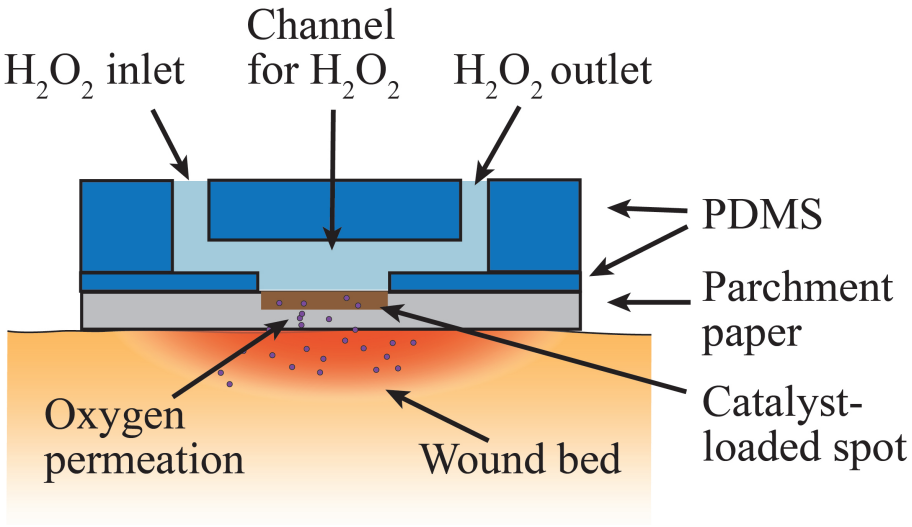

Figure 5.1. Cross-sectional illustration of platform at a single catalyst-loaded pad. Reproduced from Ref. [91] with permission from Elsevier.

an aqueous solution. For the present application, the spots are loaded with a chemical catalyst, MnO_2. When H_2O_2 is injected through the microchannel network, it reaches the spot array, and is decomposed by the catalyst, resulting in oxygen generation [98–100] as described by Equation 5.1.

$$2\,H_2O_2 \rightarrow 2\,H_2O + O_2 \tag{5.1}$$

The generated O_2 diffuses through the paper and oxygenates the wound bed below for as long as H_2O_2 flows in the microchannel. The use of biocompatible structural material allows the platform to be integrated into commercial wound dressings that are in contact with the wound bed.

5.2 Experimental

5.2.1 Platform fabrication

The fabrication process of the oxygen generating platform is shown in Figure 5.2. It consists of laser-defined patterns on parchment paper, creating microchannels on a PDMS substrate, and bonding the layers together. The entire procedure is straightforward and requires no complex cleanroom processing. First, the catalyst pattern is laser-ablated onto a parchment paper substrate (30 µm thick). The paper is then dipped (1 s) into a 0.1 N $KMnO_4$ aqueous solution followed by a dip (1 s) in a 0.1 N KI aqueous solution. This results in the deposition of $KMnO_4$ and KI only onto the ablated pattern. The two reactants yield MnO_2 via the following reaction

$$KI(aq) + 2\,KMnO_4(aq) + H_2O(l) \rightarrow KIO_3(aq) + 2\,KOH(aq) + MnO_2(s) \tag{5.2}$$

Next a 200 µm layer of PDMS (polydimethyl siloxane, Dow Corning Sylgard 184) is spin coated on a silanized silicon wafer and cured on a hotplate (100 °C, 20 min). The PDMS is transferred onto an acrylic substrate and laser-machined to create through-hole regions with the same pattern as the catalyst. The patterned PDMS is exposed to air plasma (75 W, 1 min) in a plasma etcher (PLASMOD, Tegal Corporation, Richmond, CA), stamped onto uncured PDMS, and partially cured on a hotplate (65 °C, 5 min). Next, the PDMS is bonded to the patterned parchment paper by plasma-treating both materials and bringing them in contact. Finally, 150 µm-deep microchannels are fabricated in PDMS by casting onto a laser-machined acrylic mold and bonding it to the parchment paper structure using plasma surface treatment.

5.2.2 Characterization setups

A syringe pump was used to drive H_2O_2 through the device to induce oxygen generation at the catalyst-loaded spots. A fiber-optic oxygen measurement system (NeoFox, OceanOptics, Dunedin, FL) was used to measure the oxygen concentration on the

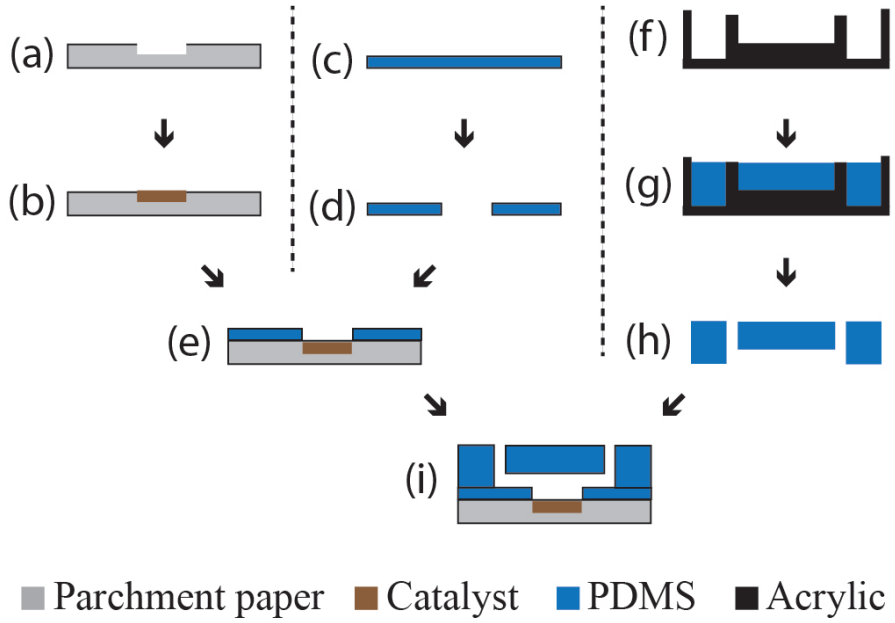

Figure 5.2. Fabrication procedure (a) laser-pattern parchment paper, (b) deposit catalyst, (c-d) laser-pattern 200 µm-thick PDMS, (e) bond paper to PDMS by stamping partially-cured PDMS, (f-h) mold PDMS microchannels, (i) bond with plasma to paper structure. Reproduced from Ref. [91] with permission from Elsevier.

opposite side of the parchment paper, recording the oxygen level at catalyst-free and catalyst-loaded regions. The oxygen level at a single spot was also monitored for 30 h to determine the long-term generation rate. The transport kinetics of the generated oxygen was explored to determine the maximum peroxide flow rate that would permit accurate delivery of oxygen at its generation location. Oxygen generated at a spot must remain at the spot for sufficient time to allow its permeation across the parchment paper; thus, if the peroxide flow rate is too high, the generated oxygen will be transported downstream and may permeate the parchment paper at an unintended location. The effect of the liquid flow rate was determined by measuring the oxygen level (using the same fiber-optic system mentioned above) across the parchment paper at various distances from the point of generation under different flow rates.

To evaluate the ability to increase the oxygen concentration in the wound bed, the oxygenation platform was tested on a surrogate wound bed, a sample of 0.3 % agarose gel was used. An acrylic chamber with open top was assembled to hold the agarose gel sample, Figure 5.3(a). The chamber includes an array of 2 mm holes on one side wall to allow insertion of an oxygen probe. Prior to testing, 0.3 % agarose gel is prepared prepared and stored in a hypoxic environment until ready for use. During testing, the agarose gel is placed in the chamber. An oxygenation platform with a single 800 µm-diameter catalyst spot (deposited as described above) is loaded with 50 µL of H_2O_2 in the PDMS microfluidics. The platform is placed on top (in contact with) of the gel. The test chamber is then sealed with Parafilm barrier to prevent significant oxygenation form the atmosphere. The same oxygen probe described above is then inserted into a hole of the test chamber, penetrating the gel until the tip is positioned 3 mm directly below the catalyst spot of the paper, Figure 5.3(b). For this test, however, the probe is covered with a protector needle to prevent mechanical damages to the probe during insertion. The remaining holes in the chamber are sealed with adhesive tape to prevent oxygen diffusion from the atmosphere. The oxygen concentration in the gel is monitored over time.

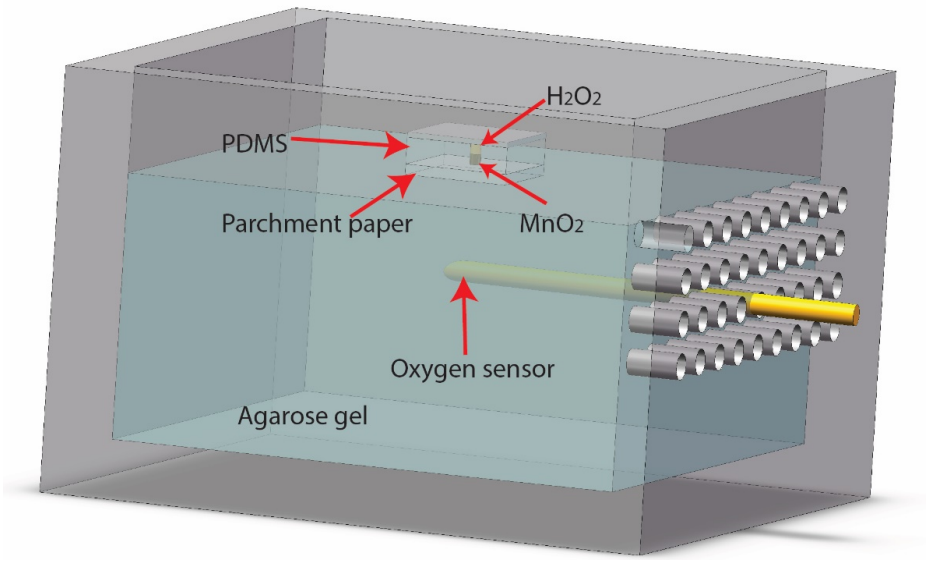

(a) Illustration of test setup

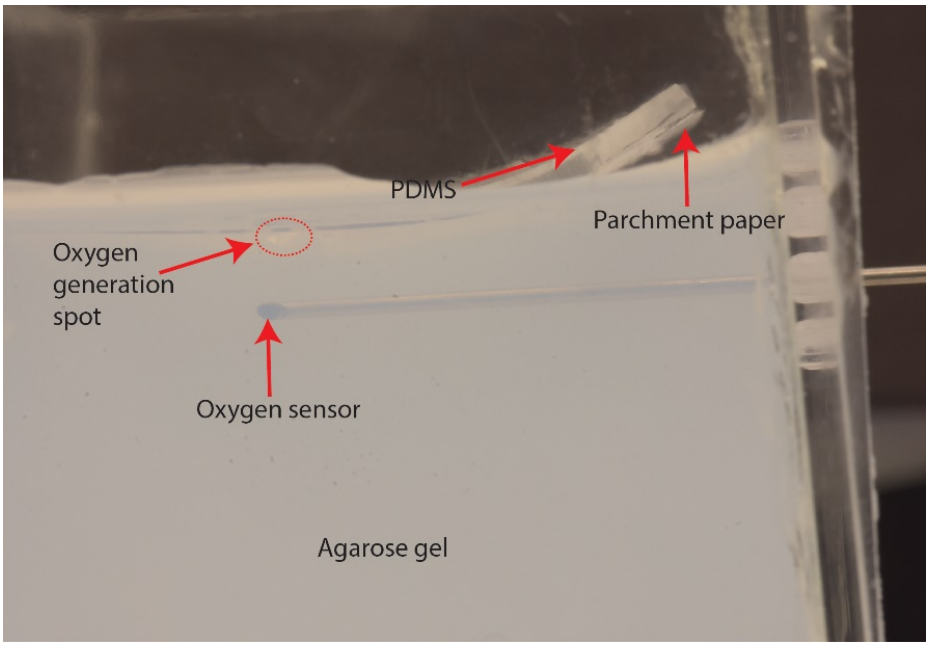

(b) Photograph during tests

Figure 5.3. Test setup for measuring oxygen diffusion into agarose gel.

In clinical applications, the oxygenation platform is expected to have an interfacial material between the parchment paper and the wound to create intimate contact with the wound bed. To simulate this, we repeated the above experiment with a commercial dermal regeneration matrix (Integra, Integra Life Sciences Corp.) as the interface. Integra wound matrix is 900 μm thick and is composed of cross-linked bovine tendon collagen and glycosaminoglycan that is indicated for the treatment of acute and chronic wounds, including diabetic skin ulcers. A 1 cm × 1 cm sample of Integra was cut with a razor blade and sandwiched between the oxygenation platform and the agarose gel. The rest of the experiment This experiment proceeded as above. As a control experiment, this test was repeated with empty microfluidics (i.e., no H_2O_2).

To determine the cytotoxicity of parchment paper, 3T3 fibroblast cells with a cell density of 10×10^4 cells/sample were seeded on the surface of the parchment paper. Since the surface of the parchment paper is hydrophobic, a short (1 min) plasma treatment was applied before the cell seeding process. Cells with the same density were seeded onto the parchment paper with catalyst, parchment paper without catalyst, and a standard well plate (as a control). After 6 hours, alamar blue assays were carried out to determine the cytotoxicity of the samples. High concentrations of H_2O_2 are known to be toxic to cells [101]; hence, separation of H_2O_2 flow from the cell-seeded region needed to be verified. Assembled PDMS-parchment paper devices were modified to include an additional 200 μm layer of PDMS bonded to the exposed parchment paper. This layer contained through-holes to form wells around the catalyst-loaded parchment paper regions. The wells were used both to contain and culture the cells, as well as to insure that the cells remained aligned on top of the oxygen-releasing spots throughout the experiment. In this experiment, the devices were first treated with plasma. Then 3T3 fibroblast cells with a density of 5×10^4 cells/sample were seeded on the surface of the devices. Next, a 3 % of H_2O_2 solution at a flow rate of 250 μL/h was introduced through the channels for 15 hours. After 15 hours of culture time, alamar blue assays were performed to measure cell proliferation. As a control group, we used some devices without any H_2O_2 flow.

5.3 Results and discussion of the platform performance

The photograph in Figure 5.4 show a fabricated oxygen generation device with four spots loaded with MnO_2, even though the accompanying microfluidic network can support eight spots. Hence, different wound-customized oxygen generating patches can be easily created by simply altering the spot pattern on the paper without requiring modifications of the microfluidics.

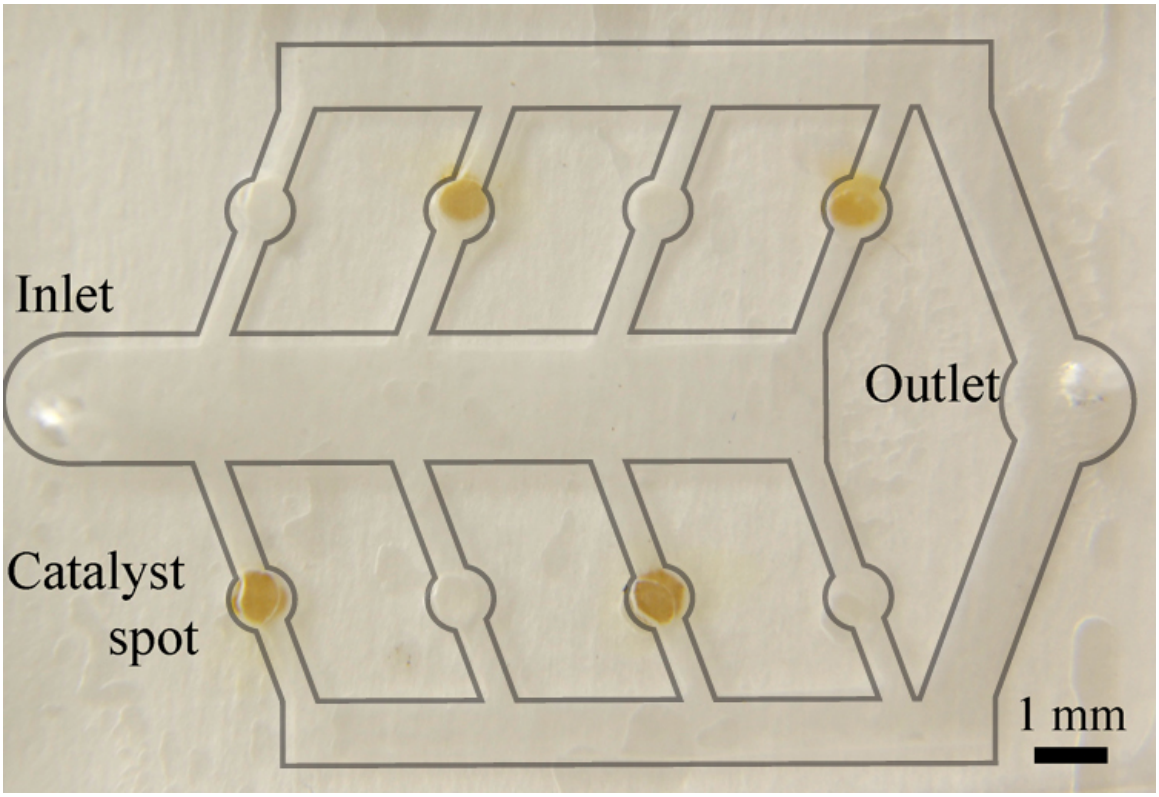

Figure 5.4. Top view of a completed device with only four patterned disks (channels are 150 µm thick; overall device thickness is 1.5 mm). Reproduced from Ref. [91] with permission from Elsevier.

The ability to increase the oxygen level across parchment paper was confirmed with direct oxygen measurements using an optical oxygen sensor positioned 1 mm above the paper surface. An increase of oxygen concentration from 20.9 % to 25.6 % was observed on the exposed side of the paper for regions with catalyst (Figure 5.5). Long-

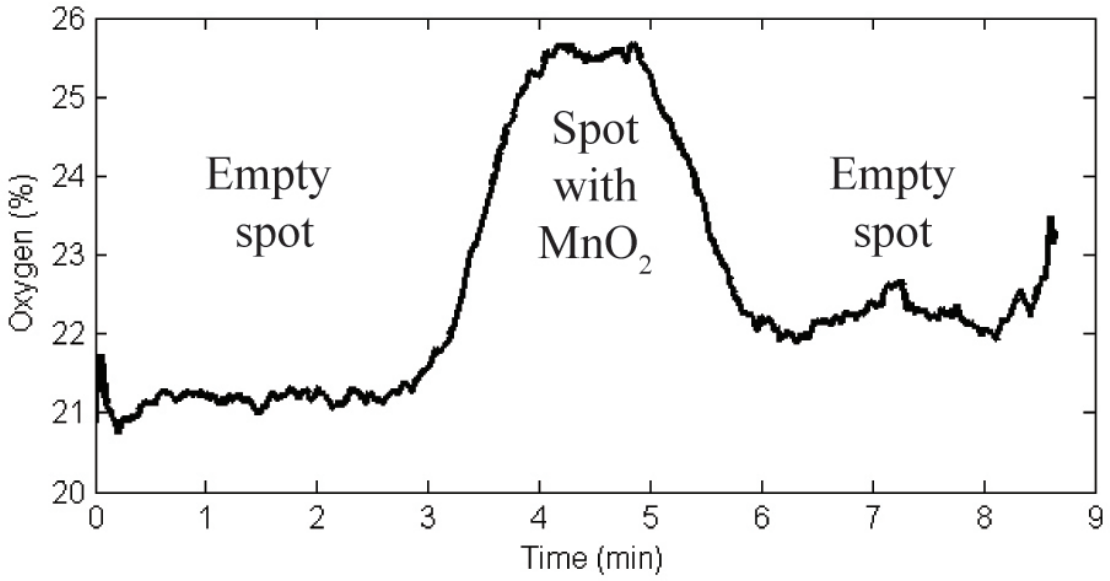

Figure 5.5. Oxygen level across parchment paper as a function of the distance from the generation location using various hydrogen peroxide flow rates. Oxygen delivery accuracy is optimum for H_2O_2 flow rates of 360 µL/h or lower. Reproduced from Ref. [91] with permission from Elsevier.

term (30 h) measurements of continuous oxygen generation revealed a constant oxygen generation rate of 0.1 µL O_2/min/mm^2 (Figure 5.6). A comparable level of oxygenation (0.3 µL O_2/min/mm^2) has been previously shown to effectively promote epithelial healing in a rabbit ear wound model [40]. Thus, our platform can generate oxygen at a sufficiently high rate to alter the oxygen level in the microenvironment of a wound and improve wound healing. Although the platform may require regular replacement (with an optionally updated catalyst pattern) throughout the duration of therapy, its replacement schedule (no more than once per day) is no more burdensome than common wound dressings. The rate of oxygenation can be further controlled by varying the amount of catalyst deposited on the spots and/or the flow rate and concentration of H_2O_2.

The results from the diffusion experiments into agarose gel are presented in Figure 5.7. For the case without Integra, the blue curve shows a monotonically-increasing oxygen

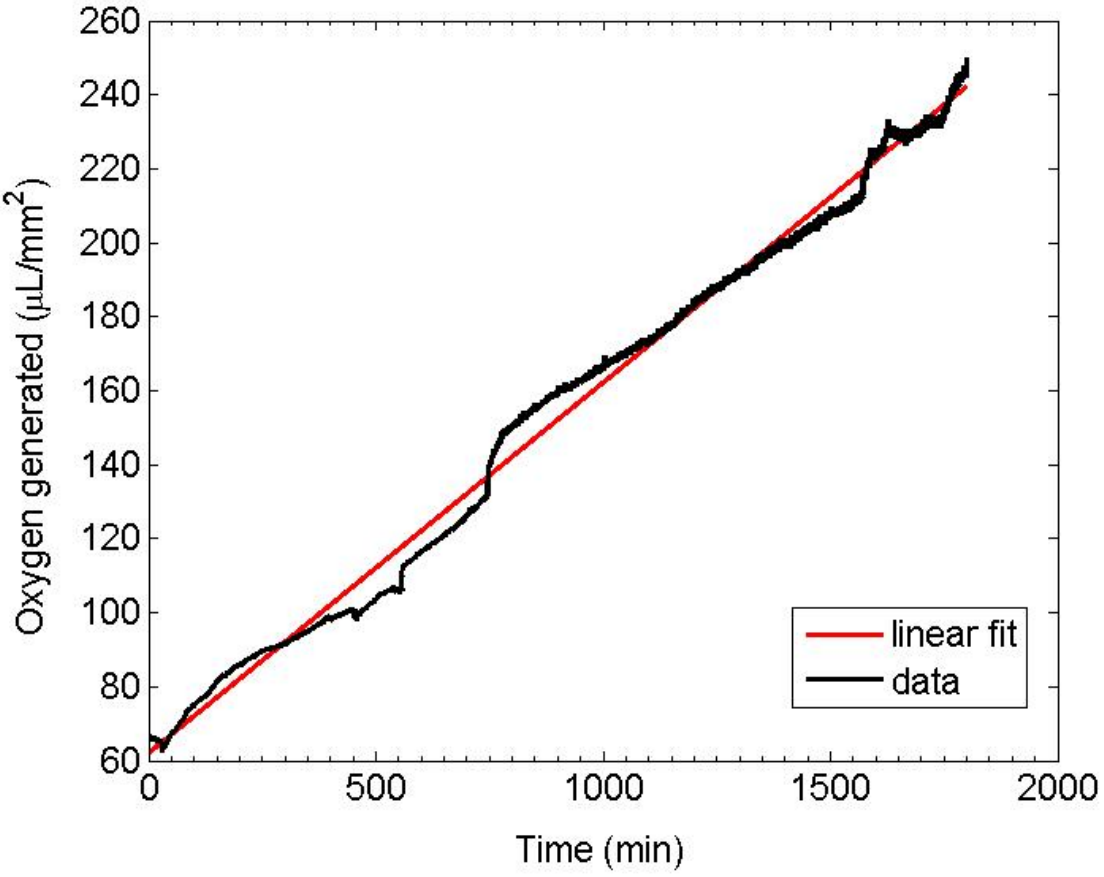

Figure 5.6. Long-term (30 h) oxygen generation profile. Oxygen is generated at a rate of 0.1 μL O_2/min/mm^2 when flowing 3 % H_2O_2 at 250 μL/h. The peroxide concentration and flowrate can be increased to achieve generation rates that have been clinically proven effectively promote epithelial healing. Reproduced from Ref. [91] with permission from Elsevier.

level (from a partially hypoxic level of 15 % to 40 % 3 hours later) in the agarose gel 3 mm below an oxygenation spot. The curves show saturation in the oxygen level since for these experiments, a fixed amount of H_2O_2 was used (rather than a continuous flow). Although the level shown here is not 100 % saturation, one can still conclude that the platform is able to successfully raise the oxygen concentration 3 mm within the gel to levels which are far from hypoxic. Therefore, if the gel were a wound, it would be reasonable to expect improved healing as deep as 3 mm as a result of the oxygenation platform.

The two remaining curves represent the tests with Integra and show a different trend. In particular, the orange curve, corresponding to the setup with Integra and peroxide-filled microfluidics contains an initial shallow slope; this lag in the increase of oxygenation can be attributed to the extra time required for oxygen to diffuse through the Integra layer. After 2.5 hours, however, the orange curve exhibits its highest rate of change in oxygen concentration (slope of 18.9 % per hour); this rate is similar to the largest rate of the sample without Integra (17.1 % per hour), suggesting that although the Integra causes an initial lag in oxygen diffusion, the eventual diffusion rate of oxygen approaches that of the oxygen generation platform. For comparison, the oxygen level does not increase during this time for the sample that does not contain peroxide in the microfluidics.

One feature of the curves that should be clarified is the initial drop in oxygen for the two Integra samples. For both of these cases, the data shows an initially normoxic oxygen level; this corresponds to the reading of the oxygen probe in atmosphere, prior to insertion into the gel (at time 0). Following insertion, the oxygen concentration drops steadily; although one would expect a quick drop in oxygen concentration (to hypoxic levels in the gel), the curves show a 20–30 minute steady decay which can be attributed to atmospheric oxygen trapped in the probe protector needle (described in the experimental setup above) which needs time to diffuse into the gel. After 30 minutes, however, the curves reach their minimum values (the oxygen level in the hypoxic gel, $\leq$15 % O_2). These data are representative examples of oxygen diffusion into agarose gels; future work will characterize the repeatability of the process to enable repeatable, reliable production of paper-based wound dressings.

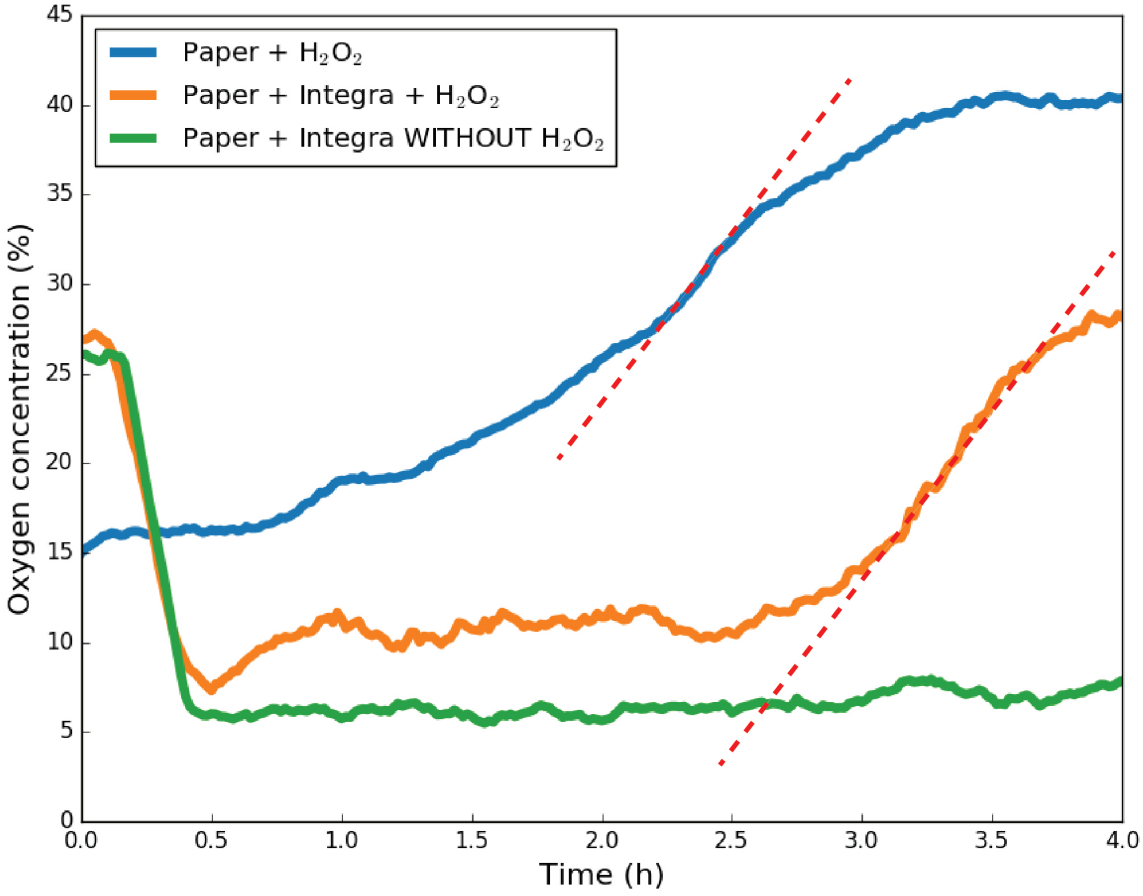

Figure 5.7. Oxygen generation and diffusion into agarose gel. The orange curve exhibits its highest rate of change in oxygen concentration (slope of 18.9 % per hour); this rate is similar to the largest rate of the sample without Integra (blue curve, slope of 17.1 % per hour). The sample with no oxygenation (green curve) does not exhibit increases in oxygen concentration in the gel.

The oxygen transport kinetics of the platform for various flow rates are shown in Figure 5.8. The plot depicts the level of oxygen as a function of the downstream distance from the point of oxygen generation for various flow rates of H_2O_2. The data show that for the channels used (rectangular cross-section of 500 µm × 200 µm), a flow rate of 300 µL/h is slow enough to provide generated oxygen with sufficient time to permeate the channel and paper at the generation spot. At higher flow rates, however, cross-paper oxygen levels peak at a location downstream from the generation spot, suggesting that flow rates higher than 300 µL/h would result in excessive lateral transport of oxygen that would prevent accurate localized delivery. Therefore, the oxygen platform exhibits satisfactory performance as long as the H_2O_2 flow rate over a spot is maintained at or below 300 µL/h. These data are representative examples of the effects of H_2O_2 flowrate on the location of oxygen permeation across parchment paper; future work will characterize its repeatability to enable repeatable, reliable production of paper-based wound dressings.

The biocompatibility results for the materials and finished devices are shown in Figure 5.9. The alamar blue assay performed for 3T3 cells on parchment paper (Figure 5.9a) showed no significant difference between the metabolic activities of cells seeded on the culture dish as a control and that of the cells seeded on the two parchment paper samples, with and without catalyst. These results imply the biocompatibility of both the parchment paper and the catalyst. Similarly, the analyses on the assembled structures with flowing H_2O_2 showed no significant difference in the metabolic activities of the cells, compared to the control (Figure 5.9b). This suggests that H_2O_2 does not come into contact with the seeded cells during device operation and implies the biocompatibility of the fabricated oxygen generators.

The overall performance of the oxygen generation platform is adequate for its intended application as a component of a disposable oxygen therapy wound dressings. Future development will focus on practical packaging measures necessary for clinical use. These include its incorporation into a commercial wound dressing as well as the implementation of an on-board hydrogen peroxide source. The microfluidic structure provides a convenient location for encapsulating H_2O_2 in a small (1–10 mL) pre-pressurized cham-

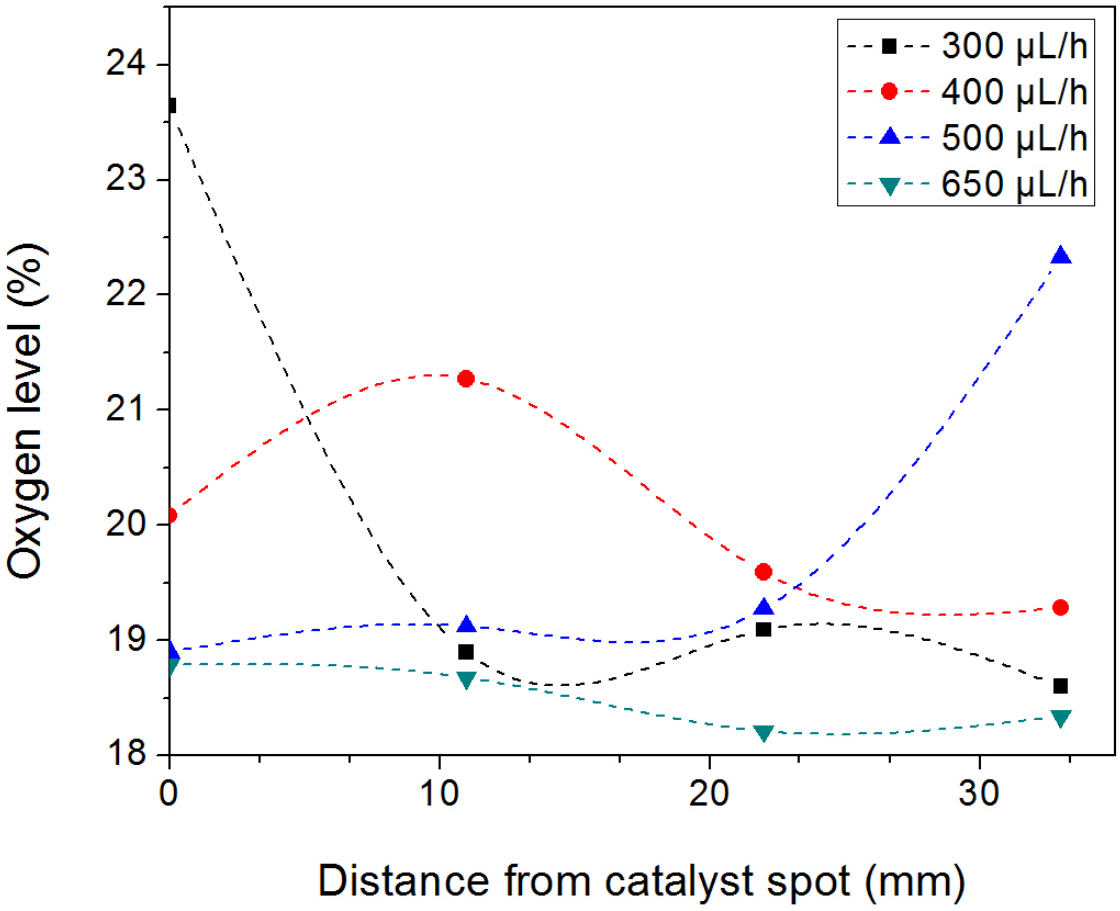

Figure 5.8. Oxygen level across parchment paper as a function of the distance from the generation location using various hydrogen peroxide flow rates. Oxygen delivery accuracy is optimum for H_2O_2 flow rates of 300 µL/h or lower. Reproduced from Ref. [91] with permission from Elsevier.

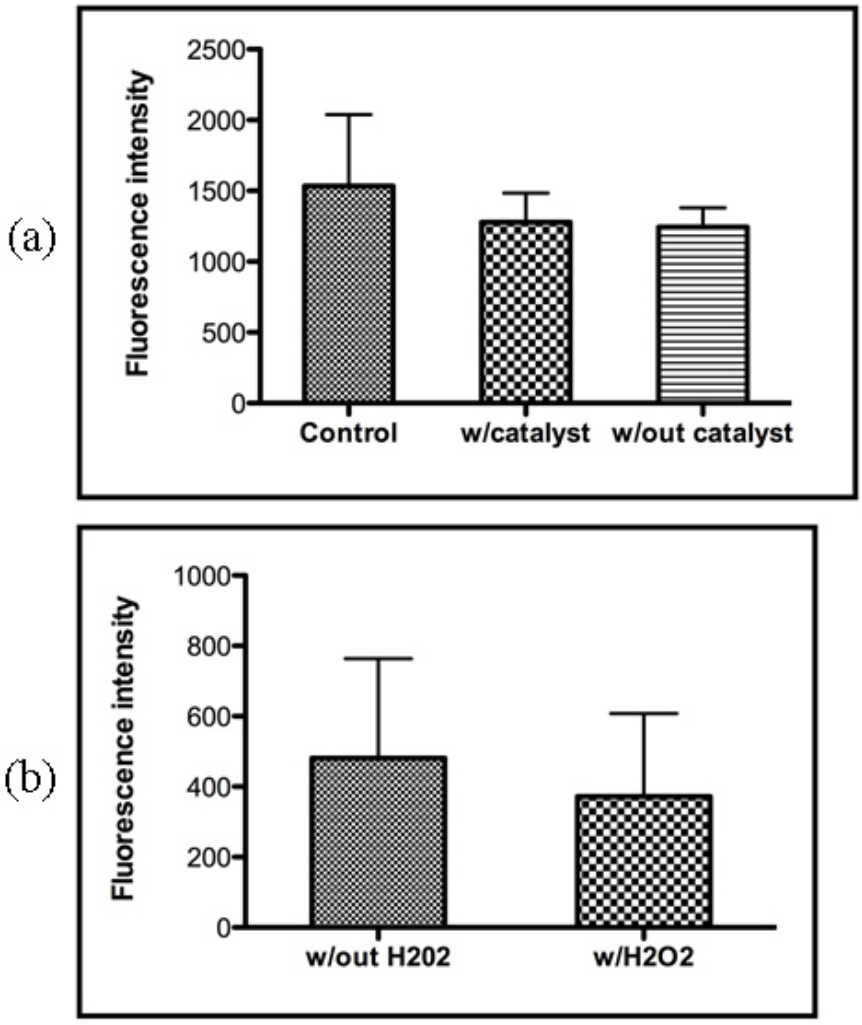

Figure 5.9. The results of alamar blue assays of (a) a control sample (standard well plate), parchment paper with catalyst, and patterned parchment paper without catalyst and (b) devices without H_2O_2, and with 3 % H_2O_2 at a flow rate of 250 µL/h. For both experiments, 3T3 fibroblast cells were seeded on the surface of the parchment paper or the channel devices. (n = 3, standard deviation). Error bars, SD±. One-way ANOVA followed by Bonferroni test were performed where appropriate to measure statistical significance. Reproduced from Ref. [91] with permission from Elsevier.

ber that delivers a continuous flow through the microchannels. For example, a reservoir of dimensions 100 mm × 100 mm × 1 mm would contain enough 3 % H_2O_2 solution to generate about 100 mL O_2, hence enabling a production rate of 100 mL O_2/h for up to 33 h. The peroxide concentration and/or reservoir dimensions can be adjusted to optimize for platform size or oxygenation capacity. The oxygen release profile for completely packaged devices will be subsequently evaluated with *in vitro* and/or *in vivo* experiments.

5.4 A practical implementation using a finger-actuated pump

The oxygenation platform can be implemented with hydrogen peroxide provided in various ways, either continuously (e.g., via an external micropump) or discretely (e.g., via on-board reservoirs). The latter design offers the simplicity required for accelerating its design to production. As such, this section describes one implementation of the system which relies on a PDMS reservoir that doubles as a finger-actuated pump.

The pump design is similar to others presented in the literature (e.g., Mosadegh et al. [102]). It consists of a reservoir connected to an output channel which contains a one-way check (flap) valve. All components are molded in PDMS; the process can be accomplished with two layers of PDMS by designing appropriate molds. As a proof-of-concept demonstration, we created mold prototypes via a stereo-lithography 3D printing process. This process provides sufficient resolution for all the pump features (which are larger than 100 µm). A photograph of the two-part mold is shown in Figure 5.10(a). The pump is created by casting PDMS in the molds, curing it, and subsequently bonding together the two PDMS components via plasma. A photograph of one such pump is shown in Figure 5.10(b), with the outlet connected directly to a glass capillary for characterization.

The pump is operated by depressing the membrane in the reservoir. Each pressing actuation outputs a specific volume via the output channel, which can be directly connected to the oxygenation platform (via tubing or as a physical extension of the platform itself). Thus, to characterize the pump performance, it was evaluated in terms of its

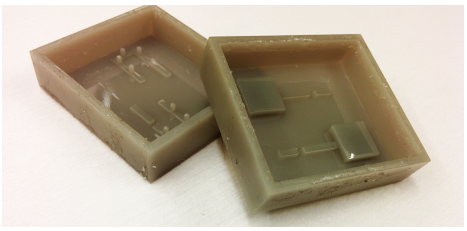

(a) 3D printed molds for pump fabrication

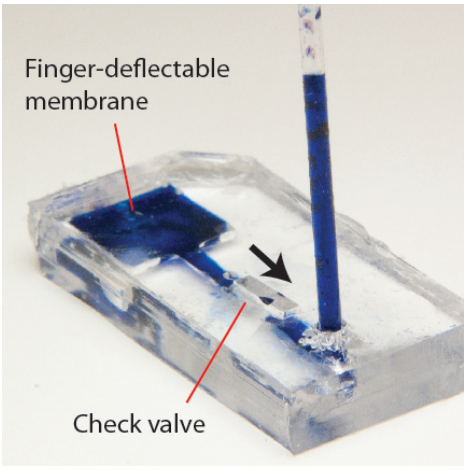

(b) Completed pump with capillary on the outlet

Figure 5.10. Implementations of the oxygenation platform with finger pumps.

volume output as a function of the number of actuations. The reservoir was first loaded with dyed water (representing hydrogen peroxide). Subsequently, the reservoir was momentarily pressed with a finger up to 7 times. The volume output after each actuation was recorded by observing the liquid output in a capillary tube connected to the output.

Figure 5.11 shows the results of the finger actuation tests, representing the average of 7 devices. Since the liquid remaining in the reservoir decreases with each actuation, the amount expelled (a fraction of the remaining liquid) is similarly decreasing with the number of actuations. The first actuation produces about 25 µL, whereas the seventh actuation produces only about 7 µL. Nevertheless, if one assumes that a patch contains 5 channels, each with dimensions 20 mm × 1 mm × 100 µm, then the amount of liquid contained in the channels is 10 µL. This value can clearly be produced by the first 5 actuations of the pump, allowing the pump to be actuated five times.

The performance of the pump is seen to be sufficient for practical applications when one considers a patch for a small wound (e.g., foot pressure ulcer of 2 cm diameter). Assuming the hydrogen peroxide is 30 % H_2O_2, 10 µL of it can produce about 3.18 mL of O_2 gas, sufficient for at least one hour of therapy. Thus, in this case, the pump can be used for 5 hours, after which a different attached pump can be used (or the entire patch can be replaced if needed). For longer usage time (and convenience), the pump dimensions can be increased, or one can create an array of pumps to attach to the platform. The device presented here serves as a proof of concept demonstration to show the practicality of a finger-actuated pump (i.e., the actuation numbers are reasonable, and the output volumes are in the range of the required values for proper oxygenation).

To evaluate the robustness of the pump, each pump was tested 10 times. Figure 5.12 graphs a comparison of the output volume as a function of actuation number for the first and tenth trial of each pump. The data reveal insignificant differences between the first and last trial for each actuation. Thus, the pump is sufficiently robust for many actuations without loss of performance due to material or structural defects.

Using this pump, we implemented various possible embodiment for integrating the pump with the oxygenation platform. Figure 5.13(a) demonstrates one approach with a

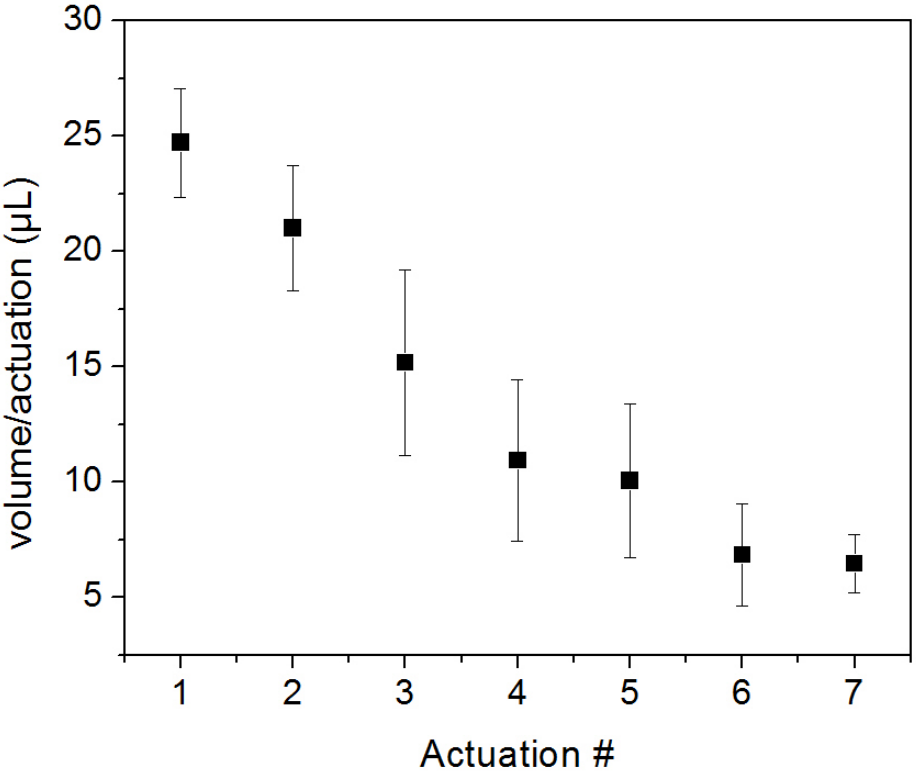

Figure 5.11. Volume output of the finger pumps as a function of actuation number.

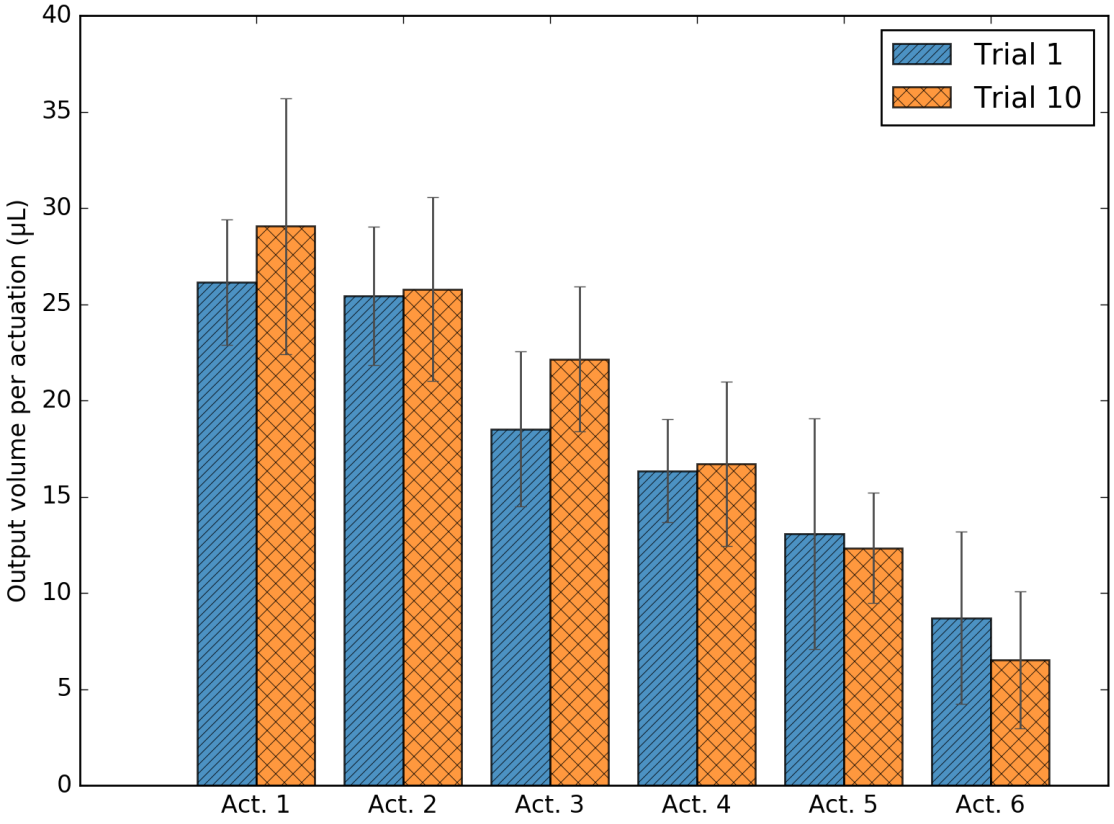

Figure 5.12. Comparison of the output volume of a finger pump as a function of actuation number for the first and tenth trial of the pump. The data represents the average of 7 pumps.

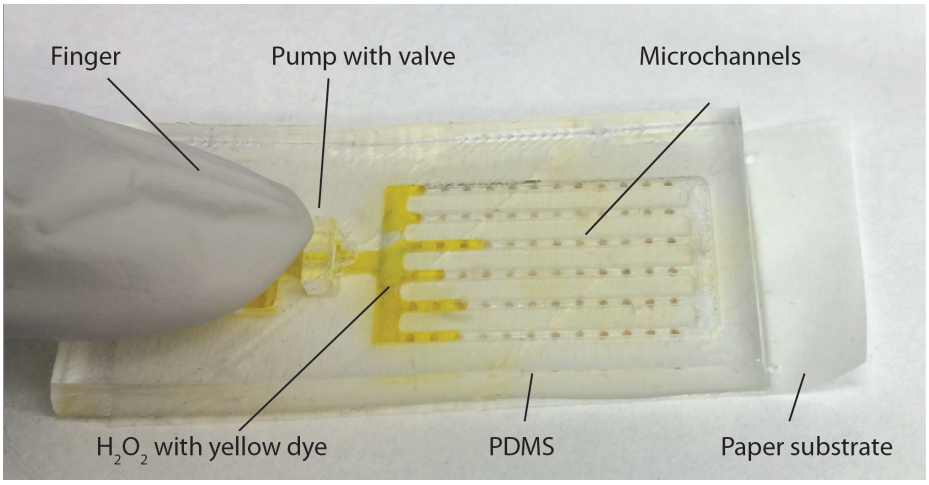

(a) Oxygenation platform with one pump. Reproduced from Ref. [26] with permission from Springer.

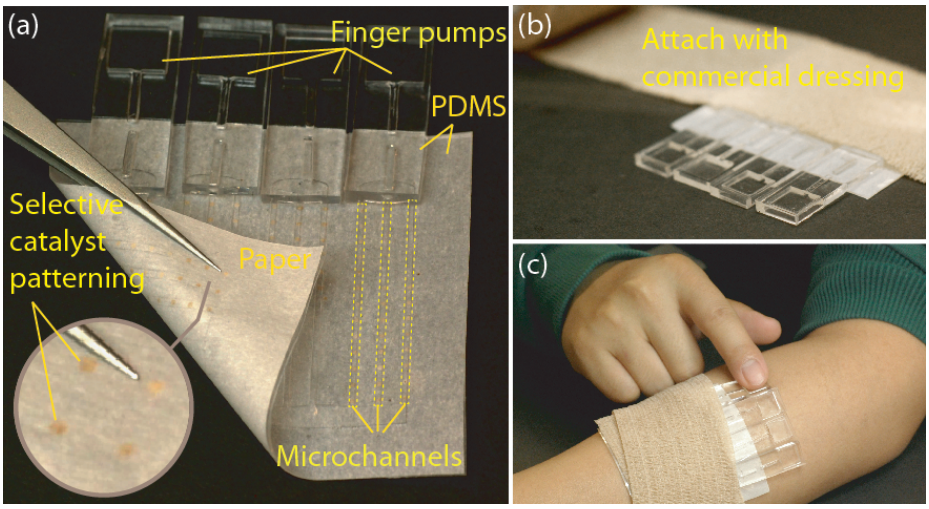

(b) Oxygenation platform with multiple pumps

Figure 5.13. Implementations of the oxygenation platform with finger pumps.

single pump; the channels are being filled with dyed water as the pump is depressed. An alternative approach with multiple pumps (for increased operation time) is demonstrated in Figure 5.13(b). Here, the pump can last as long as 20 hours using the design described above.

Overall, the finger-pump approach is a practical and effective method of supplying hydrogen peroxide to the channels for generating oxygen in the PDMS-parchment paper oxygenation platform.

5.5 Conclusions for the paper-based platform

We have developed an inexpensive, flexible, paper-based oxygen generation platform for locally generating and delivering oxygen to the microenvironment of chronic wounds. The platform consists of a PDMS microfluidic network bonded to an array of laser-defined (and hence, customizable) MnO_2-loaded hydrophilic spots on an otherwise hydrophobic parchment paper substrate. H_2O_2 is introduced into the PDMS microchannels for the generation of oxygen via catalytic decomposition at the MnO_2 spots. The generated oxygen then permeates through the parchment paper to reach the wound bed. Oxygen generation in the catalyst spots raised the oxygen level on the opposite side of the parchment paper to clinically acceptable levels. The platform generates oxygen effectively to allow its diffusion into an agarose gel (wound bed surrogate); here, oxygen concentration increases to up to 25 % within three hours when Integra (dermal regeneration matrix) is used as a wound interface, and to as much as 45 % without Integra. Both of these levels can successfully be used to treat wound hypoxia. An alamar blue assay using 3T3 cells revealed that the parchment paper with and without MnO_2 is not cytotoxic and that the fabricated structures do not expose seeded cells to H_2O_2 while in operation. Finally, finger pump-driven prototypes were presented and validated for medical practicality.

6. CONCLUSION

This work presented the development of a low-cost alternative for continuous oxygen delivery comprising of an inexpensive, paper-based, biocompatible, flexible platform for locally generating and delivering oxygen to selected hypoxic regions. The platform takes advantage of recent developments in the fabrication of flexible microsystems including the incorporation of paper as a substrate and the use of inexpensive laser machining. The use of paper simultaneously provides structural strength and flexibility as well as selective filtering functionality. In particular, the paper possesses high mechanical strength (> 70 MPa) to withstand human motion, high elastic modulus when dry (> 300 kPa) for easy handling during fabrication, low elastic modulus (< 50 kPa) when wet for interfacing with similarly soft tissue, permeability to gas and not water at low pressures, and permeable to oxygen diffusion. When laser-rastered, it offers the additional advantages of a roughened surface for deposition of particles (e.g., catalyst for oxygen generation) and a low contact angle (21 °) for adsorbing aqueous solutions as well as for promoting attachment of mammalian cells. With these characteristics, laser-treated parchment paper reveals itself to be an ideal substrate for advanced wound dressings.

Laser machining parchment paper enables the precise definition of oxygen generating regions that match the hypoxic wound profile. With this process, we have developed paper-based oxygen generation platform for locally generating and delivering oxygen to the microenvironment of chronic wounds. The platform consists of a PDMS microfluidic network bonded to an array of laser-defined (and hence, customizable) MnO_2-loaded hydrophilic spots on an otherwise hydrophobic parchment paper substrate.H_2O_2 is introduced into the PDMS microchannels for the generation of oxygen via catalytic decomposition at the MnO_2 spots. The use of manganese dioxide and hydrogen peroxide provides a low-cost catalyst-peroxide combination with fast, tunable oxygenation rate. A sample of 111 µg of the 19 µm particles of manganese dioxide investigated here, are

sufficient for achieving oxygenation rates of 3 mL/h (a typical requirement, as mentioned in Chapter 2) using 3 % H_2O_2. The generated oxygen then permeates through the parchment paper to reach the wound bed. Oxygen generation in the catalyst spots raised the oxygen level on the opposite side of the parchment paper to clinically acceptable levels. The platform was confirmed to be biocompatible via experiments with 3T3 cells. Finally, various prototypes The exact configuration of the final wound healing dressing depends on the

Together these two technologies enable the development of a low-cost patch/wound-dressing with customized, wound-specific oxygen generating regions. Table table:patches compares the present platform with existing commercial wound oxygenation platforms. The present platform is able to match the oxygenation characteristics of the other systems with a tunable, and economical approach while simultaneously providing the additional benefits of being refillable, offering selective oxygenation to specific regions of wounds via laser patterning, and allowing integration with other emerging wound healing components (due to its integrability with PDMS and pumps, as well as to its salable fabrication approach).

Healing of chronic wounds is a challenging task. Many challenges remain in creating futuristic smart wound dressings; this dissertation offers a first step towards this goal in the form of fundamental research and prototype development.

Manufacturer	Product	O2 generation rate	Continuous operation time	Selective delivery	Integratable with flexible sensor farbication	Refillable/ rechargeable	Cost ($USD) of 7 days of therapy	Notes
Ogenix	*EPIFLO*	3 mL/h	15 days	No	No	No	329	Device, separate from dressing
Inotec AMD	*Natrox*	13 mL/h	24 hours (then replace battery; use for 2-3 days)	No	No	Yes (battery)	750	Device + dressing
OxyBand	*OxyBand*	pre-filled	5 days	No	No	No	165*	Size: 7in x 9in (17.78cm x 22.86cm)
Halyard (Kimberly-Clark)	*OXYGENESYS*	221-369 mL/h	N/A	Yes (can be cut)	No	No	280*	Size: 10cm x 10cm
Our design		3 mL/h (variable up to 80)	48 h (at 3mL/h)	Yes (patterned)	Yes	Yes (H2O2)	< 100*	Size: 10cm x 10cm

Table 6.1.

Comparison of state-of-the-art, commercial oxygen-generating systems with the present paper-based platform. *For the shorter-term-use patches, the cost of 7 days of therapy is computed assuming 3 patches are used (changed every 2–3 days, as is standard for wound dressings).

7. FUTURE WORK

The oxygenation platform presented in this dissertation is only a single module of a more ambitious endeavor towards significantly improving health care for patients with chronic wounds while simultaneously reducing financial burdens. A key way to achieve this is thought he development of smart, personalized wound dressings. Currently available dressings are generic (one-size-fit-all), operate in an open loop fashion, and do not deliver therapy based on an individual's response to treatment. Furthermore, existing bandages rely on a single mode of treatment, whereas a combination of therapies (e.g., oxygen delivery, ion sensing, and drug delivery in a single bandage) can accelerate the healing process and improve the health outcome. Moreover, closing the loop around the wound by monitoring individualized response to treatment using integrated sensors that objectively capture the wound progression in real-time and tailoring the combination treatment appropriately is also expected to improve the health outcome. Figure 7.1 illustrates a vision of a smart wound dressing integrated with various sensing and delivery modules for precision wound care. In order to achieve this goal, the work in this dissertation requires further research and development on various fronts. The following subsections describe future work for the continued development of the oxygen generation platform as well as avenues for integration with other modules to enable a true, smart wound dressing.

7.1 Material characterization

The materials for the wound dressing must be completely characterized with respect to functionality, biocompatibility, and stability. This work presented material characterizations for the laser-treated parchment paper substrate and the oxygen generation kinetics of hydrogen peroxide and manganese dioxide. Further work is necessary to

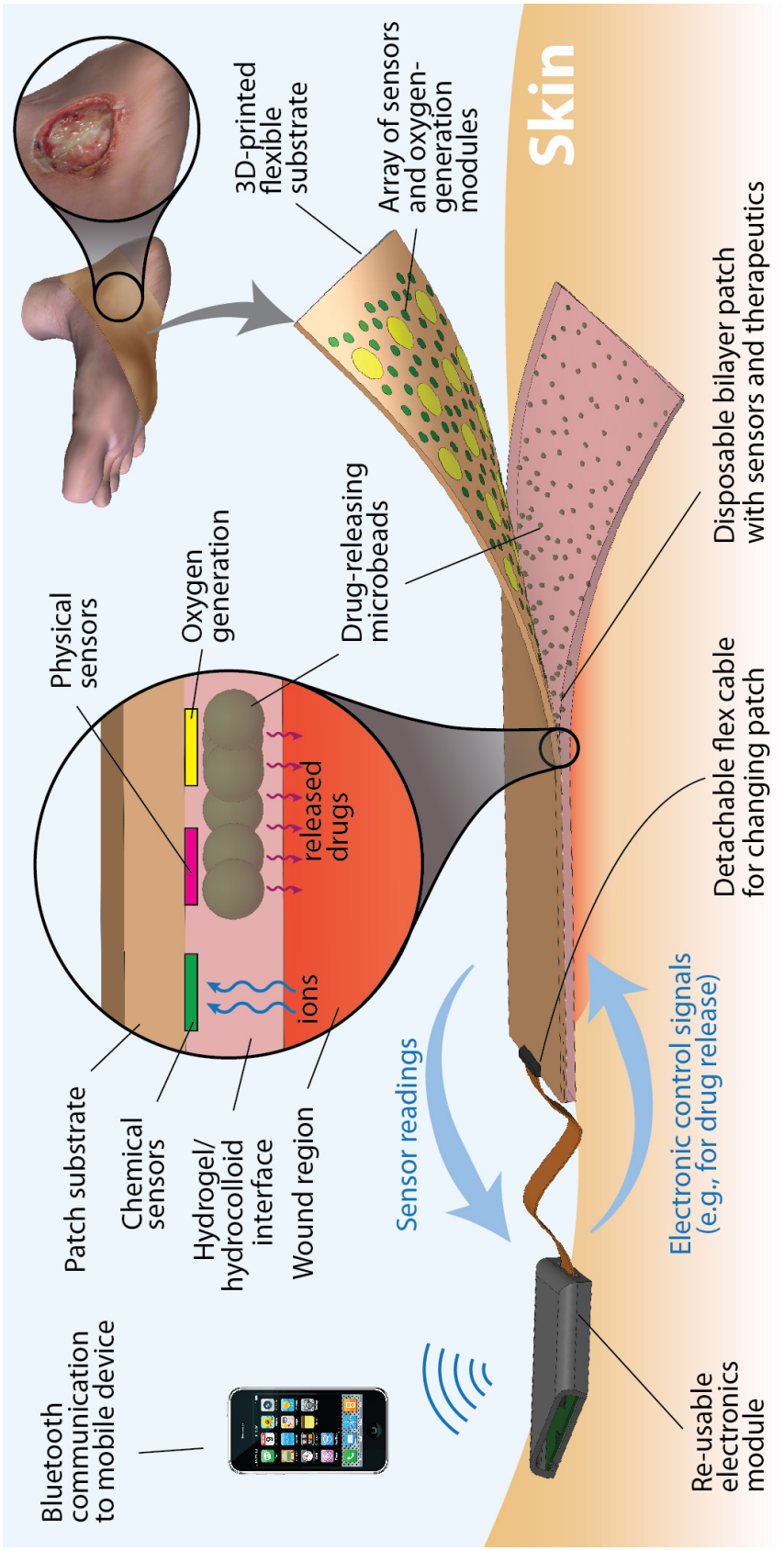

Figure 7.1. Vision of an integrated, closed-loop, smart wound dressing.

assess variability and repeatability of the various processes, in particular the repeatability of laser-rastering parchment paper. This includes conducting further experiments that, for example, compare the surface morphology across many samples of laser-treated an un-treated parchment paper (e.g., by measuring average surface roughness using a surface profilometer) while additionally comparing the material density of the samples before and after laser treatment. The mechanical properties of the paper should also be evaluated after laser machining. Since the percentage of laser-treated area can affect such properties as ultimate tensile strength and elastic modulus, paper can be treated with various area percentages and evaluated as described in Chapter 3.

Anther remaining task in the material area includes the characterization of the materials after exposure to standard sterilization techniques. This comprises exposing the materials to e-beam, gamma ray, or hydrogen peroxide vapor and subsequently evaluating their functionality.

Another task is the complete characterization of the deposition techniques for the materials (e.g., uniformity and repeatability). This includes identifying and developing a commercially-viable process for laser processing paper and depositing all the chemicals on it at a large scale. Remaining characterizations include evaluation of printing methods for the materials and print quality using various techniques (e.g., gravure, inkjet). Efforts in this area are currently underway in the Purdue-WMU collaboration as part of the NextFlex P.C. 1.0 project.

Another investigation should study the oxygenation reaction more in detail to evaluate any thermal effects occurring from the reaction. Since the oxygenation reaction is an exothermic one, any heat generated by the oxygenation platform could potentially (positively or negatively) influence the wound healing process. Temperature increases will depend on the concentration and mass of the peroxide and the catalyst used as well as the dimensions of the platform. This heat transfer problem can be best addressed by creating platform prototypes and measuring the rise in temperature on the paper using a thermal probe. This can be repeated for various concentrations of catalyst and peroxide,

as well as channel dimensions. Temperature rises should be investigates as to their effect on wounds (via literature, and eventually by *in vivo* studies.

The materials must also be characterized in terms of their long-term stability. This can be achieved by evaluating the performance of the materials after accelerate thermal aging in various environments to determine special requirements for storage and handling of the smart wound dressing.

Longer-term investigations can consider alternative materials for oxygen generation. Although not as easily available as those described in this dissertation, some chemicals, such as superoxides, may be suitable for oxygen generation in wound dressings. Superoxides are used in chemical oxygen generators which are used, for example, in airplanes. They produce oxygen rapidly but generate significant heat. Studies in this area should first evaluate the oxygen storage capabilities of such materials and then focus on precise control (triggering on and off, as well as tuning the rate) of oxygen generation, as well as maintaining proper temperature for wound dressings.

Another investigation can look into alternatives for PDMS to allow fabrication of thin ($< 500\,\mu m$) microfluidics in a more commercially-viable manner.

7.2 Device-level characterization

In addition to material characterization, the developed devices must be evaluated at the device level. This dissertation presented an oxygen platform for which the oxygen generation rate was characterized by various methods, as seen in Figures 5.5, 5.7, and 5.8. The data in these figures was collected from representative samples but do not offer a view of the variability across samples. Thus, the experiments used to create these graphs must be repeated with multiple samples to assess process/sample variability (e.g., via error bars).

Further characterization is also necessary in terms of platform biocompatibility. The platform presented in this dissertation was tested at this level using 3T3 cells. Experiments in this area must continue characterizing the platform in other clinically relevant ways.

Characterization of the devices must be performed using a simulated wound testing setup which has the potential to sense and create heterogeneous hypoxic/normoxic/hyperoxic regions to mimic the real wound micro-environment. The working performance of the oxygen sensors should be evaluated on a hydrogel wound model as a single-sensor as well as an array configuration.

The platform must also be characterized with any additional interfaces that will be used in practice. This dissertation describes one example, i.e., Integra dermal regeneration matrix. However, this is not the only interface layer which may be used commercially. Thus, future investigations should evaluate the efficacy of the platform when delivering oxygen to the wound bed via an intermediate interface materials such as alginate gel or collagen-based films. Investigations in this area should include multi-directional diffusion of the oxygen that is generated by the platform. Additionally, the mechanical properties of these interfaces must be characterized (e.g., adhesion strength to the paper).

It is also imperative to identify alternative methods for transporting hydrogen peroxide withing the microchannels of the oxygenating platform. The current platform offers one design for a finger-actuated pump; Figure 7.2 illustrates another (single-push) design. This approach is adequate as a first-generation product. However, in later generations, electronics can be integrated into the platform, and on-board micropumps can be incorporated. Thus, the pumping requirements for the system must be calculated and investigated experimentally to determine appropriate hardware.

7.3 Integration with other modules

As a step towards the vision of the smart dressing, subsequent research directions must include the integration of the wound oxygenation platform with other modules, preferably created on the same substrate for true integration. The next logical step is to integrate oxygen sensing into the platform to enable closing the loop between sensing and delivery. Efforts in this area are currently underway in the Ziaie group as part of the NextFlex P.C. 1.0 project. The successful integration of these two platforms requires

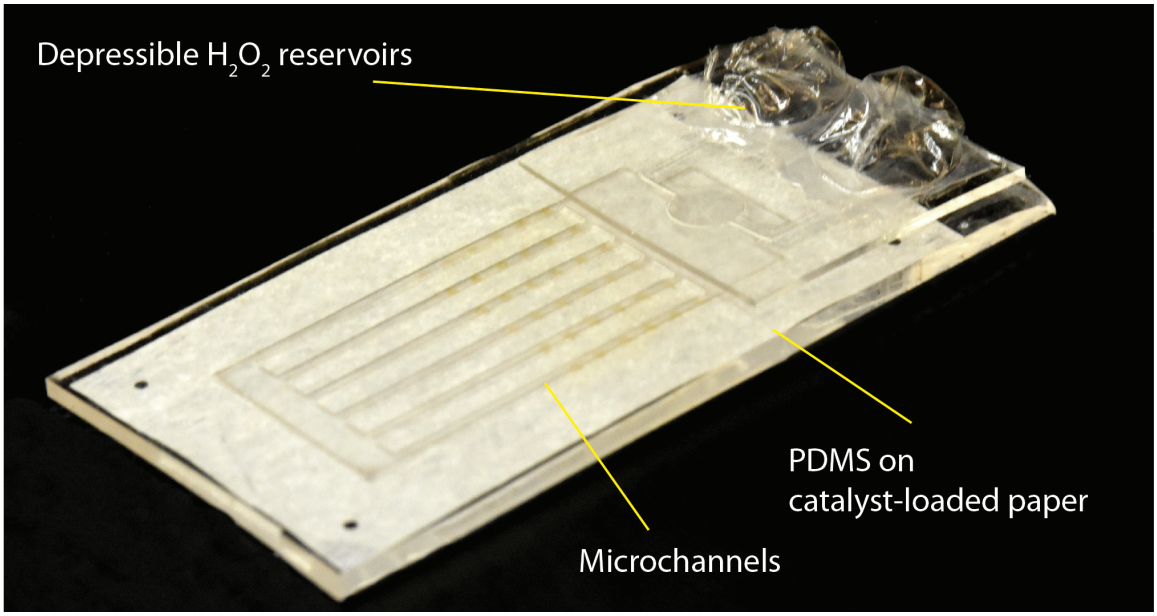

Figure 7.2. Oxygenation platform with single-actuation finger pump.

first characterizing them independently, and then combining them via a congruous fabrication process. Once combined, the two platforms (oxygen sensing and delivery) must be tested together in an array arrangement configuration prior to testing the two-module integrated system. Examples of other modules which can be subsequently integrated with this platform include electrochemical sensors, such as those developed in the Ziaie group and illustrated in Figure 7.3.

7.4 Design for scalability

Ultimately, the successful commercial adoption of the oxygen generation platform depends on its practical implementation. For this reason, it is important to develop a practical manufacturing process (with detailed diagrams) from the beginning of the design work.

One such approach that integrates two modules is as follows. First, parchment paper will be laser treat on one side to render it hydrophilic (to allow subsequent deposition of materials). Next, a chemical catalyst (MnO_2) will be deposited on the paper via *in situ* precipitation of two inkjet-printed solutions (aqueous KI and $KMnO_4$). Separately, a microfluidic network (for guiding H2O2) will be created out of PDMS by casting two films of PDMS onto a carrier substrate (PET); one will be (through-hole) patterned with laser to create microfluidic designs. The two PDMS films will then be laminated together onto the parchment paper (on the sensor side) to create closed microfluidic network. Finally, a layer of Integra/Primatrix will be laminated (and bonded) to the rest of the system using techniques similar to the ones done for the sensor platform (above). The approach is conceptualized in Figure 7.4.

7.5 In-vitro and in-vivo tests and evaluations

All fabricated devices and platform should eventually be evaluated *in vitro* and *in vivo*. These include: 1) *in-vitro* biocompatibility tests, 2) *in-vivo* biocompatibility and functionality tests, and 3) preliminary *in-vivo* efficacy tests. Biocompatibility can be assessed

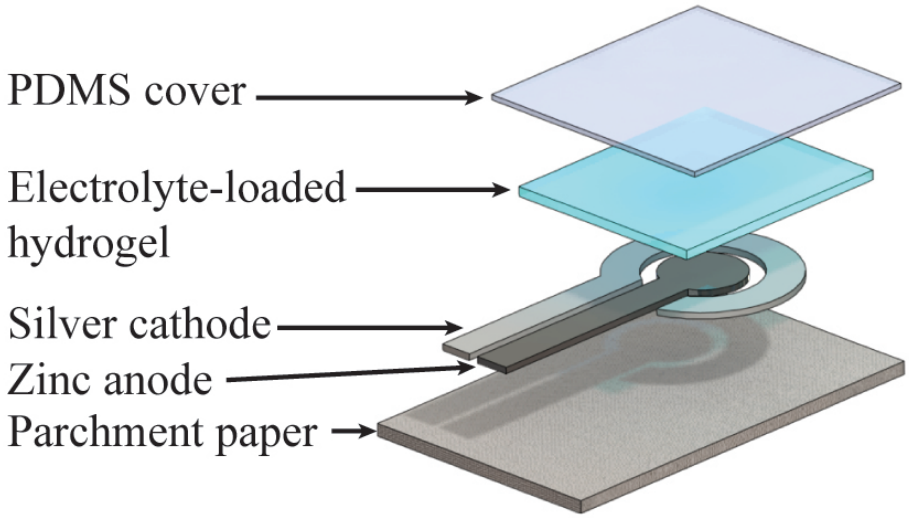

(a) Electrochemcial oxygen sensor on paper. Reproduced from Ref. [84] with permission from The Royal Society of Chemistry.

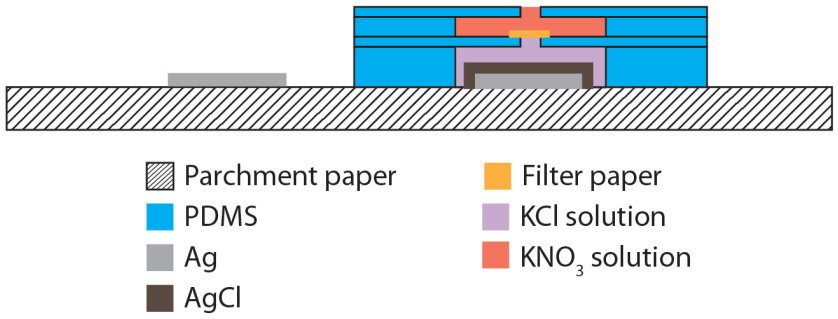

(b) Electrochemcial silver ion sensor on paper. Reproduced from Ref. [103] with permission from IEEE ®2013.

Figure 7.3. Paper-based sensors which can be integrated with the oxygenation platform for wound management.

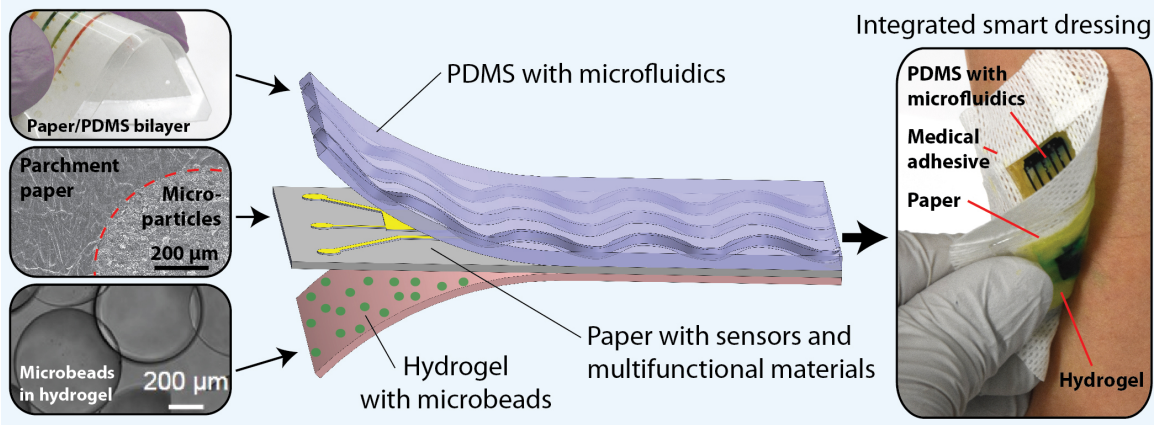

Figure 7.4. Prototype of a wound dressing with a gel interface.

in vitro by seeding a piece of Integra matrix with freshly isolated human keratinocytes or adipose stem cells, affixing the dressing to the matrix using fibrin glue and culturing the construct for 7–10 days under the appropriate conditions. The proliferation rate of cells within the construct can be assessed using the WST-1 cell proliferation reagent and significant differences in rates obtained with the complete dressing, dressings that lack catalyst, and Integra with cells but without the dressing will be used to identify cytotoxicity. Following the quantitative assessments, the constructs are formalin-fixed and processed for histological study.

In vivo biocompatibility, functionality and preliminary efficacy tests of the device can be performed using the excisional wound splinting mouse model. One approach is to use a biopsy tool to create bilateral full-thickness dermal wounds (7 mm-diameter) on the back of the SKH-1 mouse, which is a hairless mouse that is commonly used in wound healing studies. The wounds are splinted with a sterile donut shaped splint to ensure that the wound heals by the growth and migration of skin cells rather than by contraction of skin from the edges of the wound, which is how wounds heal in rodents. Once splinted, an appropriately sized disc of Integra with the affixed paper dressing is placed onto the wound and then wrapped with a self-adhering elastic bandage. To test for functionality, the device is used to deliver oxygen for 30 min. Independent oxygen measurements will be made using a fiber optic sensor. This process will be repeated every 24 h to measure the degradation of the dressing over time. Once the dressing is functionally degraded, a biopsy of the wound and surrounding tissue is collected for routine histological processing and analysis of wound healing and inflammation by a board certified pathologist. Some animals receive replacement dressings to prolong the measurement process up to two weeks before subsequent biopsy collection and histological assessment. Samples are scored for the number of inflammatory cells, evidence of angiogenesis, the number of granuloma and giant cells and the degree of infiltration of surrounding tissues.

7.6 Conclusions

The sections above outline various research directions to further develop this work, with the ultimate goal being the development of a commercially-viable product which can improve the lives of patients around the would.

REFERENCES

REFERENCES

[1] Medical Data International, "US market for chronic wound management products," Irvine, CA, 1997.

[2] C. K. Sen, G. M. Gordillo, S. Roy, R. Kirsner, L. Lambert, T. K. Hunt, F. Gottrup, G. C. Gurtner, and M. T. Longaker, "Human skin wounds: a major and snowballing threat to public health and the economy." *Wound repair and regeneration : official publication of the Wound Healing Society [and] the European Tissue Repair Society*, vol. 17, no. 6, pp. 763–71, 2009.

[3] A. Stojadinovic, J. W. Carlson, G. S. Schultz, T. A. Davis, and E. A. Elster, "Topical advances in wound care." *Gynecologic oncology*, vol. 111, no. 2 Suppl, pp. 70–80, 11 2008.

[4] R. O. Y. W. Tarnuzzer and G. S. Schultz, "Biochemical analysis of acute and chronic wound environments," *Wound Repair and Regeneration*, vol. 4, pp. 321–325, 1996.

[5] V. Falanga, "Classifications for wound bed preparation and stimulation of chronic wounds," *Wound Repair and Regeneration*, vol. 8, no. 5, pp. 347–352, 9 2000.

[6] A. A. Tandara and T. A. Mustoe, "Oxygen in wound healing–more than a nutrient." *World journal of surgery*, vol. 28, no. 3, pp. 294–300, 3 2004.

[7] C. K. Sen, "Wound healing essentials: let there be oxygen." *Wound repair and regeneration*, vol. 17, no. 1, pp. 1–18, 2010.

[8] D. M. Castilla, Z.-J. Liu, and O. C. Velazquez, "Oxygen: Implications for Wound Healing," *Advances in Wound Care*, vol. 1, no. 6, pp. 225–230, 12 2012.

[9] N. S. Greaves, S. a. Iqbal, M. Baguneid, and A. Bayat, "The role of skin substitutes in the management of chronic cutaneous wounds." *Wound repair and regeneration : official publication of the Wound Healing Society [and] the European Tissue Repair Society*, vol. 21, no. 2, pp. 194–210, 2013.

[10] M. E. Lait and L. N. Smith, "Wound management: a literature review," *Journal of Clinical Nursing*, vol. 7, no. 1, pp. 11–17, 1 1998.

[11] W. H. Eaglstein, "Moist wound healing with occlusive dressings: a clinical focus." *Dermatologic surgery : official publication for American Society for Dermatologic Surgery [et al.]*, vol. 27, no. 2, pp. 175–81, 3 2001.

[12] G. Chaby, P. Senet, M. Vaneau, P. Martel, J.-C. Guillaume, S. Meaume, L. Téot, C. Debure, A. Dompmartin, H. Bachelet, H. Carsin, V. Matz, J. L. Richard, J. M. Rochet, N. Sales-Aussias, A. Zagnoli, C. Denis, B. Guillot, and O. Chosidow, "Dressings for acute and chronic wounds: a systematic review." *Archives of dermatology*, vol. 143, no. 10, pp. 1297–304, 10 2007.

[13] N. Mehmood, A. Hariz, R. Fitridge, and N. H. Voelcker, "Applications of modern sensors and wireless technology in effective wound management." *Journal of biomedical materials research. Part B, Applied biomaterials*, vol. 102, no. 4, pp. 885–95, 5 2014.

[14] M. Ochoa, R. Rahimi, and B. Ziaie, "Flexible Sensors for Chronic Wound Management," *IEEE Reviews in Biomedical Engineering*, vol. 7, pp. 73–86, 1 2014.

[15] S. Schreml, R. M. Szeimies, L. Prantl, S. Karrer, M. Landthaler, and P. Babilas, "Oxygen in acute and chronic wound healing." *The British journal of dermatology*, vol. 163, no. 2, pp. 257–68, 8 2010.

[16] P. Kranke, M. H. Bennett, M. Martyn-St James, A. Schnabel, and S. E. Debus, "Hyperbaric oxygen therapy for chronic wounds." *The Cochrane database of systematic reviews*, vol. 4, no. 4, p. CD004123, 1 2012.

[17] M. A. Howard, R. Asmis, K. K. Evans, and T. A. Mustoe, "Oxygen and wound care: A review of current therapeutic modalities and future direction," *Wound Repair and Regeneration*, vol. 21, no. 4, pp. 503–511, 7 2013.

[18] G. M. Gordillo, R. Schlanger, W. a. Wallace, V. Bergdall, R. Bartlett, and C. K. Sen, "Protocols for topical and systemic oxygen treatments in wound healing." *Methods in enzymology*, vol. 381, no. 1968, pp. 575–85, 1 2004.

[19] A. Russo, B. Y. Ahn, J. J. Adams, E. B. Duoss, J. T. Bernhard, and J. A. Lewis, "Pen-on-paper flexible electronics." *Advanced materials (Deerfield Beach, Fla.)*, vol. 23, no. 30, pp. 3426–3430, 8 2011.

[20] C.-M. Cheng, A. D. Mazzeo, J. Gong, A. W. Martinez, S. T. Phillips, N. Jain, and G. M. Whitesides, "Millimeter-scale contact printing of aqueous solutions using a stamp made out of paper and tape." *Lab on a chip*, no. 1, pp. 3201–3205, 10 2010.

[21] A. W. Martinez, S. T. Phillips, M. J. Butte, and G. M. Whitesides, "Patterned paper as a platform for inexpensive, low-volume, portable bioassays." *Angewandte Chemie (International ed. in English)*, vol. 46, no. 8, pp. 1318–1320, 1 2007.

[22] Z. Ding, P. Wei, G. Chitnis, and B. Ziaie, "Ferrofluid-Impregnated Paper Actuators," *Journal of Microelectromechanical Systems*, vol. 20, no. 1, pp. 59–64, 2 2011.

[23] M. Ochoa, G. Chitnis, and B. Ziaie, "Laser-micromachined cellulose acetate adhesive tape as a low-cost smart material," *Journal of Polymer Science Part B: Polymer Physics*, vol. 51, no. 17, pp. 1263–1267, 9 2013.

[24] H. Klank, J. P. J. P. Kutter, and O. Geschke, "CO(2)-laser micromachining and back-end processing for rapid production of PMMA-based microfluidic systems." *Lab on a Chip*, vol. 2, no. 4, pp. 242–6, 11 2002.

[25] G. Chitnis and B. Ziaie, "Waterproof Active Paper via Laser Surface Micropatterning of Magnetic Nanoparticles." *ACS applied materials & interfaces*, vol. 4, no. 9, pp. 4435–9, 9 2012.

[26] M. Ochoa, R. Rahimi, and B. Ziaie, "Laser-Enabled Fabrication Technologies for Low-Cost Flexible/Conformal Cutaneous Wound Interfaces," in *Stretchable Bioelectronics for Medical Devices and Systems*, J. A. Rogers, R. Ghaffari, and D.-H. Kim, Eds. Springer International Publishing, 2016, ch. 11, pp. 207–226.

[27] M. Sevcova, J. Horacek, and J. Sevc, "On the thickness of the epidermis," *Cesko-Slovenska Dermatologie*, vol. 53, no. 4, pp. 223–228, 1978.

[28] J. A. McGrath, R. A. J. Eady, and F. M. Pope, "Anatomy and Organization of Human Skin," in *Rook's Textbook of Dermatology*. Malden, Massachusetts, USA: Blackwell Publishing, Inc., 2004, pp. 45–128.

[29] C. Mørk, K. Kvernebo, C. L. Asker, and E. G. Salerud, "Reduced skin capillary density during attacks of erythromelalgia implies arteriovenous shunting as pathogenetic mechanism," *Journal of Investigative Dermatology*, vol. 119, no. 4, pp. 949–953, 2002.

[30] L. A. Schneider, A. Korber, S. Grabbe, and J. Dissemond, "Influence of pH on wound-healing: a new perspective for wound-therapy?" *Archives of dermatological research*, vol. 298, no. 9, pp. 413–20, 2 2007.

[31] R. G. Frykberg and J. Banks, "Challenges in the Treatment of Chronic Wounds," *Advances in wound care*, vol. 4, no. 9, pp. 560–582, 2015.

[32] G. S. Schultz, R. G. Sibbald, V. Falanga, E. A. Ayello, C. Dowsett, K. Harding, M. Romanelli, M. C. Stacey, L. Teot, and W. Vanscheidt, "Wound bed preparation: a systematic approach to wound management," *Wound Repair and Regeneration*, vol. 11, pp. 1–28, 3 2003.

[33] T. Abdelrahman and H. Newton, "Wound dressings: principles and practice," *Surgery (Oxford)*, vol. 29, no. 10, pp. 491–495, 10 2011.

[34] D. Queen, H. Orsted, H. Sanada, and G. Sussman, "A dressing history." *International wound journal*, vol. 1, no. 1, pp. 59–77, 4 2004.

[35] S.-F. Lo, M. Hayter, C.-J. Chang, W.-Y. Hu, and L.-L. Lee, "A systematic review of silver-releasing dressings in the management of infected chronic wounds." *Journal of clinical nursing*, vol. 17, no. 15, pp. 1973–85, 8 2008.

[36] P. M. Tibbles and J. S. Edelsberg, "Hyperbaric-oxygen therapy," *The New England journal of medicine*, vol. 334, no. 25, pp. 1642–1648, 1996.

[37] B. M. Smith, L. D. Desvigne, J. B. Slade, J. W. Dooley, and D. C. Warren, "Transcutaneous oxygen measurements predict healing of leg wounds with hyperbaric therapy." *Wound repair and regeneration : official publication of the Wound Healing Society [and] the European Tissue Repair Society*, vol. 4, no. 2, pp. 224–9, 1996.

[38] C. L. Hess, M. A. Howard, and C. E. Attinger, "A review of mechanical adjuncts in wound healing: hydrotherapy, ultrasound, negative pressure therapy, hyperbaric oxygen, and electrostimulation." *Annals of plastic surgery*, vol. 51, no. 2, pp. 210–8, 8 2003.

[39] J. A. Flegg, H. M. Byrne, and D. L. S. McElwain, "Mathematical model of hyperbaric oxygen therapy applied to chronic diabetic wounds." *Bulletin of mathematical biology*, vol. 72, no. 7, pp. 1867–91, 10 2010.

[40] H. K. Said, J. Hijjawi, N. Roy, J. Mogford, and T. Mustoe, "Transdermal sustained-delivery oxygen improves epithelial healing in a rabbit ear wound model." *Archives of surgery (Chicago, Ill. : 1960)*, vol. 140, no. 10, pp. 998–1004, 10 2005.

[41] G. M. Gordillo, S. Roy, S. Khanna, R. Schlanger, S. Khandelwal, G. Phillips, and C. K. Sen, "Topical oxygen therapy induces vascular endothelial growth factor expression and improves closure of clinically presented chronic wounds." *Clinical and experimental pharmacology & physiology*, vol. 35, no. 8, pp. 957–64, 8 2008.

[42] D. Kemp and M. Hermans, "An evaluation of the efficacy of Transdermal Continuous Oxygen Therapy in patients with recalcitrant diabetic foot ulcer." *Journal of Diabetic Foot Complications*, vol. 3, no. 1, pp. 6–12, 2011.

[43] Therapeutic Surface Solutions Inc., "Topical Pressurized Oxygen Therapy (TPOT)," 2011. [Online]. Available: http://www.tsswoundcare.com/products-tpot.php

[44] P. Banks and C. Ho, "A novel topical oxygen treatment for chronic and difficult-to-heal wounds: case studies," *The journal of spinal cord medicine*, vol. 31, no. 3, pp. 297–301, 2008.

[45] Ogenix, "EPIFLO® Transdermal Continuous Oxygen Therapy [TCOT] for Wound Healing," 2012. [Online]. Available: http://www.ogenix.com/product-overview/

[46] Inotec AMD Limited, "Home Page," 2016. [Online]. Available: http://www.inotecamd.com/home-page

[47] Halyard Health Inc., "OXYGENESYS: Advanced Oxygen Technology," 2016. [Online]. Available: http://www.halyardhealth.com/solutions/advanced-wound-care/oxygenesys.aspx

[48] OxyBand Technologies, "OxyBand Technologies -Topical Oxygen Technology," 2016. [Online]. Available: http://oxyband.com/OxyBand/Images/misc/OxyBand-Wound-Dressing-1024x837px.jpg

[49] P. Boisseau and B. Loubaton, "Nanomedicine, nanotechnology in medicine," *Comptes Rendus Physique*, vol. 12, no. 7, pp. 620–636, 9 2011.

[50] M. Ochoa, C. Mousoulis, and B. Ziaie, "Polymeric microdevices for transdermal and subcutaneous drug delivery." *Advanced drug delivery reviews*, vol. 64, no. 14, pp. 1603–1616, 11 2012.

[51] N. Mehmood, A. Hariz, R. Fitridge, and N. H. Voelcker, "Applications of modern sensors and wireless technology in effective wound management." *Journal of biomedical materials research. Part B, Applied biomaterials*, pp. 1–11, 10 2013.

[52] T. R. Dargaville, B. L. Farrugia, J. a. Broadbent, S. Pace, Z. Upton, and N. H. Voelcker, "Sensors and imaging for wound healing: a review." *Biosensors & bioelectronics*, vol. 41, pp. 30–42, 3 2013.

[53] M. D. Kerstein, E. Gemmen, L. van Rijswijk, C. H. Lyder, T. Phillips, G. Xakellis, K. Golden, and C. Harrington, "Cost and Cost Effectiveness of Venous and Pressure Ulcer Protocols of Care," *Disease Management and Health Outcomes*, vol. 9, no. 11, pp. 651–636, 2001.

[54] B. Derby, "Inkjet Printing of Functional and Structural Materials: Fluid Property Requirements, Feature Stability, and Resolution," *Annual Review of Materials Research*, vol. 40, no. 1, pp. 395–414, 6 2010.

[55] S. Hengsbach and A. D. Lantada, "Rapid prototyping of multi-scale biomedical microdevices by combining additive manufacturing technologies." *Biomedical microdevices*, vol. 16, no. 4, pp. 617–27, 8 2014.

[56] D. Queen, J. H. Evans, J. D. Gaylor, J. M. Courtney, and W. H. Reid, "An in vitro assessment of wound dressing conformability." *Biomaterials*, vol. 8, no. 5, pp. 372–6, 9 1987.

[57] T. E. Wright, W. G. Payne, F. Ko, D. Ladizinsky, N. Bowlby, R. Neeley, B. Mannari, and M. C. Robson, "The Effects of an Oxygen- Generating Dressing on Tissue Infection and Wound Healing," *Journal Of Applied Research*, vol. 3, no. 4, pp. 363–370, 2003.

[58] D. W. Brett, "A Review of Moisture-Control Dressings in Wound Care," *Journal of Wound, Ostomy and Continence Nursing*, vol. 33, no. 6 Suppl, pp. S3–S8, 11 2006.

[59] J. Viventi, D.-H. Kim, J. D. Moss, Y.-s. Kim, J. A. Blanco, N. Annetta, A. Hicks, J. Xiao, Y. Huang, D. J. Callans, J. A. Rogers, and B. Litt, "A conformal, bio-interfaced class of silicon electronics for mapping cardiac electrophysiology." *Science translational medicine*, vol. 2, no. 24, p. 24ra22, 3 2010.

[60] J. A. Rogers, T. Someya, and Y. Huang, "Materials and mechanics for stretchable electronics." *Science (New York, N.Y.)*, vol. 327, no. 5973, pp. 1603–7, 3 2010.

[61] J. Seo, "Making monosaccharide and disaccharide sugar glasses by using microwave oven," *Journal of Non-Crystalline Solids*, vol. 333, no. 1, pp. 111–114, 1 2004.

[62] S. T. Hwang, C. K. Choi, and K. Kammermeyer, "Gaseous Transfer Coefficients in Membranes," *Separation Science*, vol. 9, no. 6, pp. 461–478, 12 1974.

[63] W. Li, D. C. Rodger, A. Pinto, E. Meng, J. D. Weiland, M. S. Humayun, and Y.-C. Tai, "Parylene-based integrated wireless single-channel neurostimulator," *Sensors and Actuators A: Physical*, vol. 166, no. 2, pp. 193–200, 4 2011.

[64] H.-S. Noh, Y. Huang, and P. J. Hesketh, "Parylene micromolding, a rapid and low-cost fabrication method for parylene microchannel," *Sensors and Actuators B: Chemical*, vol. 102, no. 1, pp. 78–85, 9 2004.

[65] D. C. Rodger, A. J. Fong, W. Li, H. Ameri, A. K. Ahuja, C. Gutierrez, I. Lavrov, H. Zhong, P. R. Menon, E. Meng, J. W. Burdick, R. R. Roy, V. R. Edgerton, J. D. Weiland, M. S. Humayun, and Y.-C. Tai, "Flexible parylene-based multielectrode array technology for high-density neural stimulation and recording," *Sensors and Actuators B: Chemical*, vol. 132, no. 2, pp. 449–460, 6 2008.

[66] D. Armani, C. Liu, and N. Aluru, "Re-configurable fluid circuits by PDMS elastomer micromachining," in *Twelfth IEEE International Conference on Micro Electro Mechanical Systems*. IEEE, 1999, pp. 222–227.

[67] S. Wang, M. Li, and Q. Lu, "Filter Paper with Selective Absorption and Separation of Liquids that Differ in Surface Tension," *ACS Applied Materials & Interfaces*, vol. 2, no. 3, pp. 677–683, 3 2010.

[68] M. I. Tiwana, S. J. Redmond, and N. H. Lovell, "A review of tactile sensing technologies with applications in biomedical engineering," *Sensors and Actuators A: Physical*, vol. 179, pp. 17–31, 6 2012.

[69] H. Yousef, M. Boukallel, and K. Althoefer, "Tactile sensing for dexterous in-hand manipulation in robotics–A review," *Sensors and Actuators A: Physical*, vol. 167, no. 2, pp. 171–187, 6 2011.

[70] R. R. Søndergaard, M. Hösel, and F. C. Krebs, "Roll-to-Roll fabrication of large area functional organic materials," *Journal of Polymer Science Part B: Polymer Physics*, vol. 51, no. 1, pp. 16–34, 1 2013.

[71] K. P. Cooper and R. F. Wachter, "High-rate, roll-to-roll nanomanufacturing of flexible systems," vol. 8466, no. 202, p. 846602, 10 2012.

[72] K. Jain, M. Klosner, M. Zemel, and S. Raghunandan, "Flexible Electronics and Displays: High-Resolution, Roll-to-Roll, Projection Lithography and Photoablation Processing Technologies for High-Throughput Production," *Proceedings of the IEEE*, vol. 93, no. 8, pp. 1500–1510, 8 2005.

[73] K. Burczak, E. Gamian, and A. Kochman, "Long-term in vivo performance and biocompatibility of poly(vinyl alcohol) hydrogel macrocapsules for hybrid-type artificial pancreas," *Biomaterials*, vol. 17, no. 24, pp. 2351–2356, 1 1996.

[74] C.-H. Chen, A. Torrents, L. Kulinsky, R. D. Nelson, M. J. Madou, L. Valdevit, and J. C. LaRue, "Mechanical characterizations of cast Poly(3,4-ethylenedioxythiophene):Poly(styrenesulfonate)/Polyvinyl Alcohol thin films," *Synthetic Metals*, vol. 161, no. 21-22, pp. 2259–2267, 11 2011.

[75] D. Garlotta, "A literature review of poly (lactic acid)," *Journal of Polymers and the Environment*, vol. 9, no. 2, 2001.

[76] S. Mueller, B. Kruck, and P. Baudisch, "LaserOrigami: laser-cutting 3D objects," in *Proceedings of the SIGCHI Conference on Human Factors in Computing Systems*, 2013, pp. 2585–2592.

[77] A. Toossi, M. Daneshmand, and D. Sameoto, "A low-cost rapid prototyping method for metal electrode fabrication using a CO2 laser cutter," *Journal of Micromechanics and Microengineering*, vol. 23, no. 4, p. 047001, 4 2013.

[78] J. Yuan, J. Chen, and C. He, "Research of micro removing copper foil of FCCL assisted with laser," in *2011 IEEE International Conference on Mechatronics and Automation*. IEEE, 8 2011, pp. 749–754.

[79] A. K. Yetisen, M. S. Akram, and C. R. Lowe, "Paper-based microfluidic point-of-care diagnostic devices." *Lab on a chip*, vol. 13, no. 12, pp. 2210–51, 6 2013.

[80] G. Chitnis, T. Tan, and B. Ziaie, "Laser-assisted fabrication of batteries on wax paper," *Journal of Micromechanics and Microengineering*, vol. 23, no. 11, p. 114016(5pp), 11 2013.

[81] G. Chitnis, Z. Ding, C.-L. Chang, C. A. Savran, and B. Ziaie, "Laser-treated hydrophobic paper: an inexpensive microfluidic platform." *Lab on a chip*, vol. 11, no. 6, pp. 1161–5, 3 2011.

[82] L. S. Nair and C. T. Laurencin, "Polymers as biomaterials for tissue engineering and controlled drug delivery." *Advances in biochemical engineering/biotechnology*, vol. 102, no. October 2005, pp. 47–90, 1 2006.

[83] P. B. Maurus and C. C. Kaeding, "Bioabsorbable implant material review," *Operative Techniques in Sports Medicine*, vol. 12, no. 3, pp. 158–160, 7 2004.

[84] R. Rahimi, G. Chitnis, P. Mostafalu, M. Ochoa, S. Sonkusale, and B. Ziaie, "A low-cost oxygen sensor on paper for monitoring wound oxygenation," in *The 7th International Conference on Microtechnologies in Medicine and Biology*, Marina del Rey, CA, USA, 2013.

[85] A. W. Martinez, S. T. Phillips, Z. Nie, C.-M. Cheng, E. Carrilho, B. J. Wiley, and G. M. Whitesides, "Programmable diagnostic devices made from paper and tape." *Lab on a chip*, vol. 10, no. 19, pp. 2499–504, 10 2010.

[86] C. Rivet, H. Lee, A. Hirsch, S. Hamilton, and H. Lu, "Microfluidics for medical diagnostics and biosensors," *Chemical Engineering Science*, vol. 66, no. 7, pp. 1490–1507, 4 2011.

[87] D. Nilsson, "An all-organic sensor-transistor based on a novel electrochemical transducer concept printed electrochemical sensors on paper," *Sensors and Actuators B: Chemical*, vol. 86, pp. 193–197, 9 2002.

[88] P. Spicar-Mihalic, B. Toley, J. Houghtaling, T. Liang, P. Yager, and E. Fu, "CO 2 laser cutting and ablative etching for the fabrication of paper-based devices," *Journal of Micromechanics and Microengineering*, vol. 23, no. 6, p. 067003, 6 2013.

[89] W. K. T. Coltro, D. P. de Jesus, J. A. F. da Silva, C. L. do Lago, and E. Carrilho, "Toner and paper-based fabrication techniques for microfluidic applications," *ELECTROPHORESIS*, vol. 31, no. 15, pp. 2487–2498, 7 2010.

[90] R. Rahimi, S. S. Htwe, M. Ochoa, A. Donaldson, M. Zieger, R. Sood, A. Tamayol, A. Khademhosseini, A. Ghaemmaghami, and B. Ziaie, "Paper-based in-vitro model for on-chip investigation of the human respiratory system," *Lab Chip*, 2016.

[91] M. Ochoa, R. Rahimi, T. L. Huang, N. Alemdar, A. Khademhosseini, M. R. Dokmeci, and B. Ziaie, "A paper-based oxygen generating platform with spatially defined catalytic regions," *Sensors and Actuators B: Chemical*, vol. 198, pp. 472–478, 7 2014.

[92] Xing Liang and S. Boppart, "Biomechanical Properties of In Vivo Human Skin From Dynamic Optical Coherence Elastography," *IEEE Transactions on Biomedical Engineering*, vol. 57, no. 4, pp. 953–959, 4 2010.

[93] R. H. Müller and D. L. Clegg, "Automatic Paper Chromatography," *Analytical Chemistry*, vol. 21, no. 9, pp. 1123–1125, 9 1949.

[94] L. Jeong, I.-S. Yeo, H. N. Kim, Y. I. Yoon, D. H. Jang, S. Y. Jung, B.-M. Min, and W. H. Park, "Plasma-treated silk fibroin nanofibers for skin regeneration," *International Journal of Biological Macromolecules*, vol. 44, no. 3, pp. 222–228, 4 2009.

[95] S. C. Jin, H. S. Baek, Y. I. Woo, M. H. Lee, J.-S. Kim, J.-C. Park, Y. H. Park, D. K. Rah, K.-H. Chung, S. J. Lee, and I. H. Han, "Beneficial effects of microwave-induced argon plasma treatment on cellular behaviors of articular chondrocytes onto nanofibrous silk fibroin mesh," *Macromolecular Research*, vol. 17, no. 9, pp. 703–708, 9 2009.

[96] V. P. Ribeiro, L. R. Almeida, A. R. Martins, I. Pashkuleva, A. P. Marques, A. S. Ribeiro, C. J. Silva, G. Bonifácio, R. A. Sousa, R. L. Reis, and A. L. Oliveira, "Influence of different surface modification treatments on silk biotextiles for tissue engineering applications," *Journal of Biomedical Materials Research Part B: Applied Biomaterials*, vol. 104, no. 3, pp. 496–507, 4 2016.

[97] S. Özkar, "Enhancement of catalytic activity by increasing surface area in heterogeneous catalysis," *Applied Surface Science*, vol. 256, no. 5, pp. 1272–1277, 12 2009.

[98] D. B. Broughton and R. Wentworth, "Mechanism of Decomposition of Hydrogen Peroxide Solutions with Manganese Dioxide. I," *J. Am. Chem. Soc.*, vol. 69, no. 4, pp. 741–744, 1947.

[99] D. B. Broughton, R. Wentworth, and M. Laing, "Mechanism of Decomposition of Hydrogen Peroxide Solutions with Manganese Dioxide. II," *J. Am. Chem. Soc.*, vol. 69, no. 4, pp. 744–747, 1947.

[100] S.-H. Do, B. Batchelor, H.-K. Lee, and S.-H. Kong, "Hydrogen peroxide decomposition on manganese oxide (pyrolusite): kinetics, intermediates, and mechanism." *Chemosphere*, vol. 75, no. 1, pp. 8–12, 3 2009.

[101] R. H. Burdon, "Superoxide and hydrogen peroxide in relation to mammalian cell proliferation," *Free Radical Biology and Medicine*, vol. 18, no. 4, pp. 775–794, 4 1995.

[102] B. Mosadegh, C.-H. Kuo, Y.-C. Tung, Y.-S. Torisawa, T. Bersano-Begey, H. Tavana, and S. Takayama, "Integrated elastomeric components for autonomous regulation of sequential and oscillatory flow switching in microfluidic devices," *Nature Physics*, vol. 6, no. 6, pp. 433–437, 2010.

[103] R. Rahimi, M. Ochoa, and B. Ziaie, "A low-cost flexible electrochemical sensor for monitoring silver ion concentration in alginate wound dressings," in *Proc. Sensors'13*, 2013.

VITA

VITA

Manuel Ochoa received the B.S. degree in electrical engineering from the California Institute of Technology, Pasadena, CA in 2009 and the M.S. degree in electrical and computer engineering from Purdue University, West Lafayette, IN in 2012. Since then, he has been a research assistant with the Ziaie Biomedical Microdevices Laboratory at Purdue University while pursuing a PhD degree. His research focuses on the integration of common materials for the development low-cost, multifunctional, microsystem platforms for biomedical applications, including transdermal drug delivery and treatment of chronic dermal wounds.

PUBLICATIONS

PUBLICATIONS

JOURNAL PUBLICATIONS (20)

M. Ochoa, C. K. Yoon, and B. Ziaie, "Laser-fabricated, self-forming swimmers with catalytic propulsion and magnetic navigation," *J Microelectromech S*, under review.

R. Rahimi, S. S. Htwe, **M. Ochoa**, A. Donaldson, M. Zieger, R. Sood, A. Tamayol, A. Khademhosseini, A. Ghaemmaghami, and B. Ziaie, "Paper-based in-vitro model for on-chip investigation of the human respiratory system," *Lab Chip*, accepted.

L. Yang, C. Compton, **M. Ochoa**, B. Ziaie, J. Sokol, and M. Boyce, "Early Experience with Medpor Nonporous Barrier Sheet In Orbital Fracture Repair," *Invest. Ophthalmol. Vis. Sci.*, vol. 57, no. 12, p. 710, 2016.

R. Rahimi, **M. Ochoa**, and B. Ziaie, "Direct laser writing of porous-carbon/silver nanocomposite for flexible electronics," *ACS Appl. Mater. Interfaces*, vol. 8, no. 26, pp. 16907–16913, Jul. **2016**.

M. Ochoa, H. Jiang, J. H. Park, A. Otte, R. Pinal, and B. Ziaie, "Nanoparticle-enabled wireless monitoring and characterization of physical degradation kinetics in pharmaceutical gelatin films," *Sens. Actuators A: Phys.*, vol. 241, **2016**, pp. 238–244.

R. Rahimi, **M. Ochoa**, T. Parupudi, X. Zhao, I. K. Yazdi, M. R. Dokmeci, A. Tamayol, A. Khademhosseini, and B. Ziaie, "A low-cost flexible pH sensor array for wound assessment," *Sens. Actuators B: Chem.*, vol. 229, **2016**, pp. 609–617.

W. Yu, R. Rahimi, **M. Ochoa**, R. Pinal, and B. Ziaie, "A smart capsule with GI-tract-location-specific payload release," *IEEE Trans. Biomed. Eng.*, vol. 62, no. 9, **2015**, pp. 2289–2295

R. Rahimi, **M. Ochoa**, A. Donaldson, T. Parupudi, M. R. Dokmeci, A. Khademhosseini, A. Ghaemmaghami, and B. Ziaie, "A Janus-paper PDMS platform for air-liquid interface cell culture applications," *J. Micromech. Microeng.*, vol. 25, **2015**, 055015

R. Rahimi, **M. Ochoa**, W. Yu, and B. Ziaie, "Highly stretchable and sensitive unidirectional strain sensor via laser carbonization," *ACS Appl. Mater. Interfaces*, vol. 7, no. 8, **2015**, pp. 4463–4470

R. Rahimi, **M. Ochoa**, W. Yu, and B. Ziaie, "A sewing-enabled stitch-and-transfer method for robust, ultra-stretchable, conductive interconnects," *J. Micromech. Microeng.*, vol. 24, **2014**, 095018

A. H. Najafabadi, A. Tamayol, N. Annabi, **M. Ochoa**, R. Rahimi, P. Mostafalu, M. Akbari, M. Nikkhah, M. R. Dokmeci, S. Sonkusale, B. Ziaie, A. Khademhosseini, "Biodegradable nanofibrous polymeric substrates for generating elastic and flexible electronics," *Adv. Mater.*, vol. 26, no. 33, pp. 5823–5830, Sep. **2014**.

M. Ochoa, R. Rahimi, and B. Ziaie, "Flexible Sensors for Chronic Wound Management," *IEEE Rev. Biomed. Eng.*, **2014**.

P.-A. Vidi, T. Maleki, **M. Ochoa**, L. Wang, S. M. Clark, J. F. Leary, and S. A. Lelièvre, "Disease-on-a-Chip: Mimicry of Tumor Growth in Mammary Ducts," *Lab Chip*, vol. 14, no. 1, pp. 172–177, **2014**.

M. Ochoa, R. Rahimi, Tiffany L. Huang, N. Alemdar, A. Khademhosseini, M. R. Dokmeci, and B. Ziaie, " A paper-based oxygen generating platform with spatially-defined catalytic regions for chronic wound treatment," *Sens. Actuators B: Chem*, vol. 198, pp. 472–478, Jul. **2014**.

M. Ochoa, G. Chitnis, and B. Ziaie, "Laser-micromachined cellulose acetate adhesive tape as a low-cost smart material," *J. Polym. Sci. B Polym. Phys.*, vol. 51, no. 17, **2013**, pp. 1263–1267

M. Ochoa, P. Wei, A. J. Wolley, K. J. Otto, and B. Ziaie, "A hybrid PDMS-Parylene subdural multi-electrode array," *Biomed. Microdevices*, Jan. vol. 15, no. 3, **2013**, pp. 437–443

M. Ochoa, C. Mousoulis, and B. Ziaie, "Polymeric microdevices for transdermal and subcutaneous drug delivery," *Adv. Drug Delivery Rev.*, vol. 64, no. 14, **2012**, pp. 1603–1616.

M. Ochoa and B. Ziaie, "A fermentation-powered thermopneumatic pump for biomedical applications," *Lab Chip*, vol. 12, no. 20, **2012**, pp. 4044–4048.

M. Ochoa and B. Ziaie, "Analysis of novel methods to determine the accuracy of the OmniPod insulin pump: a key component of the artificial pancreas system.," *J. Diabetes Sci. Technol.*, vol. 5, no. 6, **2011**, pp. 1519–1520.

C. Mousoulis, **M. Ochoa**, D. Papageorgiou, and B. Ziaie, "A skin-contact-actuated micropump for transdermal drug delivery," *IEEE Trans. Biomed. Eng.*, vol. 58, **2011**, pp. 1492–1498.

CONFERENCE PUBLICATIONS (31)

V. Jain, **M. Ochoa**, and B. Ziaie,"A low-cost, paper-based visual indicator patch for monitoring dehydration rate due to sweating," in *Proceedings of MicroTAS '16*, **2016**.

H. Jiang, R. Rahimi, **M. Ochoa**, T. Parupudi, and B. Ziaie,"A pH-regulated drug delivery device for targeting infected regions in chronic dermal wounds," in *Proceedings of MicroTAS '16*, **2016**.

W. Yu, J. Zhou, R. Rahimi, H. Jiang, **M. Ochoa**, and B. Ziaie,"Modular customizable 3D-printed batteries for wearable applications," in *Proceedings of MicroTAS '16*, **2016**.

C. K. Yoon, **M. Ochoa**, A. Kim, R. Rahimi, and B. Ziaie, "An integrated low-cost radiation dosimeter utilizing microorganism as radiation-sensitive material," in *Hilton Head 2016: A Solid-State Sensors, Actuators and Microsystems Workshop*, **2016**.

R. Rahimi **M. Ochoa**, S. S. Htwe, A. Donaldson, M. Zieger, M. R. Dokmeci, A. Khademhosseini, R. Sood, A. Ghaemmaghami, and B. Ziaie, "A low-cost paper-based model for on-chip human respiratory system studies," in *Hilton Head 2016: A Solid-State Sensors, Actuators and Microsystems Workshop*, **2016**.

R. Rahimi , **M. Ochoa**, T. Parupudi, W. Yu, and B. Ziaie, "Facile fabrication of flexible electronics via direct laser writing of carbon-silver nanocomposite," in *Hilton Head 2016: A Solid-State Sensors, Actuators and Microsystems Workshop*, **2016**.

J. Zhou, R. Rahimi, A. Kim, **M. Ochoa**, and B. Ziaie, "A PVDF-based flexible and shapeable acoustic power source for implantable biomedical devices," in *Hilton Head 2016: A Solid-State Sensors, Actuators and Microsystems Workshop*, **2016**.

M. Ochoa, C. K. Yoon, and B. Ziaie, "Flexible self-forming swimmers with catalytic propulsion and magnetic navigation," in *MEMS 2016, Shanghai, China*, **2016**, pp. 1161–1164.

R. Rahimi, **M. Ochoa**, M. Zieger, R. Sood, and B. Ziaie, "A wireless strain sensor for wound monitoring with direct laser-defined patterning on a commercial dressing," in *MEMS 2016, Shanghai, China*, **2016**, pp. 481–484.

J. Zhou, A. Kim, **M. Ochoa**, H. Jiang, and B. Ziaie, "An ultrasonically powered micropump for on-demand in-situ drug delivery," in *MEMS 2016, Shanghai, China*, **2016**, pp. 349–352.

C. K. Yoon, A. Kim, **M. Ochoa**, T. Parupudi, and B. Ziaie, "A low-cost wearable radiation sensor based on dose response viability of yeast cells," in *MEMS 2016, Shanghai, China*, **2016**, pp. 1066–1069.

M. Ochoa, J. Zhou, R. Rahimi, V. Badwaik, D. Thompson, and B. Ziaie, "Rapid 3D-print-and-shrink fabrication of biodegradable microneedles with complex geometries," in *Transducers 2015, Anchorage, AK*, **2015**.

H. Jiang, **M. Ochoa**, J.H. Park, A. Otte, R. Pinal, and B. Ziaie, "Wireless screenning of degradation kinetics in pharmaceutical gelatin films," in *Transducers 2015, Anchorage, AK*, **2015**.

R. Rahimi, **M. Ochoa**, W. Yu, and B. Ziaie, "A highly stretchable pH sensor array using elastomer-embedded laser carbonized patterns," in *Transducers 2015, Anchorage, AK*, **2015**.

R. Rahimi, **M. Ochoa**, W. Yu, and B. Ziaie, "A low-cost fabrication technique for direct sewing stretchable interconnetions for wearable electronics," in *Transducers 2015, Anchorage, AK*, **2015**.

L. Ben-Yehoshua, **M. Ochoa**, and B. Ziaie, "Rapid fabrication of 3D elastomeric structures via laser-machining and vacuum deformation," in *Transducers 2015, Anchorage, AK*, **2015**.

Z.B. Hughes, R. Rahimi, **M. Ochoa**, and B. Ziaie, "Rapid prototyping of piezoresistive mems sensors via a single-step laser carbonization and micromachining process," in *Transducers 2015, Anchorage, AK*, **2015**.

M. Ochoa, H. Jiang, R. Rahimi, and B. Ziaie, "Laser treated glass platform with rapid wicking-driven transport and particle separation capabilities," in *MEMS 2015, Estoril, Portugal*, **2015**.

R. Rahimi, **M. Ochoa**, W. Yu, and B. Ziaie, "A facile fabrication technique for stretchable interconnects and transducers via laser carbonization," in *MEMS 2015, Estoril, Portugal*, **2015**.

T.S. Zhang, A. Kim, **M. Ochoa**, and B. Ziaie, "Controllable 'somersault' magnetic soft robotics," in *MEMS 2015, Estoril, Portugal*, **2015**.

M. Ochoa, R. Rahimi, H. Jiang, and B. Ziaie, "Laser surface-treated glass with wicking capability for microfluidics," in *μTAS 2015, San Antonio, TX*, **2015**.

R. Rahimi, **M. Ochoa**, J. Zhou, A. Tamayol, M.R. Dokmeci, A. Khademhosseini, A. Ghaemmaghami, and B. Ziaie, "A hybrid PDMS/paper passive pump for slow-release/delivery of drugs in chronic dermal wounds," in *μTAS 2015, San Antonio, TX*, **2015**.

R. Rahimi, **M. Ochoa**, M. R. Dokmeci, A. Khademhosseini, and B. Ziaie, "A Janus-paper PDMS platform for lab-on-a-chip applications," in *Hilton Head 2014: A Solid-State Sensors, Actuators and Microsystems Workshop*, **2014**.

R. Rahimi, **M. Ochoa**, X. Zhao, M. R. Dokmeci, A. Khademhosseini, and B. Ziaie, "A flexible ph sensor array on paper using laser pattern definition and self-aligned laminated encapsulation," in *Hilton Head 2014: A Solid-State Sensors, Actuators and Microsystems Workshop*, **2014**.

R. Rahimi, **M. Ochoa**, W. Yu, and B. Ziaie, "A sewing-enabled stitch-and-transfer method for robust, ultra-stretchable, conductive interconnects," in *Hilton Head 2014: A Solid-State Sensors, Actuators and Microsystems Workshop*, **2014**.

M. Ochoa, R. Rahimi, N. Alemdar, M. R. Dokmeci, A. Khademhosseini, and B. Ziaie, "A flexible, laser-defined, paper platform for localized oxygen generation and delivery," in *Proc. Transducers 2013*, Actuators and Microsystems, **2013**.

M. Ochoa, R. Rahimi, R. Shi, and B. Ziaie, "An impact sensing platform for spinal cord injury experiments," in *Proc. Sensors '13*, **2013**.

R. Rahimi, **M. Ochoa**, and B. Ziaie, "A low-cost flexible electrochemical sensor for monitoring silver ion concentration in alginate wound dressings," in *Proc. Sensors '13*, **2013**.

R. Rahimi, G. Chitnis, P. Mostafalu, **M. Ochoa**, S. Sonkusale, and B. Ziaie, "A low-cost oxygen sensor on paper for monitoring wound oxygenation," in *The 7th International Conference on Microtechnologies in Medicine and Biology*, **2013**.

M. Ochoa, C. Mousoulis, and B. Ziaie, "A sequential-dosage fluorocarbon-actuated micropump," in *Proceedings of MicroTAS '11*, **2011**, pp. 1807–1809.

C. Mousoulis, **M. Ochoa**, and B. Ziaie,"A skin-contact-actuated dispenser/pump for transdermal drug delivery," in *Proceedings of MicroTAS '10*, **2010**, pp. 749–751.

BOOK CHAPTERS

M. Ochoa, R. Rahimi, and B. Ziaie, "Laser-Enabled Fabrication Technologies for Low-Cost Flexible/Conformal Cutaneous Wound Interfaces," in *Stretchable Bioelectronics for Medical Devices and Systems*, J. A. Rogers, R. Ghaffari, and D.-H. Kim, Eds. Springer International Publishing, **2016**, pp. 207–226.

THESES

M. Ochoa. "A piezoelectrically actuated titanium micropump for drug delivery." (Master's thesis) *ProQuest Dissertations and Theses*, pp. 82. **2012**.

PATENTS

B. Ziaie, **M. Ochoa**, and C. Mousoulis, "Touch-actuated micropump for transdermal drug delivery and method of use," US Patent 2012/0046644 A12012.

B. Ziaie, **M. Ochoa**, and R. Rahimi, "Platform for oxygen generation and delivery," US Patent Application 14/602,203.

B. Ziaie and **M. Ochoa**, "Humidity sensors and methods of fabrication," Provisional US Patent.

B. Ziaie, **M. Ochoa**, and V. Jain, "Skin-mounted sweat sensor," Provisional US Patent.